ISSN 1018-5593

European Commission

nuclear science and technology

Abrasive water-jet cutting technique from the laboratory stage into real application

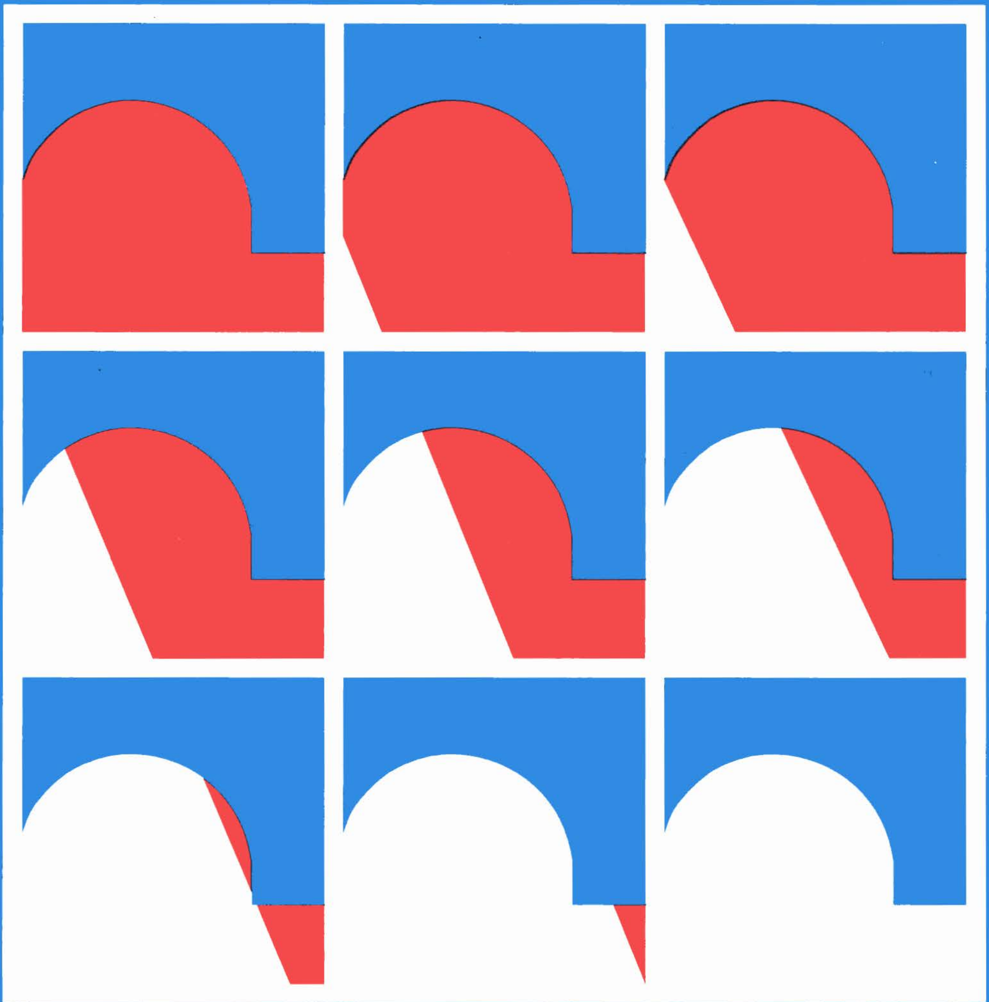

Report

EUR 15241 EN

European Commission

nuclear science
and technology

Abrasive water-jet cutting technique from the laboratory stage into real application

G. Meier[1], H. Louis[1], G. Pilot[2]
[1] **Universität Hannover IW**
Appelstraße 11A
D-30167 Hanover

[2] **CEA, DPEI/SERAC**
CEN Saclay, Bât. 389
F-91191 Gif-sur-Yvette Cedex

Contract No F12D-0009

This work was performed in the framework of the European Communities' research programme on the
decommissioning of nuclear installations (1989-93)
Section C: Alternative tests

Directorate-General
Science, Research and Development

1995

EUR 15241 EN

Published by the
EUROPEAN COMMISSION

Directorate-General XIII
Telecommunications, Information Market and Exploitation of Research

L-2920 Luxembourg

LEGAL NOTICE

Neither the European Commission nor any person acting on
behalf of the Commission is responsible for the use which might be made of the
following information

Cataloguing data can be found at the end of this publication

Luxembourg: Office for Official Publications of the European Communities, 1995

ISBN 92-827-0222-7

© ECSC-EC-EAEC, Brussels • Luxembourg, 1995

Printed in Luxembourg

Table of Content

Summary 1

Introduction 2
Abrasive Jet Generation 2
Pressure generation 2
Jet generation 3

Experimental Work and Results 5

B.1 Definition of cutting parameters 5
Minimisation of consumed water 10
Minimisation of used abrasives 12

B.2 Development of control systems 15

B.2.1 Preparation of the test equipment 16

B.2.2 Tool control 17

B.2.3 Control of the cutting result 22

B.3 Methods to replace worn parts of the cutting head 28

B.4 Characterisation and handling of secondary waste 30

B.4.1 Preparation of the test facility 30

B.4.2 Measurement and characterisation of the sec.emmissions 35
Balance of the secondary emissions 35
Size distribution of abrasives and sedimented dross 39
Characterisation of the aerosols in the exhaust duct 42
Gas 44
Kerf appearance 44

B.4.3 Methods to lower the spreading out of the emissions 46
Cutting through 46
Kerfing 49

B.4.4 Determination of the efficiency of different methods 52
Balance of the secondary emissions 54
Size distribution of abrasives and sedimented dross 56
Characterisation of the aerosols in the exhaust duct 63

Conclusions and Outlook 65

References 67

Annexes

Summary

The aim of the project was to qualify the abrasive water jet cutting technique for application in nuclear decommissioning.

First, the cutting parameters which are known from industrial application had to be adapted to the special conditions of dismantling contaminated or activated material. Mainly, the minimisation of the secondary waste was of importance. Therefore tests were carried out to reduce the amount of abrasives as well as the consumption of water by optimising the cutting parameters. The efficiency of the abrasives was increased by reducing the abrasive flow rate and by increasing the working pressure. The minimisation of the water consumption can be realised by using a high working pressure and a small nozzle diameter.

The operation during dismantling work has to be remote controlled. Therefore, methods are required to control the state of the wear of the cutting tool as well as the cutting result.

The tool control can be realised by measuring the sucked-in air flow rate. By this technique the state of wear as well as the conditions of abrasive transport can be supervised.

Experiments have shown, that sound analysis are no sufficient method to check the cutting result (cutting through or kerfing only). But in case of kerfing the reflected jet can be detected by a deflector plate and an adapted accelerometer.

Different tests have been carried out to quantify the secondary waste. Abrasive water jet cutting produces a small amount of aerosols, especially when cutting under water. Most of the waste is sedimented dross. During the cutting process the abrasive particles disintegrate, so the mean diameter of the particles is less than 150 μm in most cases.

When kerfing the use of a suction hood can lower the spreading out of the secondary waste. The adaptation of a separation unit like a hydrocyclone can help to clean the water of the cutting basin. During the tests about 70 % of the solid waste was caught and separated by the cyclone.

Using optimised cutting parameters to minimise the consumption of water and abrasives and separating the waste from the water by using a cyclone can lead to an important reduction of waste. In addition methods have to be investigated in future to recycle the separated abrasives. First tests point out that a recycling of 80-90 % of the abrasives is within reach.

Introduction

An increasing number of technical installations are hazardous by themselves (like nuclear installations) or they have taken place in inaccessible environment (like off-shore structures). When finishing lifetime all these facilities have to be removed without exposing the operation staff to danger and without contaminating the environment.

Conventional tools to do these jobs are percussive hammers, different kinds of saws, blasting techniques and thermal cutting methods like plasma cutting /1/. But unfortunately all cutting techniques have specific disadvantages: They produce a lot of dust and mechanical load (hammer, blasting, saw), the weight of the tools is quite high (saw, hammer) and it is difficult to use them remote-controlled (hammer). Plasma cutting technique is applicable to dismantle nuclear installations, but the tool produces difficult-to-handle aerosols even when working under water /2/.

An alternative non-thermal method is the abrasive water jet cutting technique: Small mineral particles accelerated by a high speed water jet, are able to cut any kind of material. Advantages of this technique are /1,3/:

- non-contacting process
- small cutting forces (for the manipulator)
- small and lightweight cutting head
- non-thermal cutting process, no fire risk
- no chemical reaction products
- small kerfs (small amount of radioactive waste when cutting activated structures)
- all kinds of material can be cut

The main disadvantage is the great amount of secondary waste produced during operation. Therefore, it is necessary in case of dismantling operations in nuclear environment to reduce the added abrasives and to reach a high cutting performance with respect to the minimisation of secondary waste. Additionally the generation of aerosols has to be investigated.
For using this cutting technique remote controlled it is necessary to adapt controlling devices to check the reliability of the tool as well as the cutting result during operation.

ABRASIVE JET GENERATION

Pressure generation

For pressurising the water slowly working pressure intensifiers are used. These intensifier pumps are normally double-ended pistons utilising differential areas to multiply pressure provided by a standard variable displacement hydraulic pump (fig. 1). With a commercial available intensifier pump pressures up to 4000 bar are achievable, but at a comparatively low level of flow rate of 2 to 4 l/min. Up to three intensifiers are mounted in one pumping set.

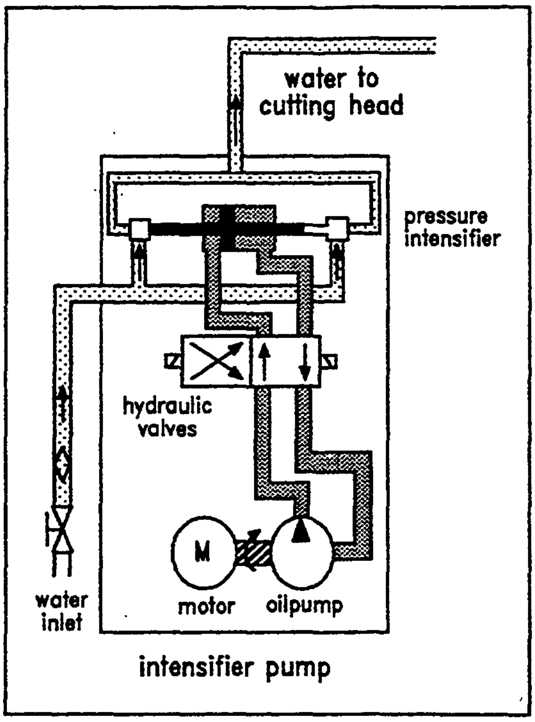

Figure 1
Draft of an intensifier pump

Jet generation

The abrasive water jet is formed in a special mixing head. First a plain water jet is produced and the abrasives are added afterwards in a hard metal or ceramic mixing nozzle.

The mixing head works according to the principle of waterjet pump, what means that the high speed water jet generates a suction pressure in the suction port, which produces a pneumatic transport of the abrasives into the mixing head.

For all the cutting tests a self-designed abrasive cutting head was used /3,4/.

To adjust the axis of the focusing nozzle on the high speed water jet a ball-and-socket joint was created (fig. 2).

So the focusing nozzle is movable around the water jet nozzle within small angles. In case of not adjusting the cutting head the irregular wear in the focusing nozzle increases rapidly and cutting efficiency decreases because of friction loss.

After adjusting, the movable part of the cutting head is fixed by adjusting screws.

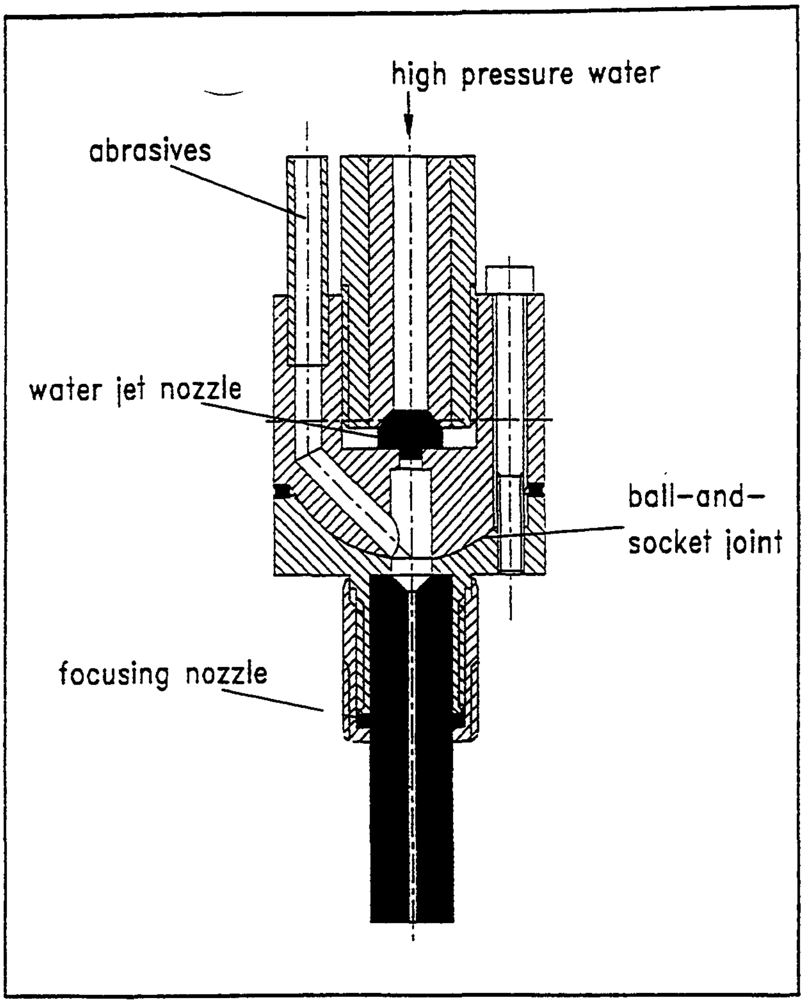
high pressure water
abrasives
water jet nozzle
ball-and-socket joint
focusing nozzle

Figure 2 Abrasive cutting head

The abrasive feed is realised by a vibration feeder, the particles are transported by air stream. Figure 3 shows SEM-pictures of new and used garnet sand.

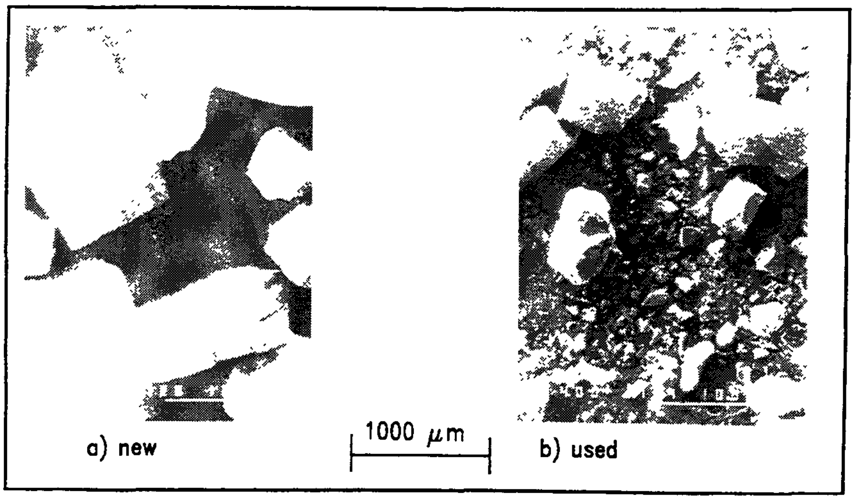
a) new
1000 µm
b) used

Figure 3 New and used garnet sand

Obviously there is a disintegration of the particles during the cutting process.
For the cutting experiments samples of austenitic steel X2 CrNi18 8 (1.4301)) and aluminium alloy (AlMgSi 0.5) have been used. All the samples were not cut through but kerfed to measure and compare the depth of kerf. For measuring aerosols also samples made out of copper have been used.
Figure 4 gives an overview of an abrasive water jet cutting system. In addition to the equipment mentioned before a handling system is necessary as well as a catcher unit to protect the environment from the hazardous jet.

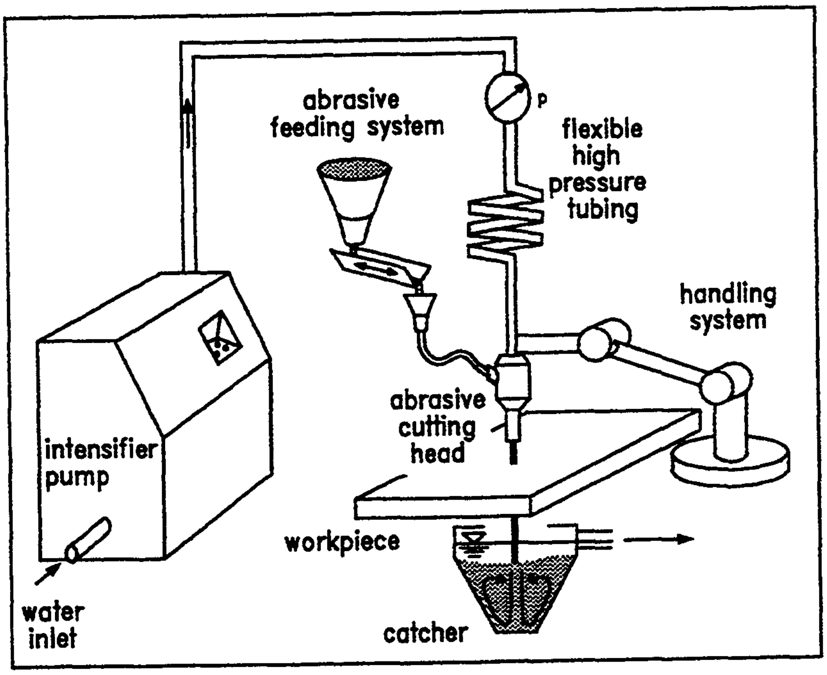

Figure 4 Abrasive water jet cutting system

The reported tests were carried out in a water basin with a numerical-controlled 2-dimensional traverse mechanism. All tests took place under water.

Experimental Work and Results

B.1. Definition of cutting parameters

For the application of abrasive water jets in case of decommissioning nuclear facilities it is necessary to reduce the abrasive flow rate as well as the amount of used water to minimum values due to the problems of handling the secondary waste.
Up to now there is no recycling technique available to reuse the abrasives several times. The used abrasives are mixed with removed workpiece material - so they have to be treated as radioactive waste in case of cutting contaminated or activated material. Also the handling of the water is quite difficult because it has to be cleaned very carefully.

Due to these facts the cutting performance related to the amounts of used abrasive and water has to be optimised. Important process parameters are

- traverse rate
- distance
- pressure
- nozzle diameter
- abrasive flow rate

All tests carried out were kerfing tests. The sample materials were not cut through but kerfed only. The depth of kerf gives an easy method to determine the cutting performance.

There are several ways to compare the cutting performances:

- The cutting performance is defined as the area of the shoulder of the cut related to the time used for the production. It can be calculated by multiplying the obtained depth of kerf with the traverse rate being used (units: mm^2/min).
- To quantify the efficiency of water and abrasives specific cutting performances were defined: The obtained area of the shoulder of the cut can be divided by the consumed amount of water or abrasives (units: mm^2/l or mm^2/g).

The cutting performance related to the energy consumption (mm^2/J) was not investigated in this contract, because providing energy is neither a technical nor an economical problem for decommissioning purposes.

To start the optimisation process it is necessary to know about the influence of different parameters to find the right starting position. At first the influence of the traverse rate on the depth of kerf was investigated. Figure 5 gives the results for different pressures.

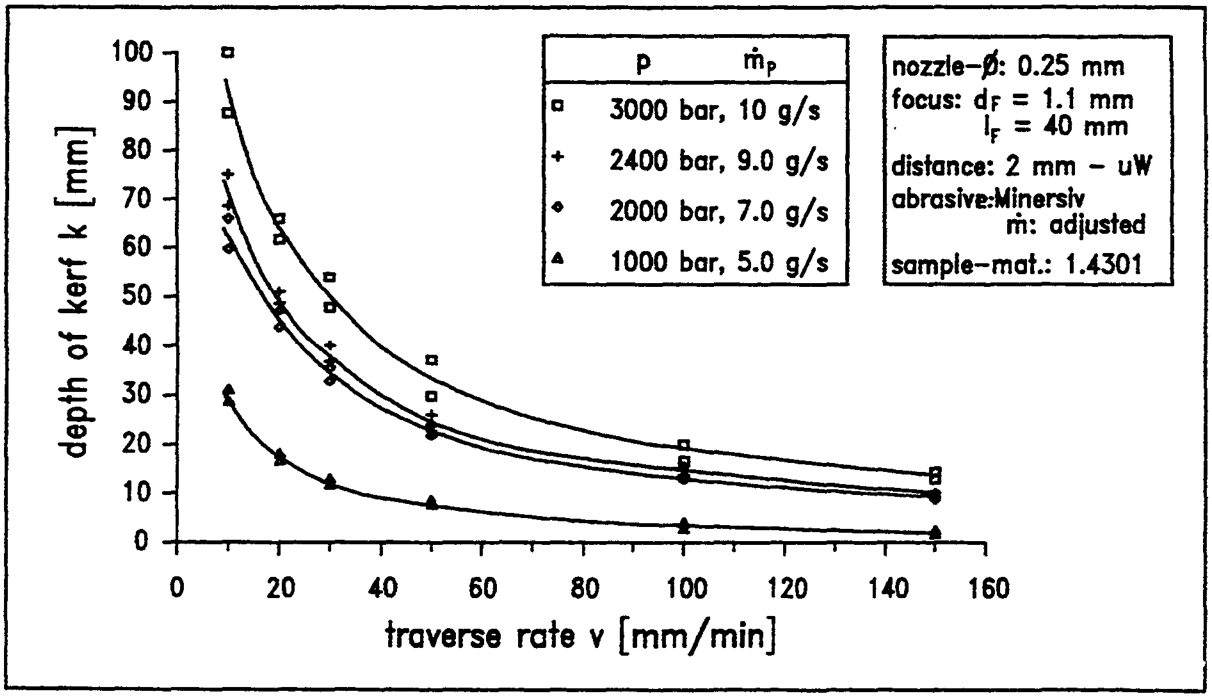

Figure 5 Effect of traverse rate on depth of kerf

The relation appears approximately inverse proportional: Increasing the traverse rate causes a decrease in depth of kerf by the same factor. Figure 6 shows the attainable cutting performance for the variation of the traverse rate.

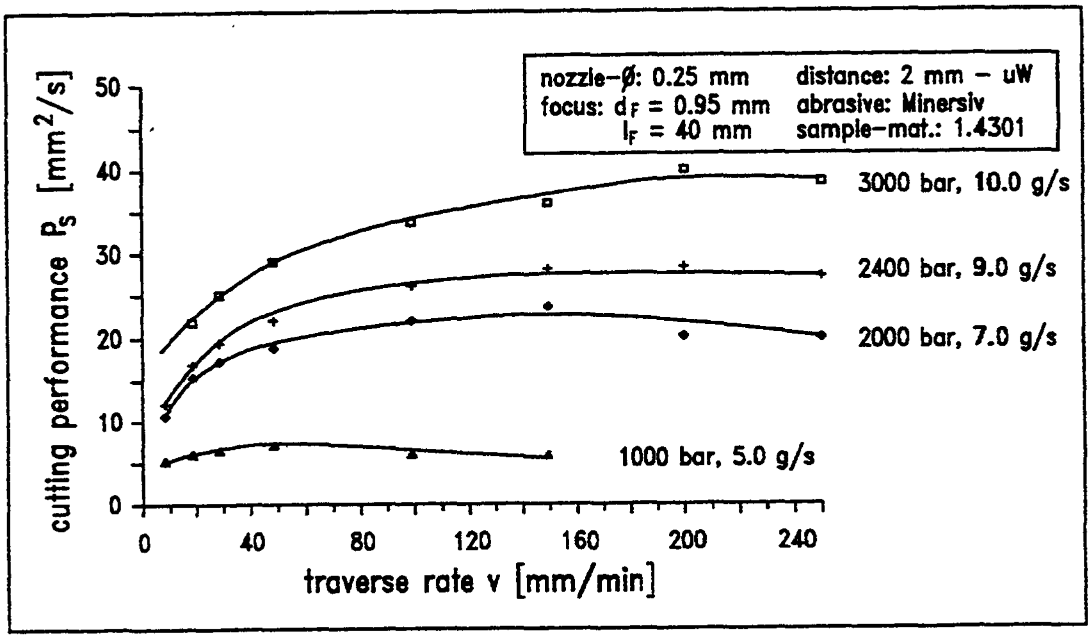

Figure 6 Effect of traverse rate on cutting performance

When reaching a specific traverse rate for all pressures the cutting performance is not affected by increasing traverse rates. For these traverse rates the depth of kerf is inverse proportional to the traverse rate.

For any lower traverse rate the obtained kerfing depth increases not as much as predicted. The reason can be found in figure 5. For example when using 3000 bar at a traverse rate of 20 mm/min a depth of kerf of more than 60 mm can be reached in austenitic steel. For a further reduction of cutting speed the depth of kerf will grow further on, but the friction between abrasive water jet and the shoulder of the cut and the increasing distance between cutting head and the bottom of the kerf will cause a loss of hydraulic power. So for kerfs deeper than about 30 mm (calculated from fig. 6) the cutting process is not as effective as for less deep kerfs.

The conclusions of these tests are:

- To compare the cutting performances for different parameters it is useful to take traverse rates which allow to kerf less than 30 mm deep. For these conditions the product of traverse rate and depth of kerf is nearly constant, so the results for different traverse rates are comparable.
- For real cutting jobs which make it necessary to cut deeper than 30 mm the decrease in cutting efficiency has to be taken into account.

According to figure 7 the best cutting performance resp. depth of kerf is attainable for small working distances. Increasing the distance causes a decrease in depth of kerf for kerfing in air as well as under water. As reported in /5/ the decrease of the depth of kerf under water is more important than in air, but when using special methods /5,6/ the effect can be reduced. Nevertheless, if possible, a working distance of 2 mm seems to be the best.

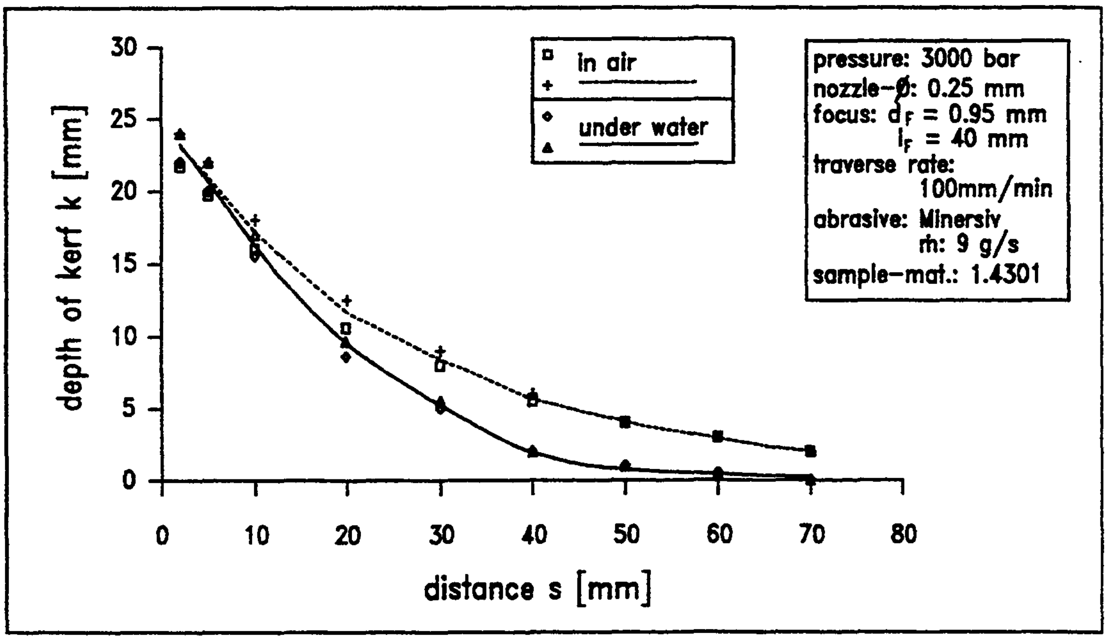

Figure 7 Effect of working distance on depth of kerf

For the comparison of cutting performances for different pressures and nozzle diameters it is necessary to use the most favourable abrasive flow rate for each parameter set. For that reason the influence of the abrasive flow rate on the depth of kerf was investigated for different pressures (fig. 8) and nozzle diameters (fig. 9).

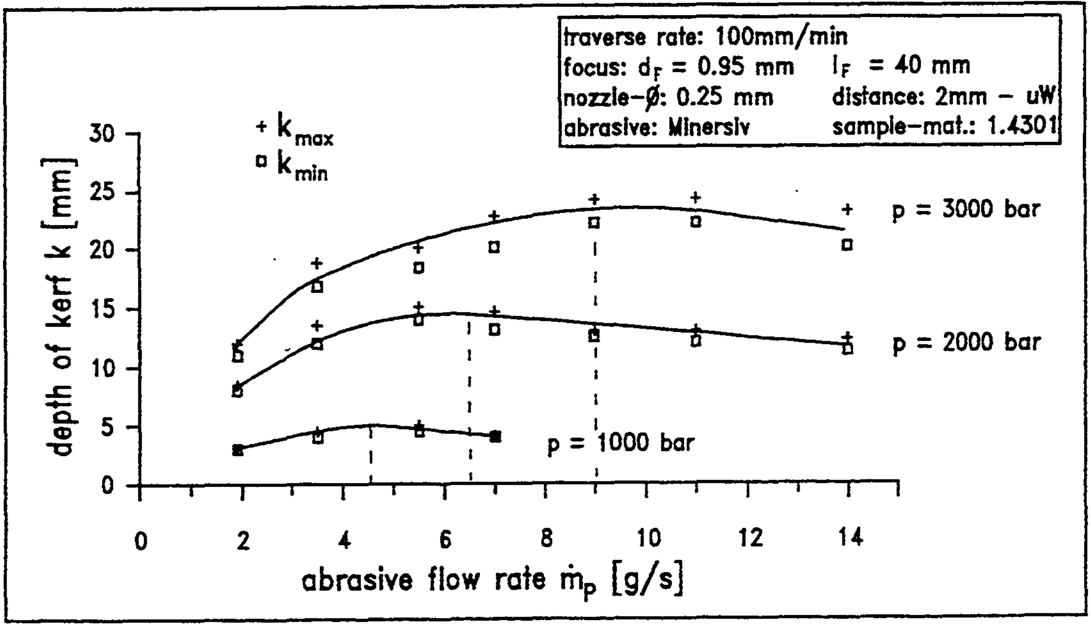

Figure 8 Effect of abrasive flow rate on depth of kerf

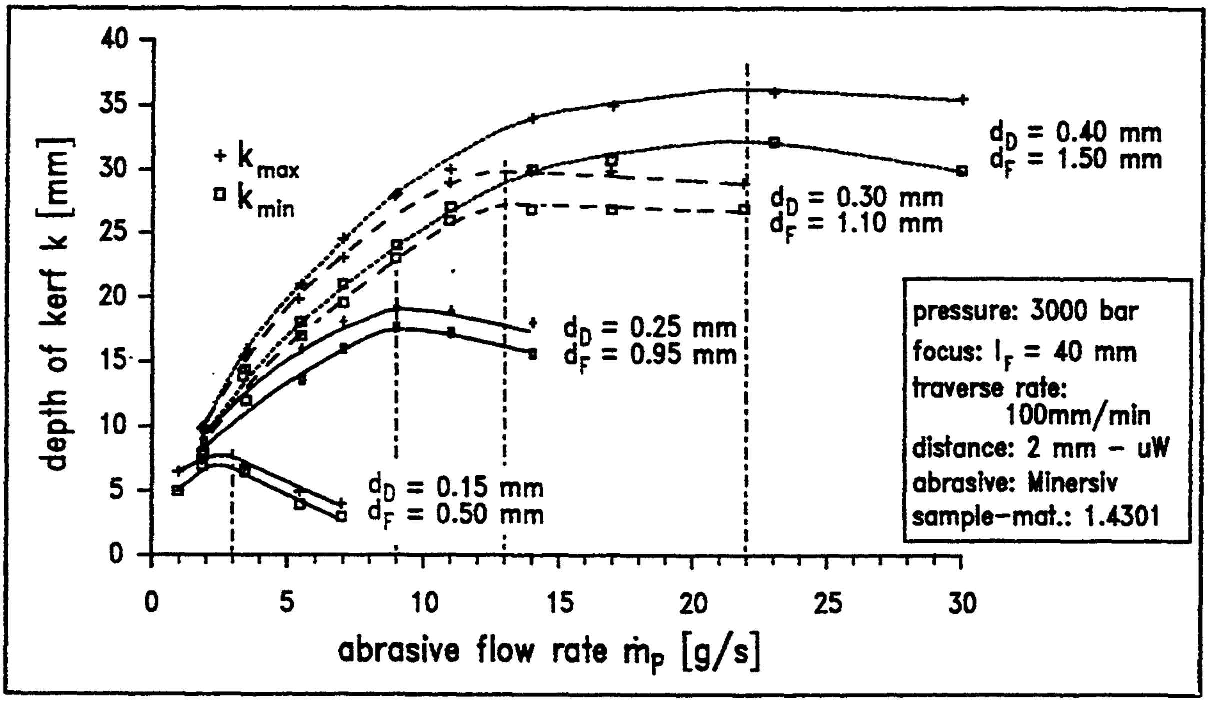

Figure 9 Effect of abrasive flow rate on depth of kerf (d_D: nozzle diameter; d_F: focus diameter)

For all pressures and nozzle diameters being used there is an optimal abrasive flow rate existing. Lower as well as higher flow rates lead to a decrease in depth of kerf. The optimal flow rates are corresponding very good to the water flow rates, as figure 10 shows. The water mass flow can be calculated by the first equation of figure 11.

nozzle diameter d_D [mm]	water flow rate $\dot{m}_W$ [g/s]				opt. abrasive flow rate $\dot{m}_P$ [g/s]				opt. mass ratio R ($\dot{m}_P/\dot{m}_W$)			
pressure p [bar]	1000	2000	2400	3000	1000	2000	2400	3000	1000	2000	2400	3000
0.15	5.2	7.3	7.8	9.2			*2.6*	3.0			*0.33*	0.33
0.20	10.0	14.0	15.5	17.5			*5.1*	*5.8*			*0.33*	*0.33*
0.25	15.0	20.8	24.0	26.7	4.5	6.5	8.0	9.0	0.30	0.31	0.33	0.34
0.30	21.7	30.0	33.4	38.3	*6.5*	*9.3*	*11.0*	13.0	*0.30*	*0.31*	*0.33*	0.34
0.40	36.6	52.0	59.1	64.9			20.0	22.0			0.34	0.34

measured *calculated*

Figure 10 Water flow rates
Optimal abrasive flow rates
Abrasive mass ratio R

$Q = v * d_D^2 * \frac{\pi}{4}$ water flow rate: Q

jet velocity: v

$v = \sqrt{\frac{2}{\rho} * p}$ nozzle diameter: d_D

pressure: p

$\rightarrow \quad Q \sim \sqrt{p}$ density of water: ρ

Figure 11 Calculation of the water flow rate

According to the results in figure 10 for all tests a mass ratio R of about 0.33 has been used to reach the optimal cutting performance.

Minimisation of consumed water

As shown in figure 11 the water flow rate is influenced by the pressure and the nozzle diameter. The effect of both parameters on the specific cutting performance will be described in the following figures.

Figure 12 gives the effect of the pressure on the cutting performance as well as on the specific cutting performance related to the water consumption.

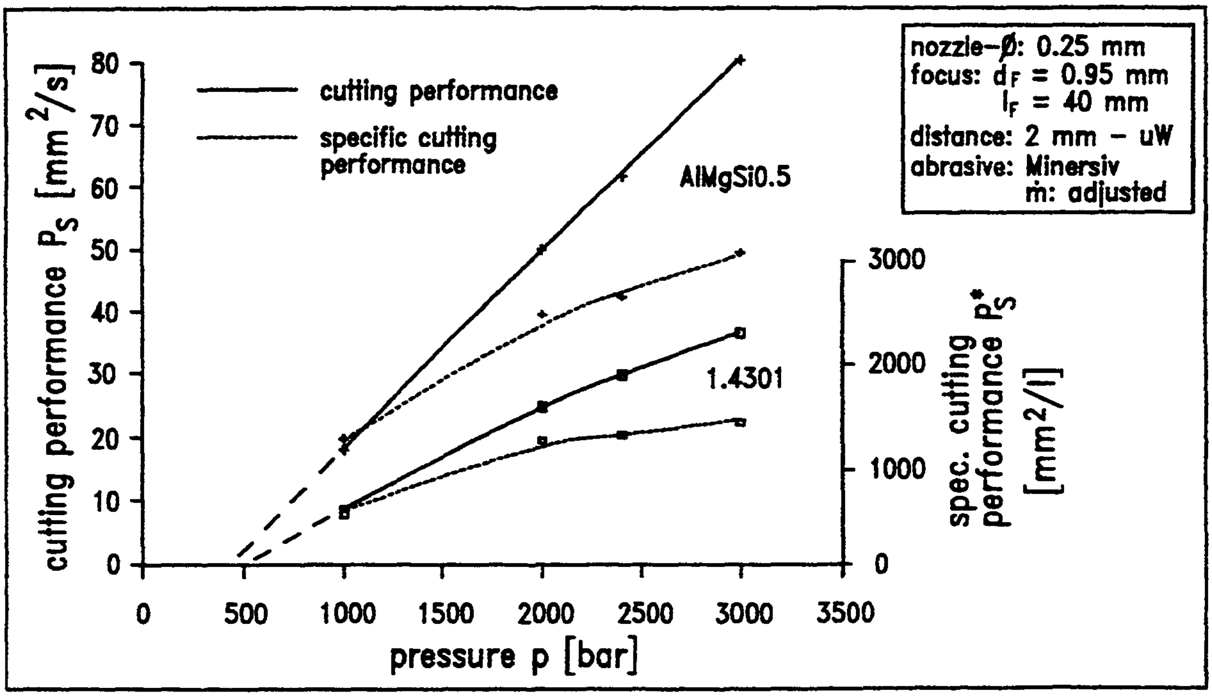

Figure 12 Effect of pressure on cutting performance

An increasing pressure causes a linear increase in cutting performance and also a better specific cutting performance. For the highest pressure the exploitation of the water is the best. So it is useful to increase the pressure to values above 3000 bar, but in that case the tool life of the pressure pump (sealing) and the nozzles will be decreasing rapidly. For the tests the abrasive flow rate was adjusted to the water flow rate according to figure 10 (R = 0.33).

The results of a variation of the nozzle diameter are given in figure 13.

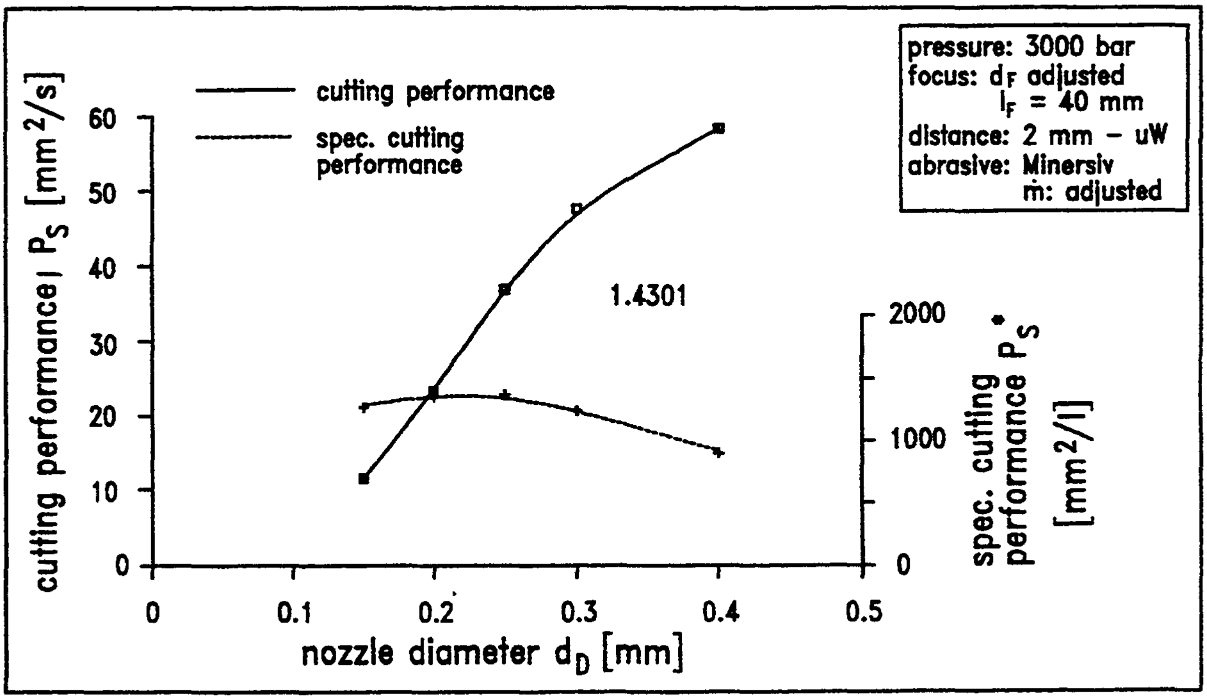

Figure 13 Effect of nozzle diameter on cutting performance

Although the cutting performance is increasing for bigger nozzles the specific performance has an optimum for medium sized nozzles because of the rapid increase of the water flow rate for bigger nozzles. The abrasive flow rate was adjusted in the way already mentioned. To reach the optimal efficiency related to the water consumption a nozzle with a diameter of 0.20-0.25 mm should be used.

Summing up for an optimal exploitation of the water the pressure should be as high as possible using a medium sized nozzle. The abrasive flow rate should be fixed to a mass ratio of about 0.33 according to figure 10. In addition it has to be mentioned that for these chosen parameters the machining time for a given job is not minimal, because the cutting performance (related to the time) is not maximal (see fig. 13) because of the smaller nozzle size.

Minimisation of used abrasives

To find parameters for the best exploitation of the abrasives two strategies can be used. On one hand the best values regarding pressure and nozzle diameter can be determined for the optimal abrasive flow rate (fig. 10), on the other hand the abrasive flow rate can be lowered to values smaller than mentioned in figure 10. In that case the cutting performance related to the cutting time will be decreased (see fig. 8, 9), but the exploitation of the abrasives will be better as shown later in the report.

Figure 14 gives the effect of the abrasive flow rate on the specific cutting performance (related to the abrasive flow rate) for different pressures.

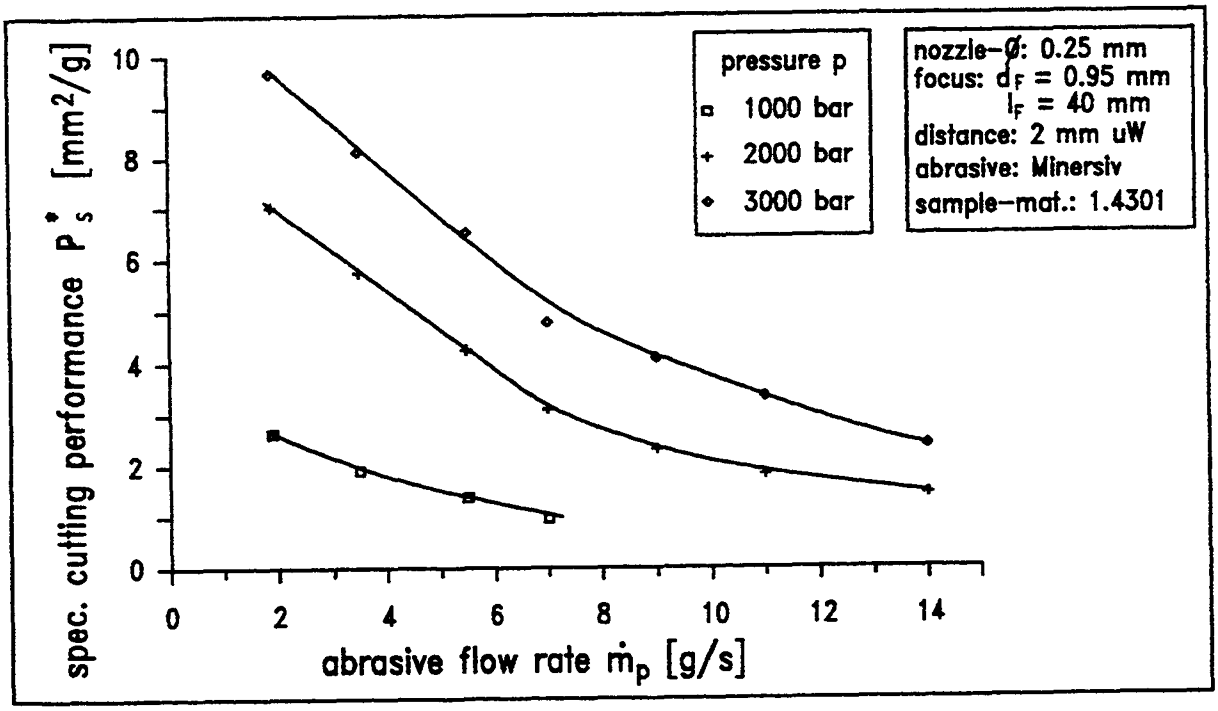

Figure 14 Effect of abrasive flow rate on specific cutting performance

The increase of pressure causes a better exploitation of the abrasives. Additionally the smaller flow rates result in a better specific cutting performance. The smallest flow rate causes the best exploitation regarding the abrasives. But, to fulfil a given cutting job, for smaller flow rates the time which is necessary to do the job will increase and so does the consumption of water and energy.

For using different nozzle sizes the effect is is given in figure 15.

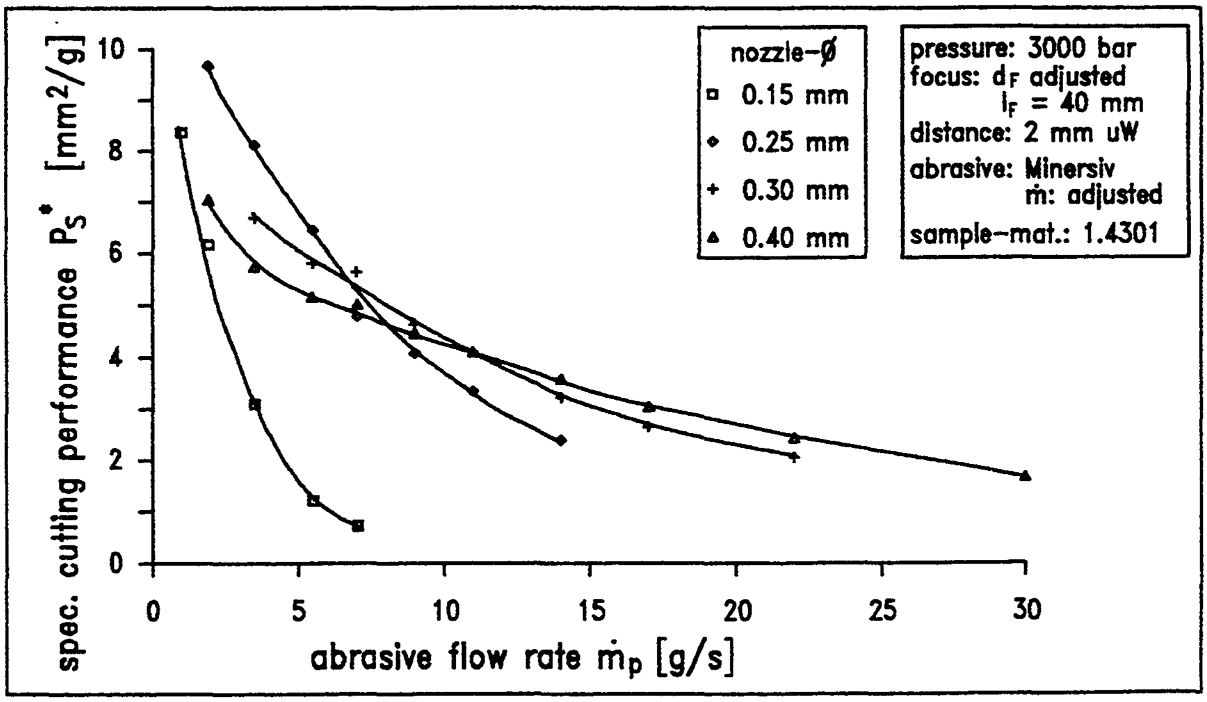

Figure 15 Effect of abrasive flow rate on specific cutting performance

Smaller abrasive flow rates cause a better exploitation of the abrasives. For high flow rates bigger nozzle are being more useful, but a decrease of the abrasive flow rate for smaller nozzle diameters leads to a faster increase of the specific cutting performance. Again it has to be mentioned that using smaller nozzles and lower abrasive flow rates help to save abrasives but leads to an increasing machining time, energy and water consumption. Figure 16 gives an example for this effect.

	pressure [bar]								
	2000			2400			3000		
	abrasive flow rate [g/s]								
	2	10	20	2	10	20	2	10	20
t [min]	33.3	25.0	33.3	28.6	20.0	25.0	25.0	12.5	16.7
m_A [g]	4000	15000	40000	3430	12000	30000	3000	7500	20000
V_W [l]	41.5	31.2	41.6	41.2	28.8	36.0	40.0	20.0	26.8
E [kJ]	8300	6240	8320	9890	6912	8640	12000	6000	8040
Δm [g]	160								

nozzle diameter: 0.25 mm
material: austenitic steel, 20 mm thickness
cutting length: 1 m

	nozzle diameter [mm]								
	0.40			0.30			0.25		
	abrasive flow rate [g/s]								
	2	10	20	2	10	20	2	10	20
t [min]	25.0	9.1	7.7	25.0	10.0	11.1	25.0	12.5	16.7
m_A [g]	3000	5460	9240	3000	6000	13320	3000	7500	20000
V_W [l]	97.5	35.5	30.0	57.5	23.0	25.5	40.0	20.0	26.8
E [kJ]	29250	10650	9000	17250	6900	7650	12000	6000	8040
Δm [g]	250			200			160		

pressure: 3000 bar
material: austenitic steel, 20 mm thickness
cutting length: 1 m

Figure 16 Cutting of steel, 20 mm thickness

The upper part gives the results for a variation of pressure and abrasive flow rate using a fixed nozzle diameter, the lower part shows the effect of different nozzle diameters.
The increasing pressure (upper part) leads to a decrease in used machining time (1. line). The consumption of abrasive, water and energy decreases, too (line 2, 3, 4). The smallest abrasive flow rate causes the best abrasive efficiency per meter of cut, but leads to a high energy and water consumption compared to higher flow rates of abrasive.
An increasing nozzle diameter (lower part of fig. 16) causes a better exploitation of the abrasive (line 2) but also an increase of the water and energy consumption (line 3 and 4). In general smaller abrasive flow rates effect a better exploitation of the abrasives, but lead to a much higher consumption of water.
So it is necessary to find a compromise between the amount of abrasives and the amount of water and the cutting time.

B.2. Development of control systems

For remote controlled operation of abrasive water jets it is necessary to control the state of the tool as well as the cutting process (cutting result) /7/.
Controlling the state of the tool means both supervising the **geometry** inside the cutting head (water nozzle and abrasive mixing nozzle) and monitoring the **operation conditions** of the cutting tool like the generation of the water jet or the abrasive transport (broken or clogged transport hose) (fig. 17).

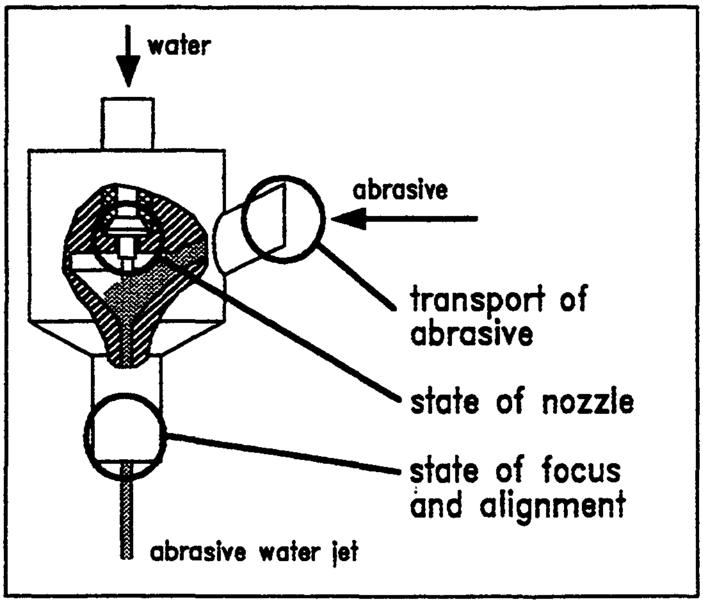

Figure 17 Aspects of tool control

Controlling the cutting result means the detection if cutting through or kerfing only. Additionally it would be helpful to supervise the quality of the shoulder of the cut during operation.

B.2.1. Preparation of the test equipment

To develop useful sensor systems tests were carried out in a water basin (fig. 18).

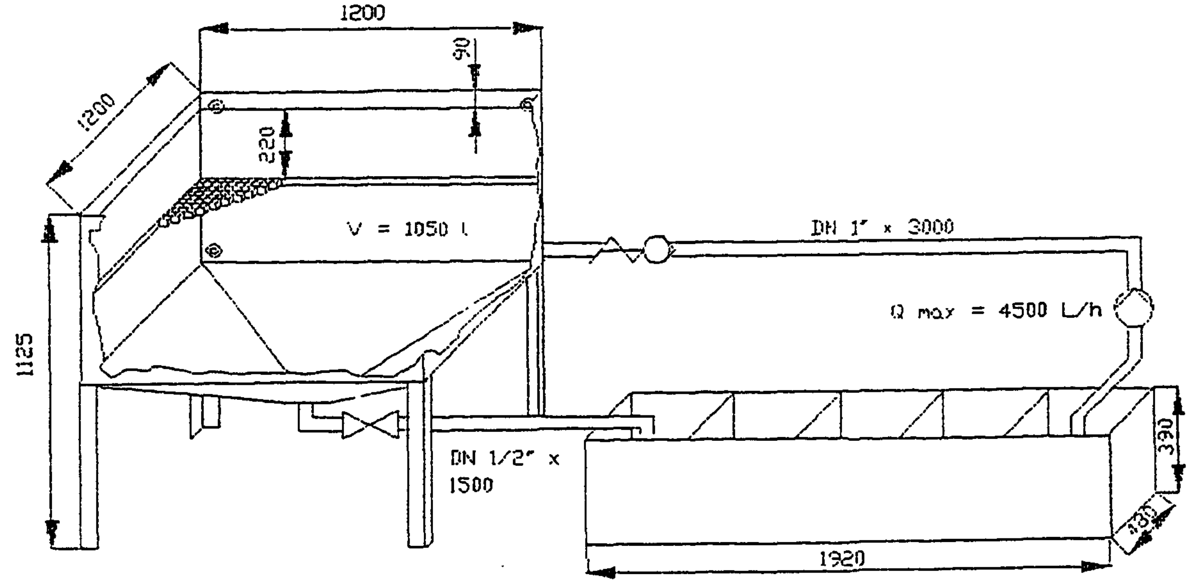

Figure 18 Water basin

For controlling the tool different measuring devices were installed (fig. 19).
The supervision of the state of the water jet nozzle can be realised by measuring the water flow rate passing the pressure pump (# 1)
To supervise the conditions of the abrasive transport tests were carried out to use sound analysis. For this purpose a hydrophone (bruel & kjaer 8103) was installed near the cutting head (# 2).
For the supervision of the state of the cutting head a system to measure the sucked-in air flow rate was adapted /4/ (# 3).
Additionally it has been tried to detect the pressure loss in a special part of the transport hose (hose length L_h) and to correlate this with the air flow rate (# 4).
For both measuring methods it has been tried to correlate the measuring results with the diameter of the focusing nozzle.

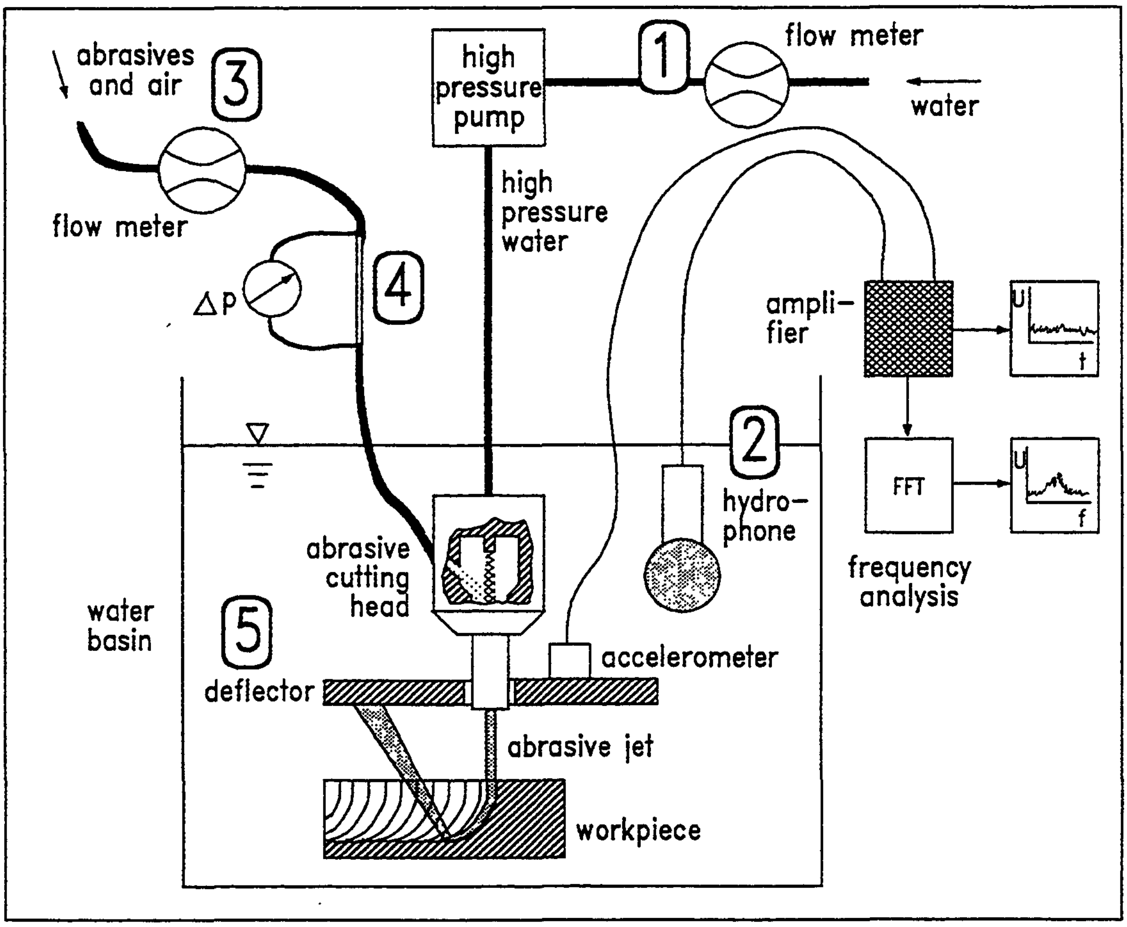
abrasives and air
3
flow meter
ΔP
4
high pressure pump
1
flow meter
water
high pressure water
ampli-fier
U
t
FFT
U
f
frequency analysis
2
hydro-phone
water basin
5
deflector
abrasive cutting head
accelerometer
abrasive jet
workpiece

Figure 19 Experimental setup

The hydrophone was used also for the detection of the cutting result (# 2). The frequencies of the sound pressure were analysed by Fourier-Transformation. Sound frequencies were measured for cutting through and kerfing a standard workpiece (austenitic steel).

In addition it has been tried to use the reflected abrasive water jet in case of kerfing the workpiece to detect this fact. On the cutting head a deflector with an accelerometer was installed (# 5) to measure signals produced by the deflected jet.

B.2.2. Tool control

The reliability of the cutting tool mostly depends on the conditions of the feeding (water and abrasives) and the state of the water jet nozzle and the focus.

The state of the water nozzle can be supervised by measuring the water flow rate. In case of broken nozzle plate or water hose leakage the flow rate will increase rapidly, in case of a clogged nozzle the flow rate decreases. The flow rate can be measured at the water inlet of the pump which means that the measurement system can be adapted at the low pressure side of the pump (pressure level of drinking water).

One possibility to supervise the conditions of the abrasive transport is measuring the sound pressure produced by the cutting head. Figure 20 shows the results of the sound measurements.

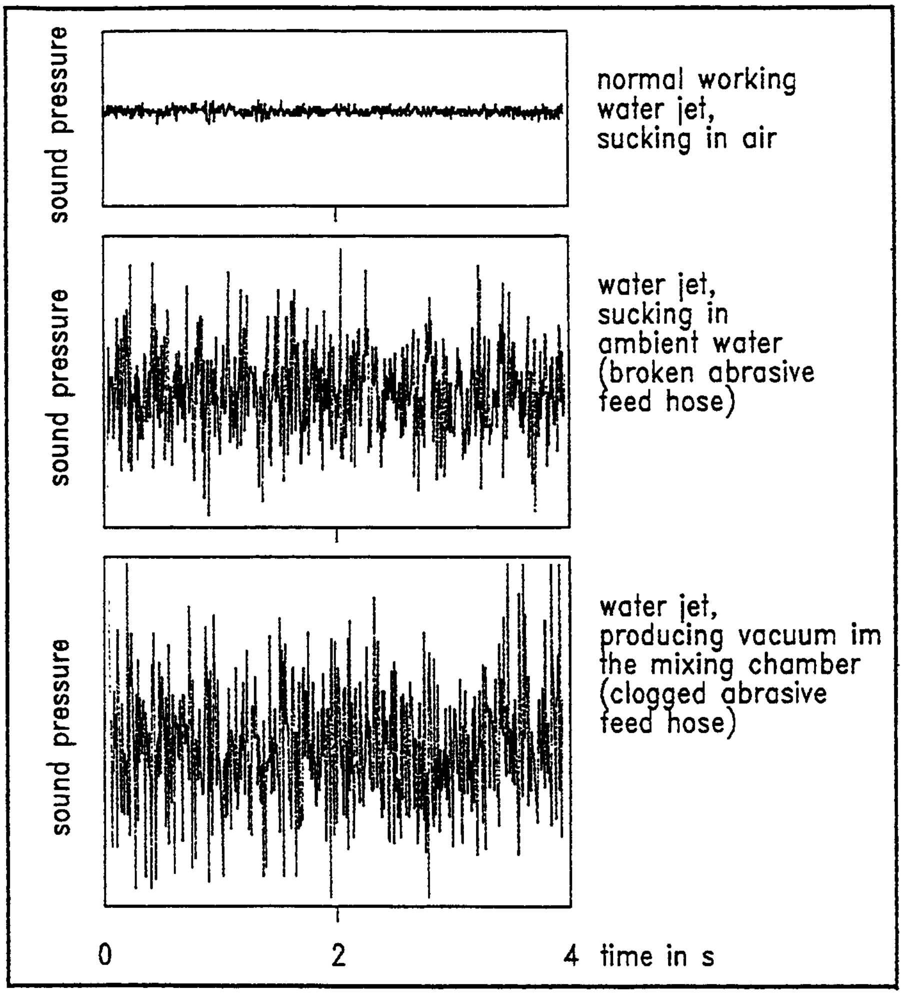

Figure 20 Control of the abrasive transport by sound analysis

For normal conditions (abrasives sucked in by air) the sound pressure is very low. In case of sucked-in water (broken transport hose) the sound level increases rapidly. Also when the transport hose is clogged (in that case the cutting head produces a vacuum) the sound level is very high because of cavitation effects.

The focusing nozzle can be controlled by measuring the flow rate of the sucked-in air. Figure 21 gives the results of some tests for different pressures.

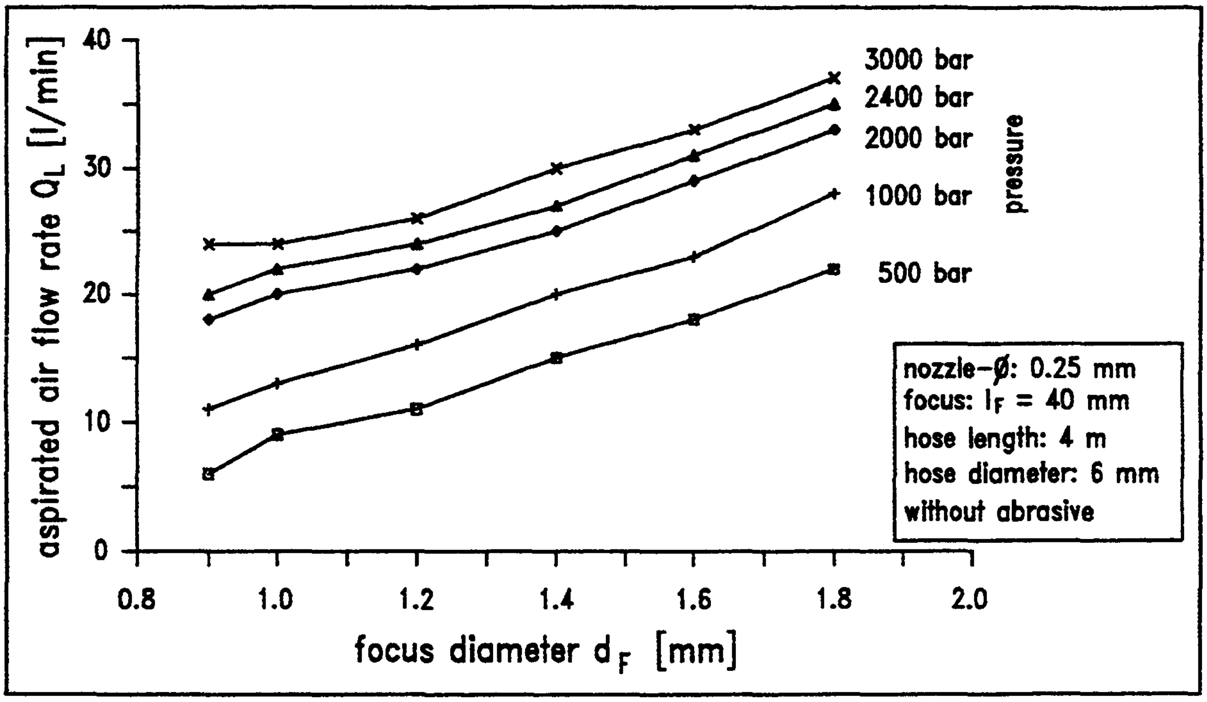

Figure 21 Effect of focus diameter on sucked-in air flow rate

The air flow rate is nearly linear with the diameter of the focusing nozzle for a constant diameter of the water jet nozzle. An increasing water pressure causes an increase in air flow.

For different nozzle diameter the results are given in figure 22.

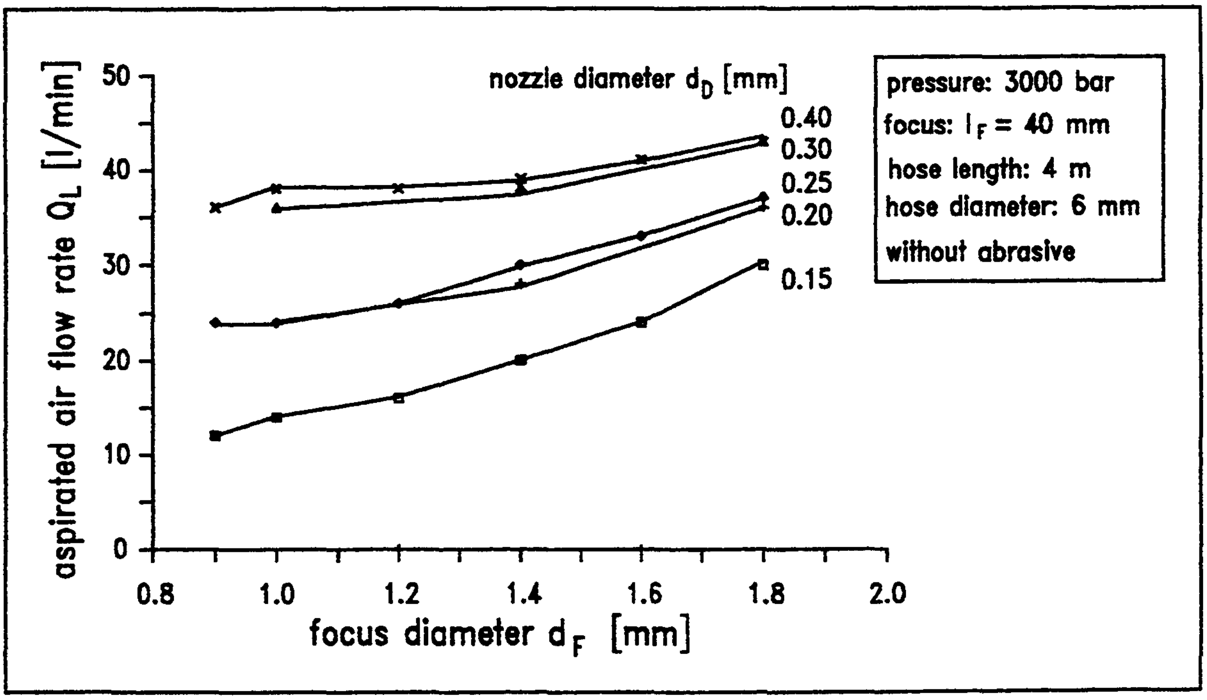

Figure 22 Effect of focus diameter on sucked-in air flow rate

Bigger water jet nozzles cause a higher air flow rate. The results of the nozzles 0.25 and 0.40 mm are not in the usual range of air flow, because for these tests nozzles with a changed inlet geometry were used. This changed geometry effects a better jet stability and so the efficiency of the water jet pump (abrasive cutting head) decreases.

All the tests were carried out without feeding abrasives into the air flow because of the prevention of wear of the measurement device and the focusing nozzle.

Figure 23 gives a comparison of results obtained with and without abrasives.

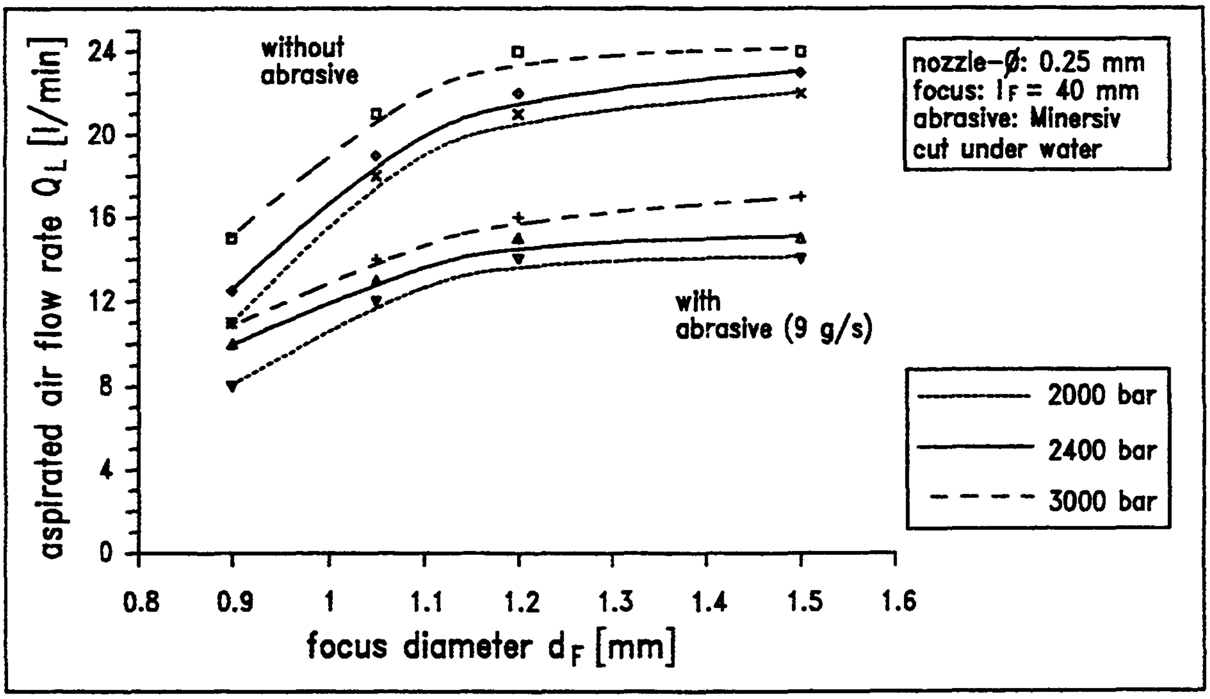

Figure 23 Effect of focus diameter on sucked-in air flow rate

Feeding abrasives into the air flow causes a decrease in flow rate due to friction and momentum loss. But the results show the same dependence of flow rate and focus diameter for both with and without abrasives.

As mentioned before the problem of measuring the flow rate during cutting is the flow of abrasives. To measure the flow rate of air two possibilities are practicable (fig. 24).

On one hand the flow rate has to be measured in the hose between abrasive feed mechanism and cutting head (1). In that case the abrasives pass the measurement device, too, and cause wear. On the other hand the abrasive feed unit has to be encapsulated to measure the ingoing air flow rate (2). Both methods are difficult to handle and not useful for practical application.

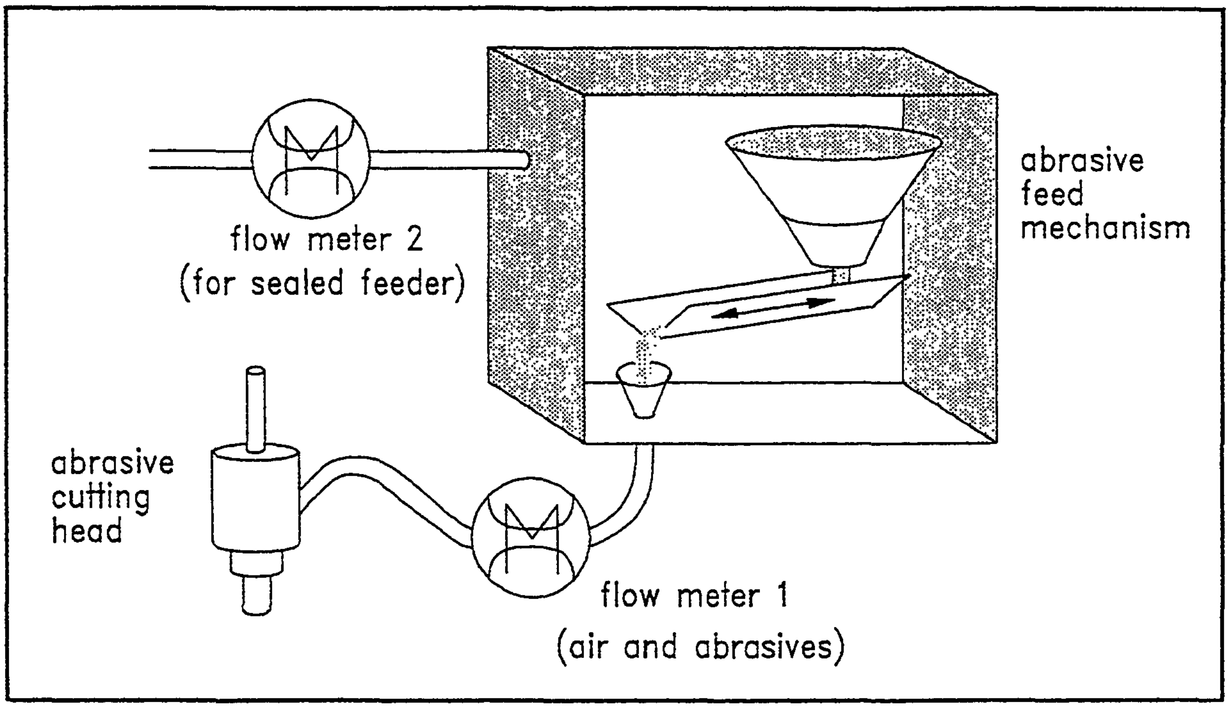

Figure 24 Methods for controlling the air flow rate

So, according to #4 in figure 19 the pressure drop in a specific length of the transport hose was measured.

The relation between this pressure difference ($p_1 - p_2$) and the air flow rate is as follows:

$$p_1 - p_2^2/p_1 = c * l * Q^2$$

p_1; p_2: pressure
c: constant
l: hose length
Q: air flow rate

Figure 25 gives the results of detailed tests for different nozzle diameters. The cutting parameters are the same as in figure 22.

An increasing nozzle diameter causes an increase in air flow rate and therefore an increase in pressure loss.

The pressure loss of the nozzles with a diameter of 0.25 and 0.40 mm again indicates a smaller air flow rate compared to the other nozzles.

Nevertheless, the pressure loss can be correlated with the focus diameter. For fixed cutting parameters like pressure, abrasive flow rate and water nozzle diameter it is necessary to prepare calibration curves at first with different focusing nozzles of known diameters. After this, the change in diameter during operation can be calculated from the measured pressure loss by using the calibration curves.

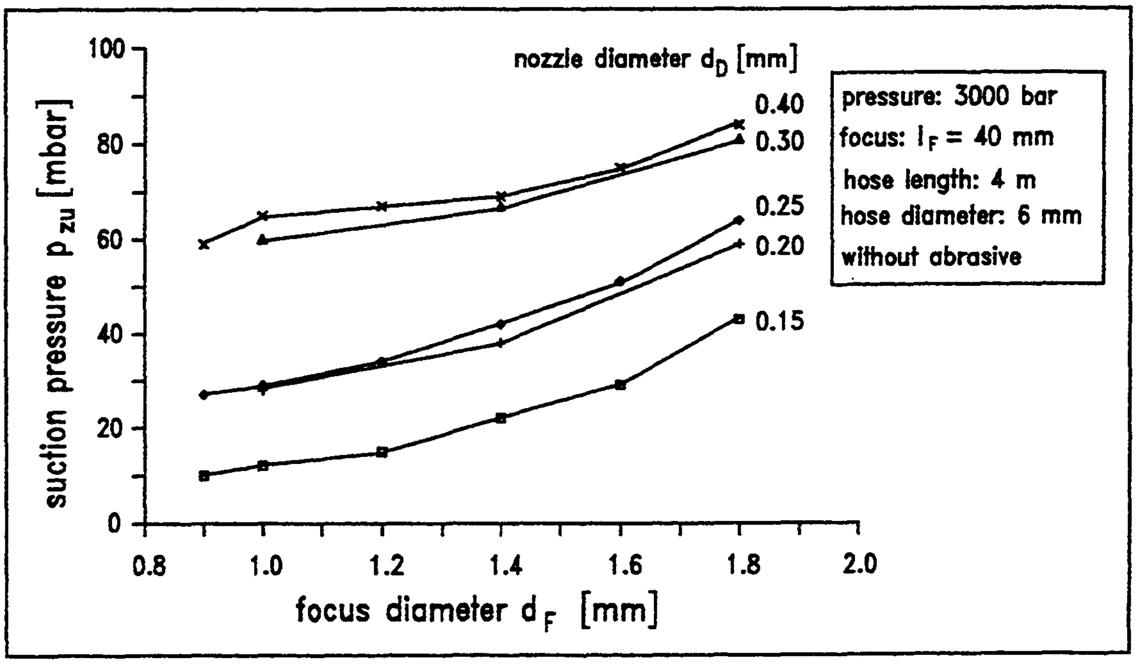

Figure 25 Effect of focus diameter on pressure loss

Additionally rapid changes of the pressure loss indicate irregular changes in tool behaviour. The reasons could be changes in the condition of transport, damages of the water jet nozzle or changes in alignment of water jet and focusing tube due to a collision with the workpiece. Measuring the air flow rate or, better, the pressure loss gives the opportunity to detect such defect.

B.2.3. Control of the cutting result

For remote controlled operation of the abrasive cutting process a special method is necessary to detect the cutting result. In case of using abrasive water jets optical and mechanical sensor systems are difficult to apply. Because of the suspended particles the optical conditions in the water are very bad, additionally optical parts and mechanical systems can be destroyed by reflected abrasives. The produced kerf is very small so there is no possibility to bring in sensor systems.

Additionally when cutting irregular structures (offshore structures with marine growth) all contacting sensor systems are not applicable because of the risk of sticking.

So the measurement of the sound pressure (according to #2 of fig. 19) seemed to be one useful method to detect the cutting result, because it is a non-contacting system which also is not sensitive against the particle load. To distinguish between cutting through and kerfing sound frequencies were analysed.

Figure 26 gives the typical analysis of cutting through.

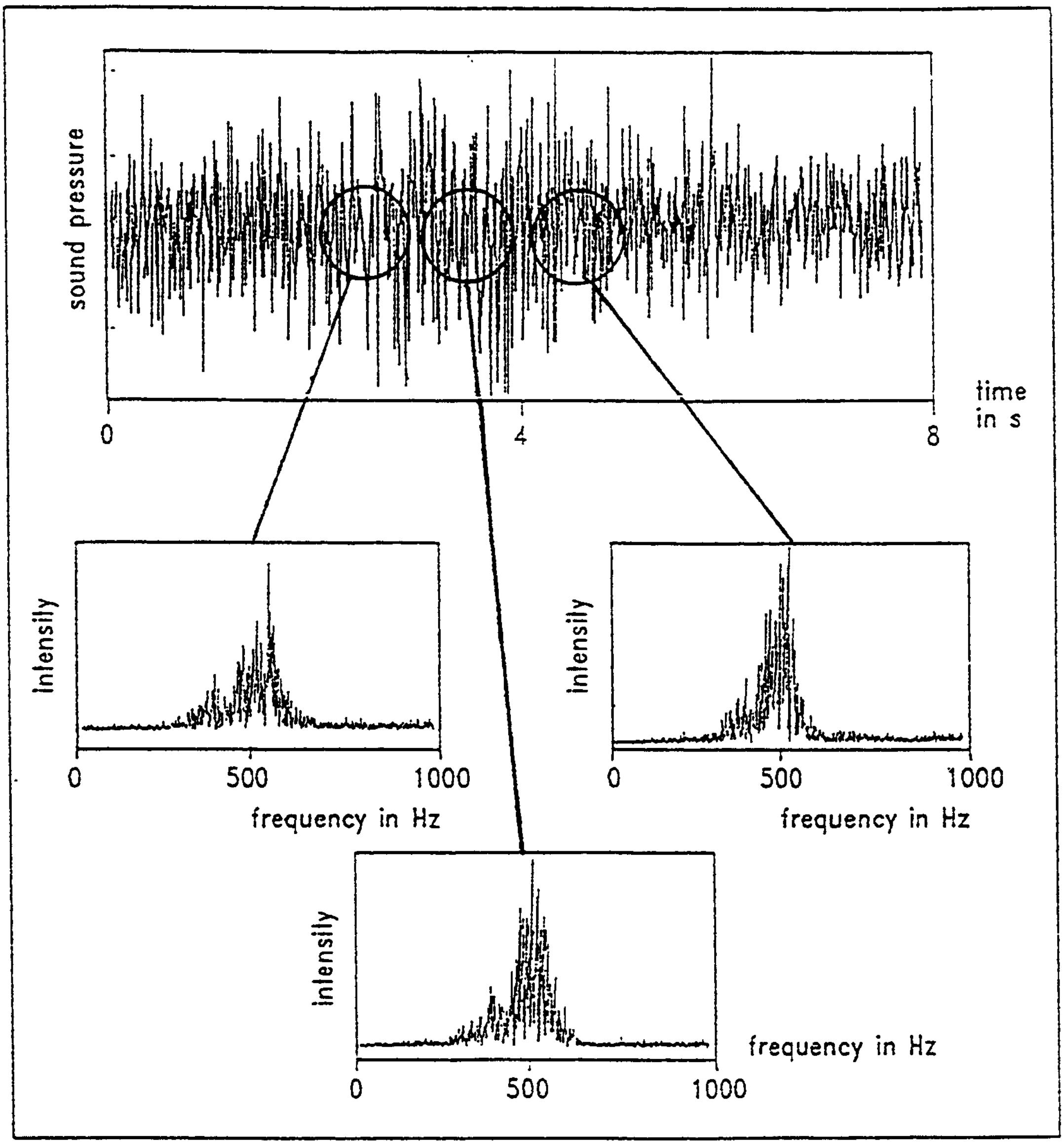

Figure 26 Sound analysis of cutting through

The upper part of the figure gives the sound intensity, the lower part gives the frequency analysis.

This analysis shows a significant maximum between 400 and 500 Hz. The signals were analysed up to frequencies of 1000 Hz. Higher levels show no significant intensity. The position of the hydrophone was fixed by carrying out different preliminary tests. The optimal position for a good sound pressure input seems to be quite close to the surface of the workpiece upside (close to the cutting head). The instrument should not be fixed in the reflection zone of particles but perpendicular to the feed direction of the cutting head. All tests were carried out with this measurement geometry.

Figure 27 gives the results for the kerfing tests. The magnification of the sound intensity signal (upper part of the figure) is the same as in figure 26.

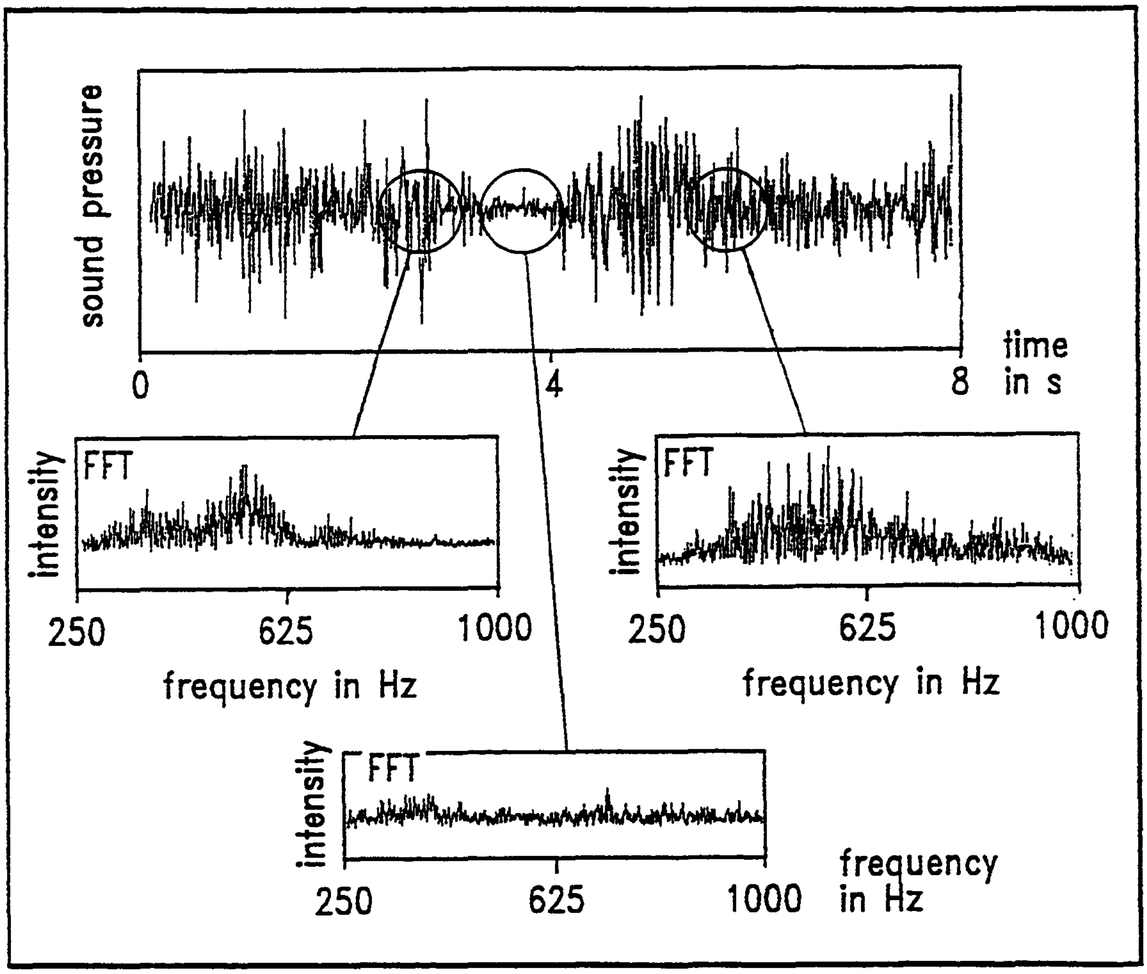

Figure 27 Sound analysis of kerfing

The measured value for the sound pressure in case of kerfing is not as constant as for cutting through. For this reason, also frequency analysis are different at different times.

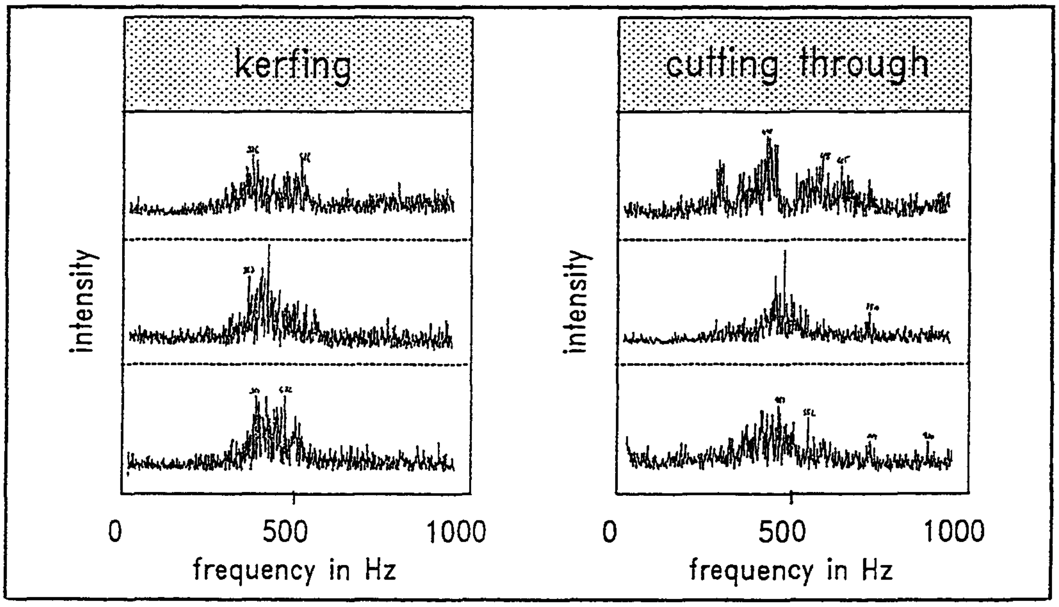

Figure 28 Frequency analysis for kerfing and cutting through

Unfortunately for a number of kerfing and cutting tests different results were obtained. Also cutting through causes different frequency maxima for constant cutting parameters. Figure 28 gives different frequency analysis of cutting through and kerfing. There is no significant difference to distinguish kerfing and cutting through.

All the tests were carried out on standard samples (size, material) under similar conditions (cutting parameters, position in the water basin). So, there should be no influence of these parameters on the results.
But, unfortunately, the **frequency** analysis does not seem to be a reliable method to detect the cutting result, because besides the results of figures 26 and 27 different analysis are occurring often, too. Up to now there isn't found out any reason for this scattering of the occurring frequencies.

Also differences in the sound **intensity** have not been reproducable. So they can't be used for the detection of the cutting result, either.
Finally, there are differences in the sound pressure signal for kerfing and cutting through (cutting through: constant intensity - kerfing: changing intensity like in fig. 27) but to use these differences for controlling the cutting result during cutting a specialised equipment is necessary.

For this reason another method to detect the case of kerfing has been tested /8/. A deflector plate was fixed at the cutting head (see #5 in fig. 19) and an accelerometer was adapted. During kerfing the reflected jet hits the plate and the accelerometer can detect the excitation of the plate. When cutting through there is no excitation of the plate.
During preliminary tests the optimal position and size of the plate was tested. It is necessary to take care about the wear of the deflector plate due to the reflected particles. On the other hand the measuring position has to be close enough to the kerf to receive signals which are significant for kerfing.
Especially for deep kerfing the reflected particles are slowed down by the friction at the shoulder of the cut. To reach a sufficient impact on the deflector plate the distance to the surface of the sample has to be 10 mm or less. Due to this small distance there is a high rate of wear on the plate for kerfing not as deep as mentioned.
Figure 29 gives the comparison of the signals for cutting through and kerfing.

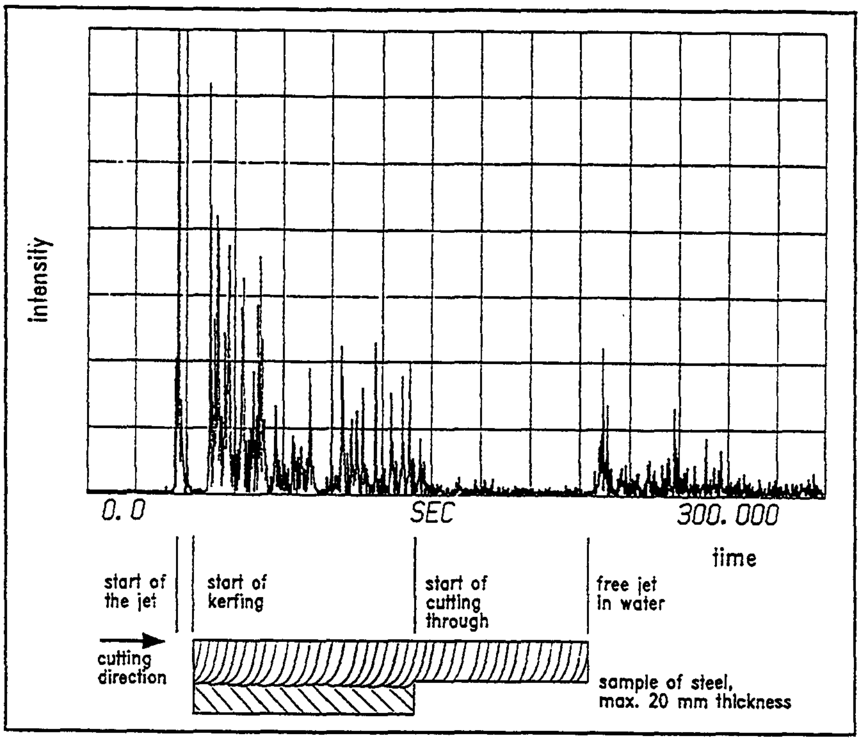

Figure 29 Signals for cutting through and kerfing, measured by deflector plate and accelerometer

The first peak is caused by opening the water jet valve. When kerfing there is a signal produced by the reflected particles (left side of the sample). In case of cutting through there is no excitation of the deflector. When the abrasive water jet runs in water without cutting bubbles hit the deflector (right side of fig. 29); when cutting through the workpiece it is like a shield - no bubbles can reach the deflector.
During a series of tests sometimes a time delay was measured regarding the signal when changing from kerfing to cutting through. This effect is caused by particles, which are reflected from the shoulder of the kerfed workpiece. Because of the track of striation the particles hit the part of the sample which was already cut (see fig. 30).

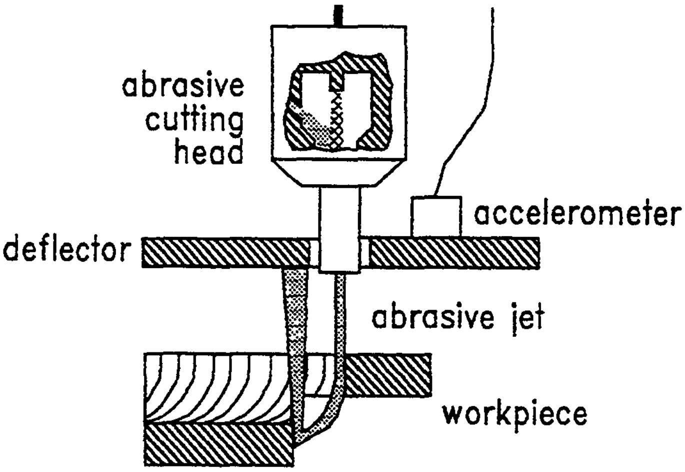

Figure 30 Reflection of particles in case of cutting through after kerfing

Changing from cutting to kerfing causes a significant signal in time. For normal application this is the more interesting situation because in cause of kerfing only the traverse speed has to be lowered immediately.

To make the method of detection more reliable it can be combined with a suction device as shown in figure 31.

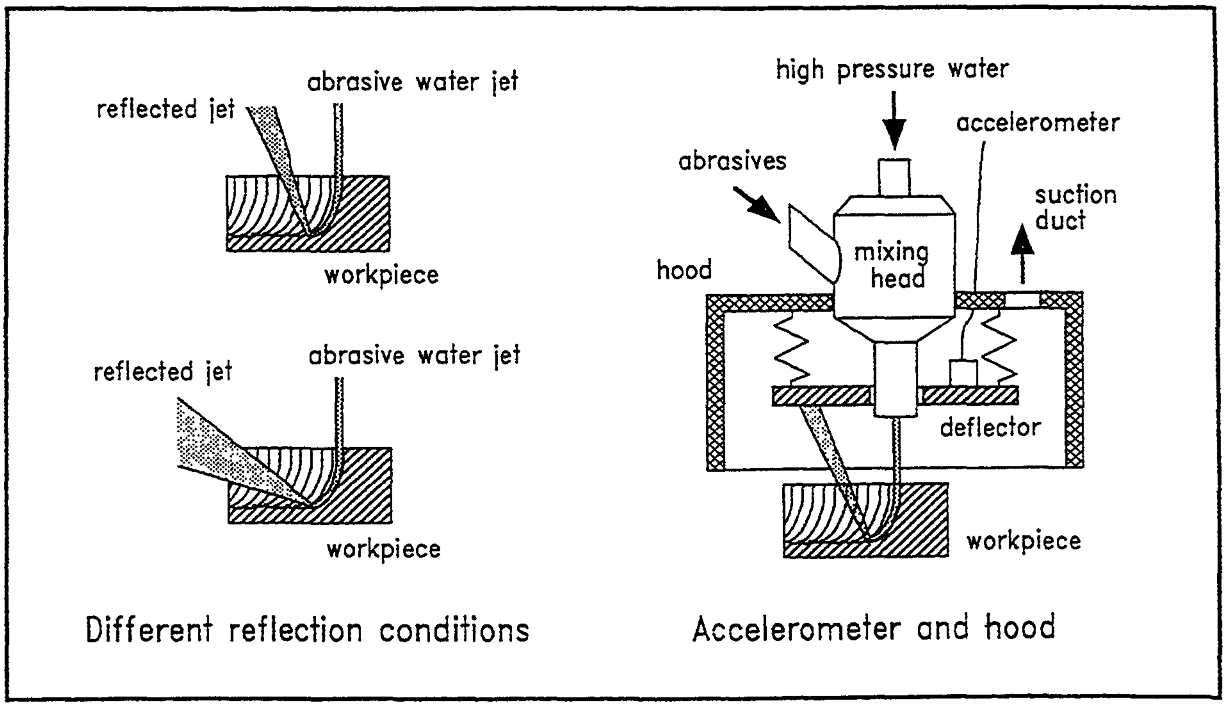
abrasive water jet
reflected jet
workpiece
reflected jet
abrasive water jet
workpiece
Different reflection conditions
high pressure water
accelerometer
abrasives
suction duct
mixing head
hood
deflector
workpiece
Accelerometer and hood

Figure 31 Deflector plate and suction hood

During kerfing the angle of reflection changes periodically due to the machining process. Also when producing very deep kerfs or very small kerfs the detection of the reflected particles is difficult because the friction between the reflected jet and the shoulder of the cut is quite high. So the kinetic energy of the particles reaching the deflector plate is low. This facts might cause problems in measuring the impact of the reflected particles by the deflector plate. In addition it seems to be useful to reduce the spreading of the secondary waste. To protect the environment from reflected particles a suction device can be used during kerfing. Inside of this device, as shown in figure 31, the deflector plate can be adapted.

Additionally the flow of water, air and abrasives, which is sucked away, can be controlled regarding the particle load of this flow. For cutting through the loading rate has to be very small because the particles pass the gap to the opposite side of the workpiece. For kerfing the particle loading will be increased as well as the amount of air in the flow, because the air as well as the particles are not able to move through the finished cut. For controlling purposes the amount of air or abrasives in the aspirated flow gives an information about kerfing or cutting through. Using an air separator to measure the

air or adapting a cyclone to separate the solid particles can give this additional information.
When cutting through often it is not possible to fix a suction device at the cutting head to move it during cutting on the backside of the workpiece to suck away the used abrasives. The reason is that in most cases the backside is not accessible or structures are too big to move a suction hood parallel. But when kerfing 90 % of the thickness of the workpiece during a first pass and cutting through the remnant with a much higher traverse rate in a second pass it can be a useful method to catch as much waste as possible.

Summing up only the analysis of changes of sound intensity during cutting resp. kerfing has the potential to be a method to control the cutting result when research work will be done in future.
Measuring the present intensity of the sound only or analysing the frequency of the sound signal are no sufficient methods for supervising the cutting process.

The method of using the reflected jet to excite an accelerometer gives sufficient results. It is possible to distinguish between cutting through and kerfing by measuring the intensity of the excitation of the plate. This measuring method is also non-contacting and easy to apply. The reliability of this technique can be increased by combining it with the detection of the air or particle amount in the flow sucked away by a special hood.

B.3. Methods to replace worn parts of the cutting head

When cutting large structures remote controlled under water it can be necessary to replace worn parts of the tool by handling systems. In case of abrasive water jet cutting mainly the focusing nozzle has to be changed.
The tool life for a normal tungsten carbide nozzle (as used as state of the art up to 1991) is about 5 - 10 hours, however these values depend on the chosen cutting parameters. But new developments in material science result in more resistant materials for these nozzles. Since 1991 a substitute of the Dow Chemical Company in USA sells focusing tubes out of composite carbides, which have a highly increased tool life /9/. Figure 32 gives the comparison of both kind of nozzles.
For the given parameters the tool life of composite carbide tubes is increased by the factor of more than 30. The prize of such nozzles is about 250 US-$.

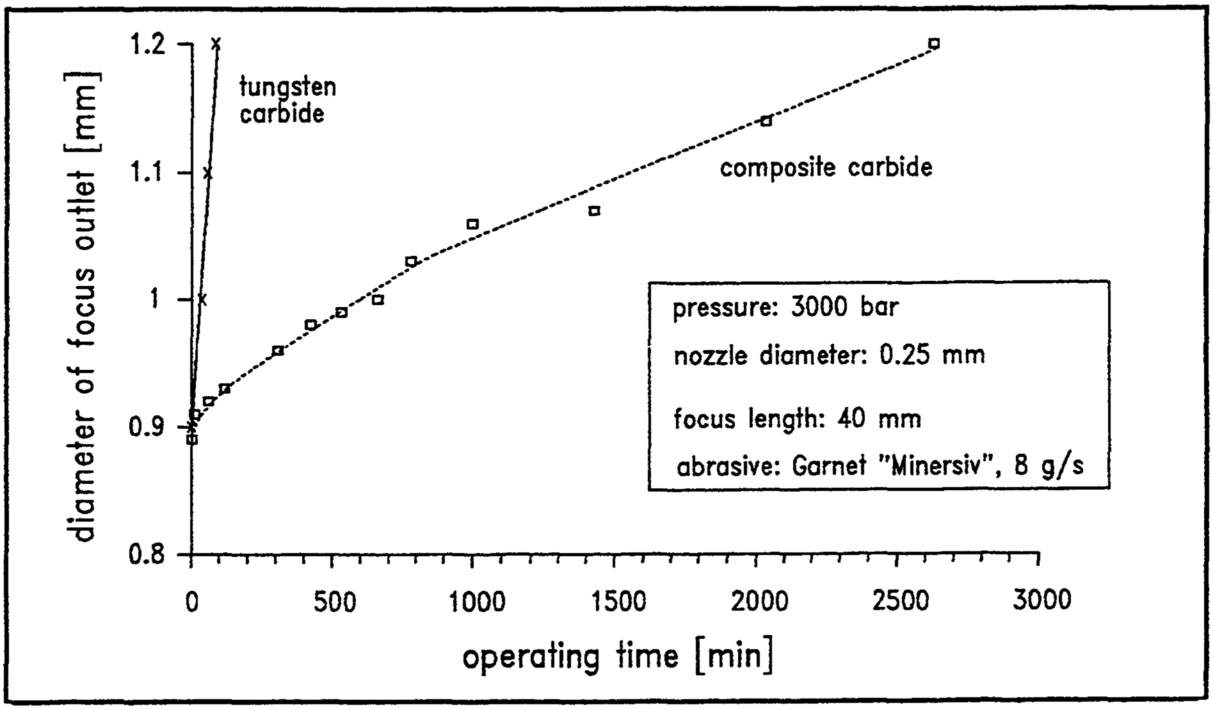

Figure 32 Wear rate of focusing nozzles

Figure 33 gives the influence of the diameter of the focusing nozzle on the attainable depth of cut.

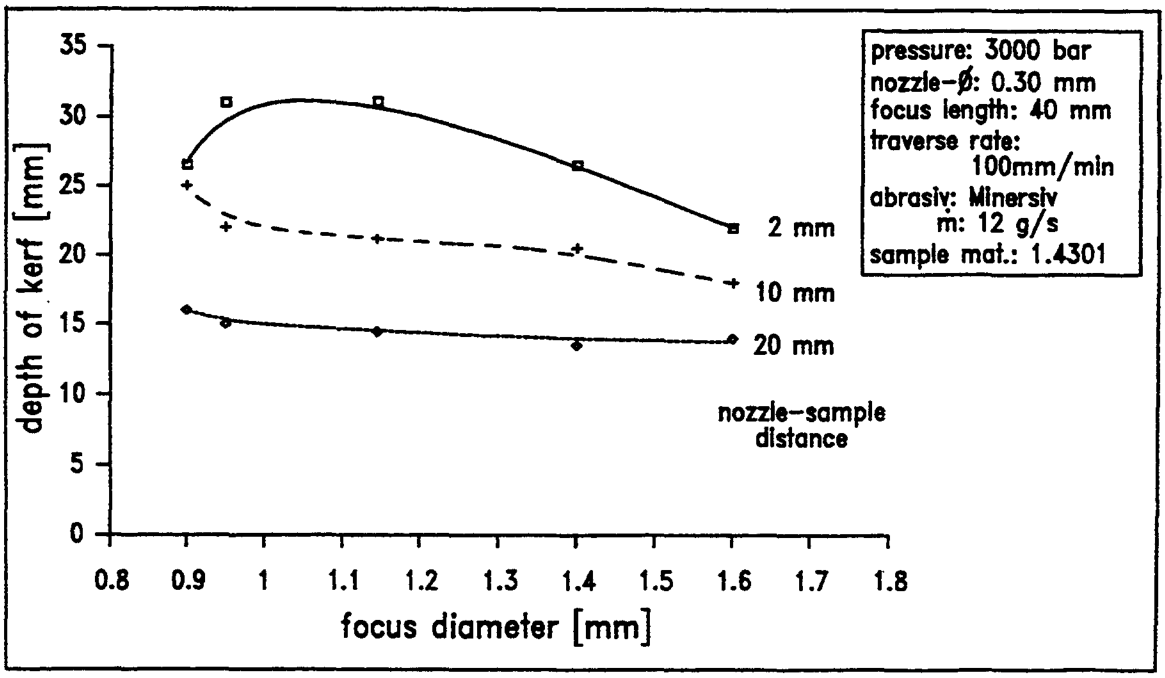

Figure 33 Effect of focus diameter on attainable depth of kerf

Defining a scattering range of 10 % of the maximal depth of kerf the focusing tube has to be changed when the diameter reaches about 1.4 mm. According to figure 31 this fact enables to cut up to 100 h without changing the focusing nozzle for the given conditions. Especially the kind of abrasive has an important effect on the wear rate. For corundum the tool life is less than 10 % of the tool life for garnet sand.

But for normal cutting jobs (steel, aluminium, concrete) the properties of garnet sand are a good compromise between wear of the tool and cutting efficiency.

So, for the given cutting conditions, the tool life of the focusing nozzle has reached the same level as the life time of the water jet nozzle. Due to this fact it does not seem to be useful to adapt a handling system, which is able to replace the focusing nozzle remote controlled. For maintenance work the whole tool (water nozzle, focusing tube, alignment, condition of the mixing chamber, status of the abrasive feed hose) has to be checked; for that purpose the tool has to be removed from the cutting job to a job shop anyway.

4. Characterisation and handling of secondary waste

To reduce the waste produced by cutting with abrasive water jets at first cutting parameters have to be optimised. This is done under B.1.

On the other hand for the treatment of the remaining waste it is necessary to quantify and analyse the sedimented waste as well as the aerosols. Results of doing so are given in the following.

B.4.1. Preparation of the test facility

To characterise the produced waste tests were carried out in cooperation of IW and CEA. In a hermetically sealed water basin steel and copper samples were cut and kerfed. Particles suspended in water as well as aerosols were measured and analysed. Figure 34 shows the setup of the test equipment.

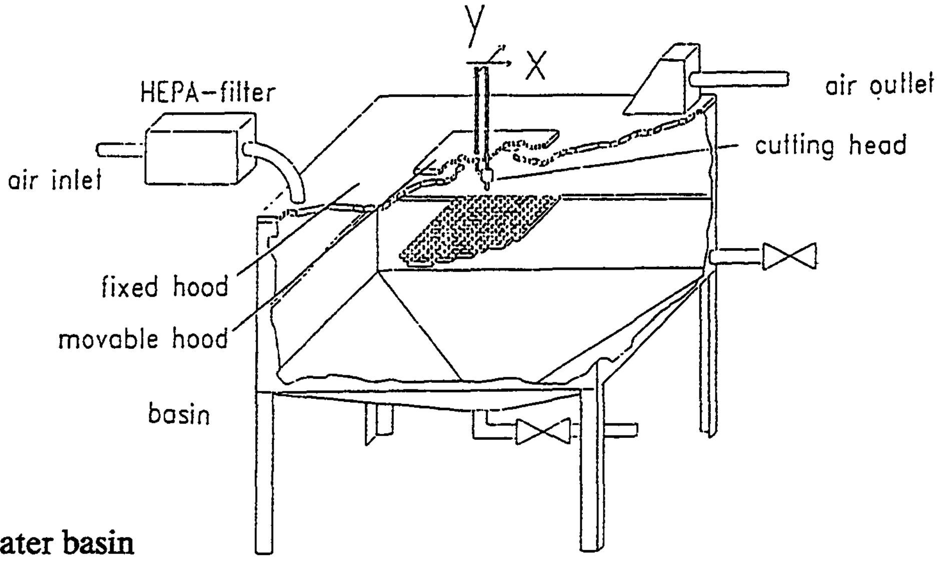

Figure 34 Water basin

The top of the basin was covered by a plate. The traverse mechanism of the cutting head was sealed against this plate. All the water used for cutting as well as the suspended particles remained in the basin. After settlement the sediments were removed and analysed. Water samples were taken to quantify suspended particles a certain time after finishing cutting.

The plates to be cut were either placed underwater (for cutting and kerfing underwater) or the water level is lowered to cut in air. However water is kept in the tank in order to absorb the water jet.
The experimental device with the associated samplings is schematised on the figure 35 (comparable to the tests described in /10/); a view of the exhaust duct with some samplings and the cutting basin is given in figure 36.

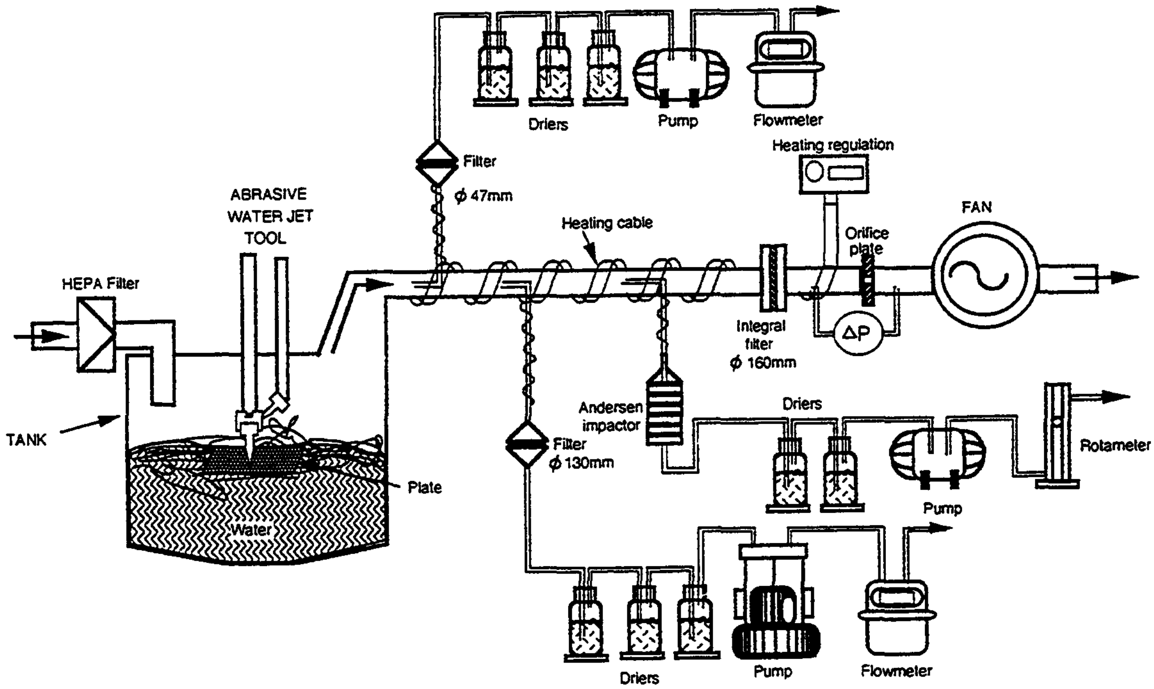
Driers
Pump
Flowmeter
Heating regulation
Filter
ϕ 47mm
ABRASIVE WATER JET TOOL
Heating cable
Orifice plate
FAN
HEPA Filter
ΔP
Integral filter
ϕ 160mm
TANK
Andersen impactor
Filter
ϕ 130mm
Driers
Rotameter
Pump
Plate
Water
Driers
Pump
Flowmeter

Figure 35 Schematic drawing of the ventilation system and the associated samplings

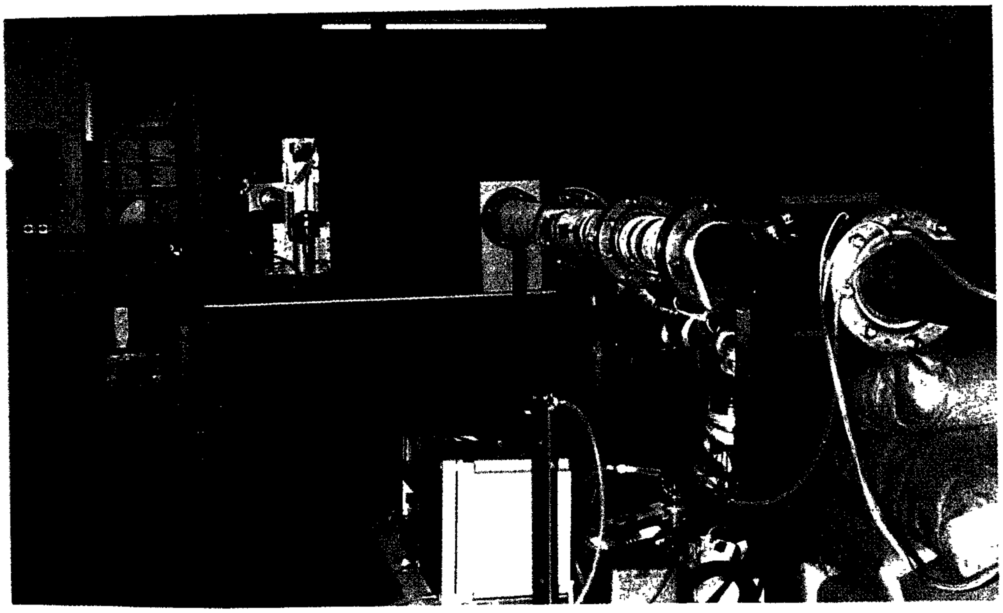

Figure 36 View on the exhaust duct with associated samplings (right) and the cutting basin with the water jet valve (left)

The ventilation circuit is composed of an inlet HEPA filter (in order to filtrate the air entering into the tank), an integral filter of 160 mm diameter (in order to collect all the aerosols drawn into the exhaust duct), an orifice plate (which has been calibrated and allows to know the flow rate) and a fan. The ventilation flow rate is set up to 24 $m^3.h^{-1}$.
Nozzles are installed in the exhaust duct to allow isokinetic sampling into:

- a filter of 130 mm diameter
- a filter of 47 mm diameter
- an Andersen impactor

Total aerosol mass concentrations are measured by filtration and weighing. The fibre glass filters are 130 mm and 47 mm in diameter. They have a collection efficiency of more than 99.99 % for particles of size superior to 0.3 micrometer.

The Andersen impactor in which the collection of particles is made on 8 stages allows to determine the aerosol size distribution between 0.35 and 15 micrometers.

The exhaust duct and the pipes until the sampling filters are heated with a regulated heating cable in order to avoid any condensation.

The three dryers put in series after the sampling filters enable to know the quantity of vapour water drawn into the exhaust duct. Dryers are also put between the impactor and the pump for its protection.

The sedimented drosses are collected manually at the bottom of the tank and their size distribution is determined with the use of several sieves which openings are respectively 0.032, 0.063, 0.125, 0.250 and 0.500 mm.

The mass concentration of particles remaining in suspension after a cut was measured by filtration and weighing. The samples of water (1 l) were taken 5 minutes after the end of cutting or kerfing.

When the cut took place under water, an hydrogen analyser was being used which sampled the air after the integral filter in the exhaust duct.

About 80 samples (suspended particles in water, abrasives, and mainly deposits on filters) have been analysed by ICP (Inert Coupled Plasma) in order to measure the proportion of several elements (Cu, Fe, Mg, Ni, Cr).

Figure 37 gives a diagram of the investigated masses and their abbreviations used in this report.

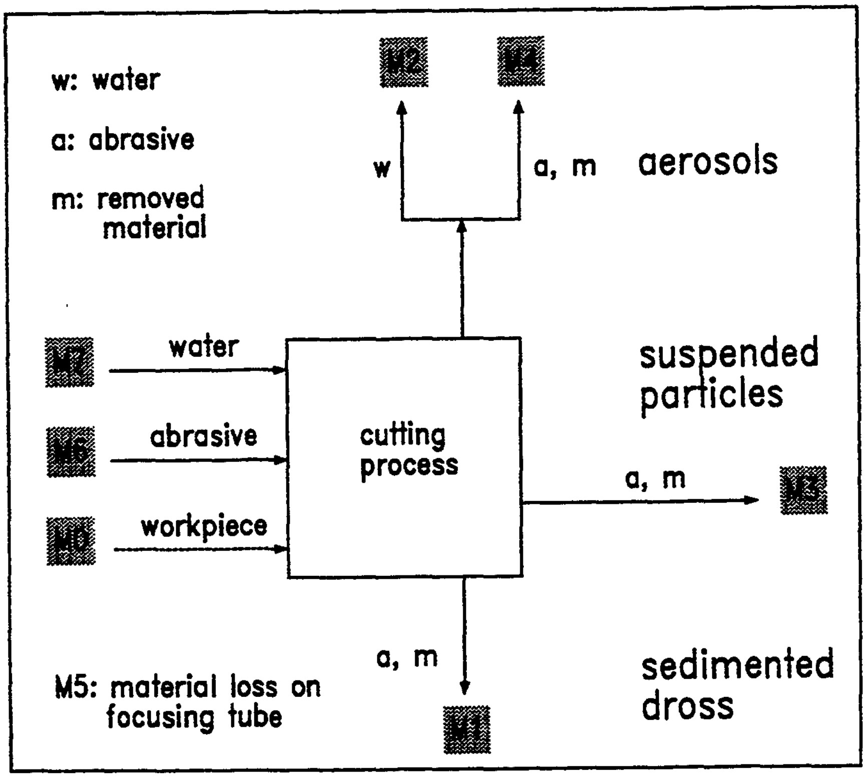
w: water
a: abrasive
m: removed material
M2
M4
w
a, m
aerosols
M7
water
M6
abrasive
M0
workpiece
cutting process
suspended particles
a, m
M3
a, m
M1
M5: material loss on focusing tube
sedimented dross

Figure 37 Diagram of material flow

The common operating conditions were as follows:

- volume of the tank:	1.140 m^3
- pressure of water:	3.000 bar
- nozzle:	0.25 mm
- focus diameter:	1 mm
length:	40 mm
- abrasive:	Garnet Minersiv
- size distribution of abrasive:	see figure 38
- water flow rate:	1.63 l/min

- standoff distance: 2 mm
- air ventilation flow rate: 24 m^3/h
- air flow rate cutting head: 2 m^3/h

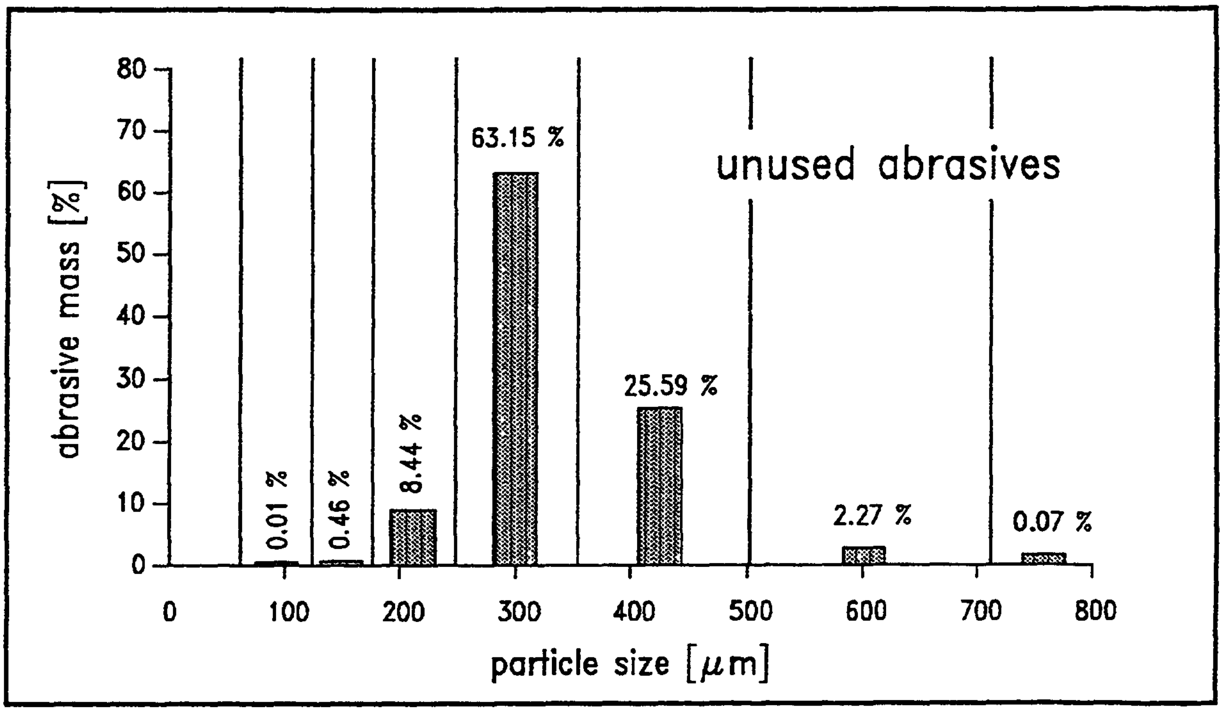

Figure 38 Size distribution of unused Garnet "Minersiv"

The used copper plates were out of Cu 99.9 %; the steel and abrasive compositions are indicated in the tables I to II.

Duplex steel: 60 % ferritic, 40 % austenitic

	C	Si	Mn	P	S	Cr	Mo	Ni	N	Fe
min (%)	-	-	-	-	-	21.0	2.5	4.5	0.08	63.7
max (%)	0.03	1.0	2.0	0.03	0.02	23.0	3.5	6.5	0.20	72.0

Table I Steel composition

Composition of abrasives (Garnet)

Al_2O_3	20 %
FeO	30 %
SiO_2	36 %
MnO	1 %
CaO	2 %
MgO	6 %

Table II Composition of abrasive garnet "Minersiv"

Copper was chosen as material to be cut in order to distinguish by chemical analyses the secondary emissions coming from the cut plate on one part and from the abrasives on the other part (Garnet contains an important proportion of FeO).
The duplex (austenitic/ferritic) steel was chosen to find cut material by magnetism.

B.4.2. Measurement and characterisation of the secondary emissions

Eight experiments were carried out in a first series as indicated in table III.

No. of experiment	Operation	Place	Material nature	Material thickness (mm)	Abrasive flow rate (g/s)
1	cutting	underwater	copper	10	7.2
2	cutting	air	copper	10	6.8
3	cutting	air	steel	10	6.8
5	kerfing	air	copper	20	6.3
6/7	kerfing	underwater	copper	20	5.9
8	kerfing	air	steel	20	7.1
9	cutting	air	copper	10	3.4
10	cutting	air	copper	10	1.8

Table III Main features of the experiments

The total secondary emissions were evaluated for all the experiments (see fig. 37). The sedimentation times were very different, so suspended particles for some experiments had no time to sediment. The sedimented dross on the walls and on the bottom of the tank were collected after 16 hours (a night) for the experiments No. 1 and No. 2.
The sedimentation behaviour for test No. 1 is shown in B.4.4 together with other results (fig. 53).

The thickness of the plates of copper and steel was 10 mm for cutting and the depth of kerfing was 15-18 mm (experiments No. 5 and No. 6/7) and 17-19 mm (experiment No. 8).

A) Balance of secondary emissions

Solid emissions

The results of weight analyses are given in table IV.

Cut No.	Material thickness	Operation place	Cut length mm	Workpiece mass loss $g.m^{-1}$	Used abrasive $g.m^{-1}$	Sedimented dross		Suspended particles		Aerosols		Used water $g.m^{-1}$	Water in exhaust duct		Aerosols
						$g.m^{-1}$	% TC	$g.m^{-1}$	% TC	$g.m^{-1}$	% TC		$g.m^{-1}$	% of used water	$g.m^{-2}$ of cut edge
1	copper 10 mm	cutting underwater	6 528	99.6	3 074.4	3 003.5	97.5	77	2.4	$1.2\ 10^{-4}$	$3.6\ 10^{-6}$	11 688	4.7	0.04	$1.2\ 10^{-2}$
2	copper 10 mm	cutting in air	6 528	110.1	2 914	2 819.2		-		0.027	$9.7\ 10^{-4}$	11 688	19.5	0.17	2.7
3	steel 10 mm	cutting in air	3 672	80.3	3 704	3 464.9		-		0.035	$9.8\ 10^{-4}$	14 788	23.6	0.16	3.5
5	copper 20 mm	kerfing in air	3 672	158.5	2 693	2 674.6		-		0.136	$5\ 10^{-3}$	11 683	194.9	1.7	8.2
6/7	copper 20 mm	kerfing underwater	6 533	152.9	2 532	2 324	98.7	31.5	1.3	$7\ 10^{-4}$	3.10^{-5}	11 679	5.5	0.05	$4.2\ 10^{-2}$
8	steel 20 mm	kerfing in air	3 672	143.5	3 860	3 196.3		-		0.211	$6.5\ 10^{-3}$	14 788	268	1.8	11.7
9	copper 10 mm	cutting in air	6 528	100.3	1 862	1 419.1		-		0.0165	$1.1\ 10^{-3}$	14 813	40.4	0.27	1.65
10	copper 10 mm	cutting in air	6 528	98.0	1 534	1 515.5		-		0.0136	$8.8\ 10^{-4}$	23 284	71.1	0.30	1.36

TC = total solid mass collected

Table IV Recapitulative secondary emissions results

For the given working conditions following results can be given:

- 4.10^{-6}% to 7.10^{-3}% of the total solid mass is drawn into the exhaust duct (M4).
- When the cutting or the kerfing takes place underwater (depth = 100 to 200 mm), the quantity of aerosols is divided by about 200 (comparison between experiments No. 1 and 2 and experiments 5 and 6/7).
- The amount of aerosols increase linearly with the amount of used abrasives (fig. 39).

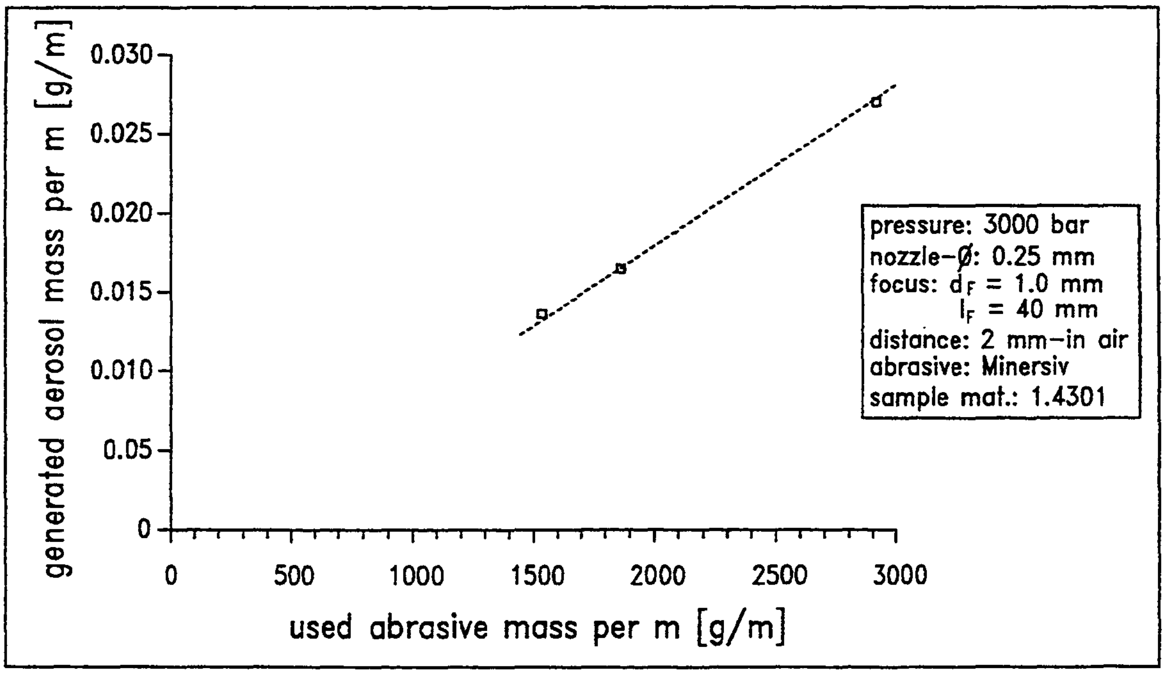

Figure 39 Effect of amount of used abrasives on the production of aerosols

- The kerfing produces three to four times more aerosols than the cutting as indicated in the table V.

	Aerosols g/m^2 of cut edge	Aerosols $g/m^2/kg$ of used abrasives per meter	$\frac{\text{Aerosols by kerfing}}{\text{Aerosols by cutting}}$
Copper kerfing underwater	$4.2\ 10^{-2}$	$1.7\ 10^{-2}$	4.3
Copper cutting underwater	$1.2\ 10^{-2}$	$0.39\ 10^{-2}$	
Copper kerfing in air	8.2	3.0	3.2
Copper cutting in air	2.7	0.93	
Steel kerfing in air	11.7	3.0	3.2
Steel cutting in air	3.5	0.94	

Table V Comparison of aerosol production by kerfing and cutting

There is no significant difference between copper and steel.
The water placed beneath the plate when the cutting takes place in air probably minimises the amount of aerosols.

- 1 to 3 % of the total solid mass is composed by suspended particles (M3) when the operation takes place under water.
  The kerfing induces less suspended particles (754 $g/(m^2*kg/m)$ - mass of suspended particles per m^2 of shoulder of the cut and per kg of used abrasive per meter) than the cutting (2505 $g/(m^2*kg/m)$).

By chemical analyses of the water of experiments No. 2 and No. 6/7 (annex 3) it can be noted:

- taking into account the composition of the abrasives there is a good agreement between the chemical results and the mass M3 of suspended particles indicated in the sheets of annex 1 (within 13 %),
- the proportion of copper and abrasives in solution in the sampling bottles three months after the experiments is in the range 1 to 3 % for copper, inferior to 0.1 % for particles of abrasives,
- the ratio of

$$\frac{\text{mass of particles of copper}}{\text{mass of particles of abrasives + mass of particles of copper}}$$

in the suspended particles five minutes after the cut is comprised between 7 and 9 %.

This seems to indicate that the particles of copper suspended in the water after an operation underwater (kerfing and cutting) have a smaller diameter than the particles of abrasives because the ratio mentioned above is higher than the same ratio in sedimented dross (3 to 5.7 %) for the two concerned experiments, and this whereas the density of copper is higher than the density of abrasives. The sedimentation of copper needs more time.

- The remainder of the solid emissions is composed by dross sedimented in the tank (M1).

  The proportion of abrasives in the sedimented dross is dependent on the type of operation (cutting or kerfing), the nature of the material and of course the flow rate of abrasives as indicated in the table VI. As sedimented dross represents almost all the solid secondary emissions especially when the operation takes place under water, the ratio

  $$\frac{\text{used abrasives}}{\text{used abrasives + workpiece mass loss}}$$

  can be considered coarsely as a representative of the proportion of abrasives in the sedimented dross.

Cut No.	Material	Operation place	Abrasive flow rate g/s	% of abrasives in the sedimented dross
1	copper	cutting underwater	7.2	97.0
2	copper	cutting in air	6.8	96.4
3	steel	cutting in air	6.8	97.9
5	copper	kerfing air	6.3	94.4
6/7	copper	kerfing underwater	5.9	94.3
8	steel	kerfing in air	7.1	96.4
9	copper	cutting in air	3.4	94.9
10	copper	cutting in air	1.8	94.0

Table VI   Proportion of abrasives in the sedimented dross

The proportion of abrasives in the sedimented dross increases for cutting (compared to kerfing), for steel (compared to copper) and there is no difference for operation in air or under water.

Liquid emissions (vapours)

Between 0.15 to 2 % of the used mass of water is drawn into the exhaust duct (M2), mainly in the vapour phase.
The kerfing induces 10 times more water in the exhaust duct than the cutting in air.
Underwater operation decreases the amount of water in the exhaust duct compared to operation in air (divided by 4 for cutting and 35 for kerfing).

B) Size distribution of abrasives and sedimented dross

The size distributions of abrasives are illustrated by the figures 40 to 43.

The analysed samples are a mixture of samples taken at different places in the basin. According to the location of sampling a wide spread of results regarding the size distribution occurs.
Figures 40 and 41 give the comparison of cutting and kerfing for application in air (right) and under water (left).

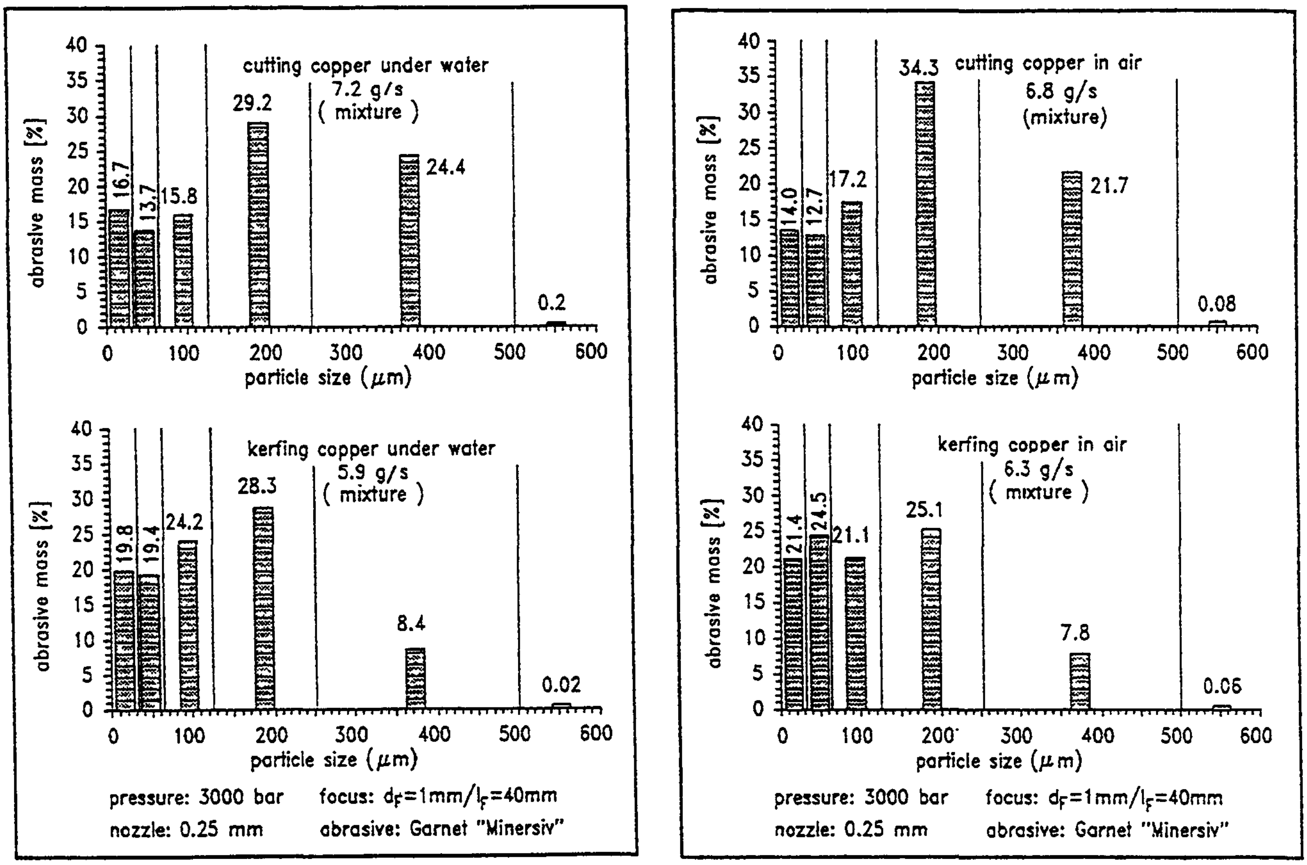
cutting copper under water 7.2 g/s (mixture)

kerfing copper under water 5.9 g/s (mixture)

cutting copper in air 6.8 g/s (mixture)

kerfing copper in air 6.3 g/s (mixture)

pressure: 3000 bar focus: d_F=1mm/l_F=40mm
nozzle: 0.25 mm abrasive: Garnet "Minersiv"

pressure: 3000 bar focus: d_F=1mm/l_F=40mm
nozzle: 0.25 mm abrasive: Garnet "Minersiv"

Figure 40, 41 Size distribution of used abrasives

Kerfing produces a bigger amount of smaller particles than cutting through. This effect is the same for machining steel as well as copper.

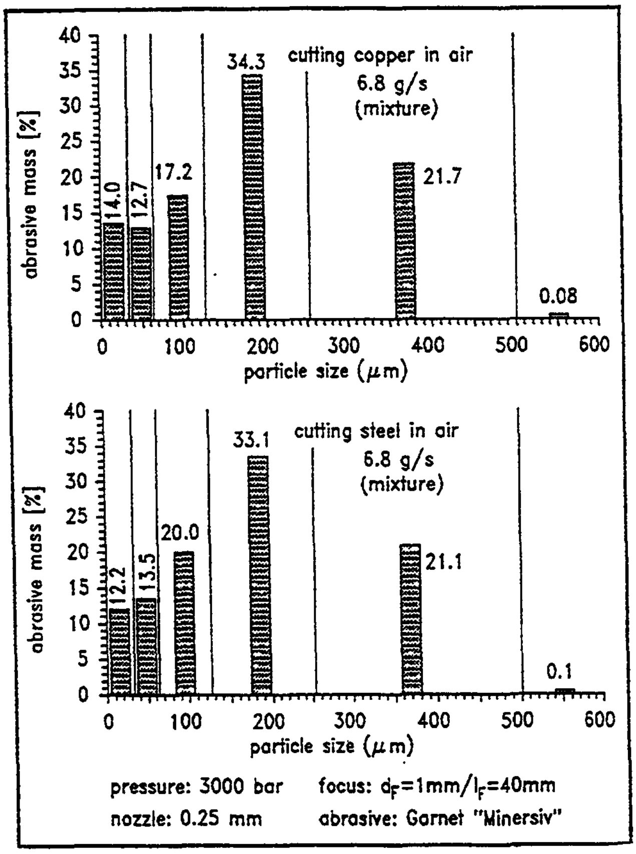

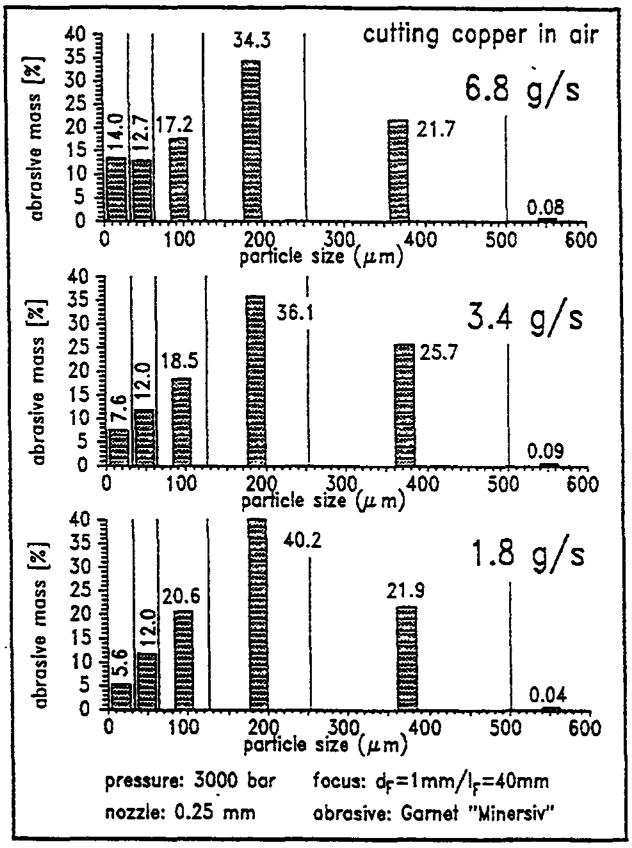

Figures 42, 43 Size distribution of used abrasives

Figure 42 shows that there is no big difference between machining copper and steel. For both materials nearly the same size distribution is given for cutting in air.

Using different abrasive flow rates (figure 43) has nearly no influence on the size distribution of the used abrasives. For lower abrasive flow rates the mass mean diameter is a little bit bigger than for higher flow rates.

As indicated in table VII, the mass mean diameter (see next page) of the abrasives which value is between 250 and 350 µm when unused, becomes comprised between 125 and 250 µm after cutting and between 65-125 µm after kerfing. For some experiments samples were taken in the bottom of the tank and on the top (along the walls of the tank) and obviously the mass mean diameter is bigger for the bottom samples.

No.	Material	Operation	Abr. flow rate (g/s)	Mass median diam. (μm)	% of abr. < 250 μm
1	copper	cut u. w.	7.2	171	75.4
2	copper	cut air	6.8	170	78.2
3	steel	cut air	6.8	166/169	80.8
5	copper	kerf air	6.3	111	91.5
6/7	copper	kerf u. w.	5.9	120	90.4
8	steel	kerf air	7.1	108/122	94.7
9	copper	cut air	3.4	189	74.3/87.8
10	copper	cut air	1.8	184	77.7
-	new abrasive			330	8.9

Table VII   Particle disintegration

The resulting mass median diameter is calculated according to the method of momentum. Using the percentage in each particle range (C_i) the average particle size can be calculated according to the mechanical momentum. For each particle range the product (momentum) of the mean particle size (x_i - lever-arm) and the corresponding percentage (C_i - power) is calculated. The sum of these values divided by 100 results in a particle size (d_{Mo} - replacement lever-arm) where 100% (replacement power) had to be placed to balance the corresponding distribution.

$$d_{Mo} = \frac{\sum_{i=1}^{n} x_i * C_i}{100}$$

Considering the particles of abrasive inferior to 250 μm (table VII), it can be said that more than 66 % of the total particles are broken during cutting and more than 80 % during kerfing.

Abrasives were more easily broken from kerfing than from cutting.

Kerfing steel and copper seems to break the abrasives into the same size.

There is no significant difference between underwater operation and operation in air for the size distribution of sedimented dross (table VII and figures 40 and 41).

When the flow rate of abrasives is decreasing, the proportion of the smaller particles of sedimented dross (<32 μm) appears to decrease (figure 43); this unexpected result could be explained by a smaller friction in the focusing nozzle and highlight that a non negligible proportion of abrasives is broken before reaching the plate when the flow rate of abrasives is high.

C. Characterisation of the aerosols in the exhaust duct

The concentration of aerosols in the exhaust duct has varied from 0.04 mg/m^3 to 58.7 mg/m^3 depending on the place of operation (under water or in air), on the nature of operation (cutting of kerfing) and on the abrasive flow rate of abrasives (1.8 to 7.2 g/s). By calculating the aerosol material mass and the total aerosol mass (aerosol material mass + aerosol abrasive mass) from the chemical analyses (annex 2) or by calculating the aerosol material mass and by taking the total aerosol mass from the weighing of sampling filters (sheets of annex 1), the ratio can be estimated as

$$\frac{\text{aerosol material mass loss}}{\text{total aerosol mass}}$$

The value of this ratio is roughly the same as the value of the ratio

$$\frac{\text{material mass loss}}{\text{used abrasives + material mass loss}}$$

Cut No.	Material	Operation place	$\frac{\text{aerosol material mass}}{\text{total aerosol mass}}$ (in %)	$\frac{\text{material mass loss}}{\text{used abrasives + material mass loss}}$ (in %)
1	copper	cutting underwater	0.7 - 9.9	3.1
2	copper	cutting in air	4.0 - 4.8	3.6
3	steel	cutting in air	1.4 - 2.1	2.1
5	copper	kerfing air	5.0 - 10.0	5.6
6/7	copper	kerfing underwater	4.4 - 5.6	5.7
8	steel	kerfing in air	4.3 - 4.8	3.6
9	copper	cutting in air	3.2 - 4.8	5.1
10	copper	cutting in air	3.1 - 5.3	6.0

Table VIII Aerosol calculation

Considering the very small masses collected on each stage of the impactor Andersen during the underwater operations (experiments No. 1 and 6/7), the size distribution

cannot be determined without a big uncertainty, even versus a chemical element.
To characterise the size distribution of the aerosols, the mass mean aerodynamic diameter (MMAD) is used. The real diameter can be calculated from the MMAD by dividing by the square root of the density of the particles

$$d_{real} = \mathrm{MMAD} * \delta^{-0.5}$$

The MMAD is 4 μm (geometric standard deviation = 2.9) for the particles produced by cutting copper or steel in air (figures 1 and 2 of annex 3), the MMAD becomes equal to 6 μm (geometric standard deviation = 2.36) for kerfing copper or steel (figures 3 and 4 of annex 3).

The sheets in annex 3 give dM/M.dlogD. That means

$$\frac{\text{dM (mass in particle size class)}}{\text{M(total mass)} * (\log D_{upper} - \log D_{lower})}$$

Cut n°	Material	Operation place	Abrasive flow rate g/s	Reference	Mass median aerodynamic diameter. 10^{-6} m	Geometric standard deviation
1	copper	cutting underwater	7.2	weight Cu, Fe	ND ND	
2	copper	cutting in air	6.8	weight Cu	4.02 4.93	2.87 3.00
3	steel	cutting in air	6.8	weight Fe	3.99 2.60	2.95 3.21
5	copper	kerfing in air	6.3	weight	6.31	2.36
6/7	copper	kerfing underwater	5.9	weight Cu, Fe	ND ND	
8	steel	kerfing in air	7.1	weight Fe Cr Ni	6.25 6.25 7.16 5.59	2.36 2.47 2.10 3.58
9	copper	cutting in air	3.4	weight	NA	
10	copper	cutting in air	1.8	weight Cu	NA NA	

ND : not determined
NA : not applicable (the size distributions are bimodal)

Table IX Aerosol size

The size distribution becomes more and more bimodal when the flow rate of abrasives decreases (figures 5 and 6 of annex 3) with one mode around 6 μm and another around 1.5 μm. The aerosol size distributions obtained from weight and from chemical analyses (figures 7 to 12) are relatively similar.

The mass mean aerodynamic diameter based on weight and on chemical elements (Cu for the plates of copper, Fe, Cr and Ni for the steel plates) have similar values (table IX).

D) Gas

During the operations under water we have used the hydrogen analyser. There is no discernible production of hydrogen (< 0.05 l.min^{-1}).

E) Kerf appearance

The bottom and top widths of the kerfs are resumed in the table X.

Cut No.	Material	Operation place	Abrasive flow rate g/s	Bottom kerf width mm	Top kerf width mm
1	copper	cutting underwater	7.2	0.9	1.2
2	copper	cutting in air	6.8	1.0	1.3
3	steel	cutting in air	6.8	1.0	1.3
5	copper	kerfing in air	6.3	0.9	1.2
6/7	copper	kerfing underwater	5.9	0.9	1.2
8	steel	kerfing in air	7.1	1.1	1.4
9	copper	cutting in air	3.4	1.0	1.3
10	copper	cutting in air	1.8	1.0	1.3

Table X Kerf widths

The top kerf width is always larger than the bottom kerf width (by about 30 %).

There are no significant differences between underwater operation and operation in air and between kerfing and cutting. There is no influence of the abrasive flow rate in the studied range.

As an example the kerfs of experiments No. 1 are shown in figure 44. Figure 45 gives a view of a cross-section of a kerfing test in copper (thickness 20 mm).

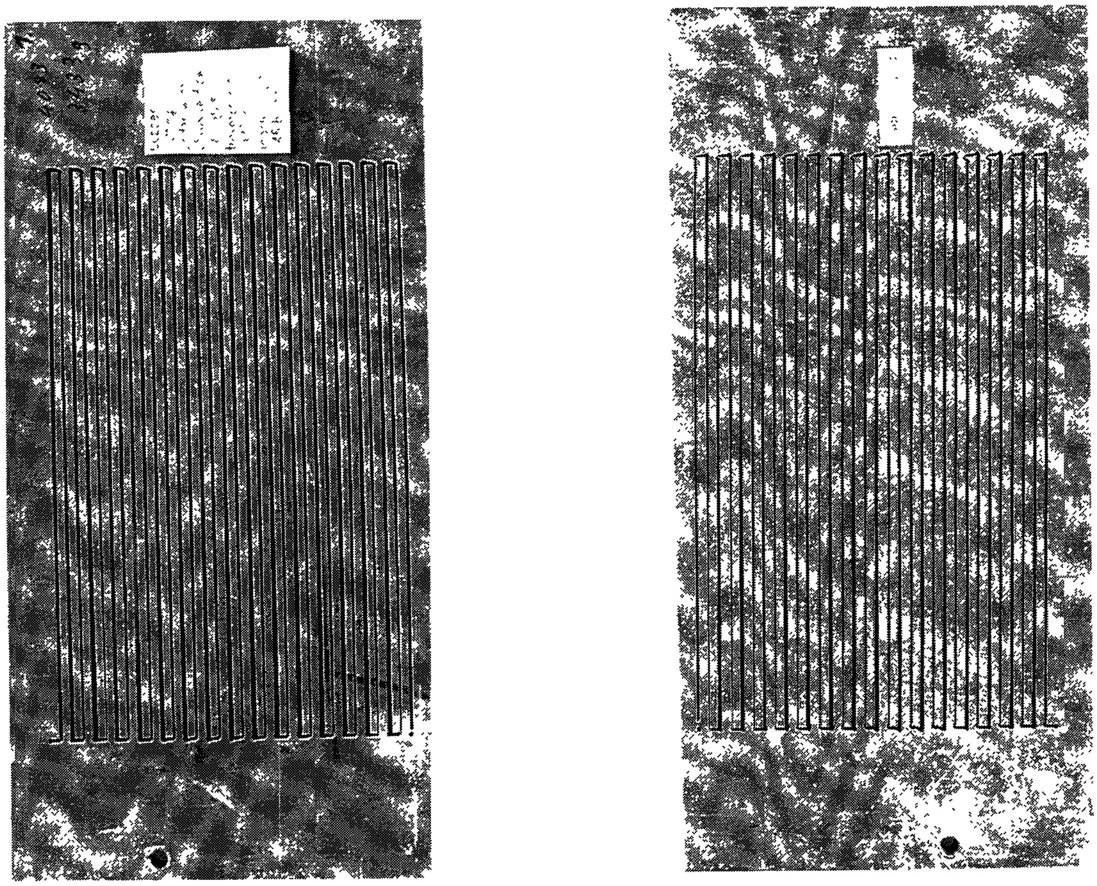

Figure 44 Front and rear view of test plate 1 (cutting through of 10 mm copper)

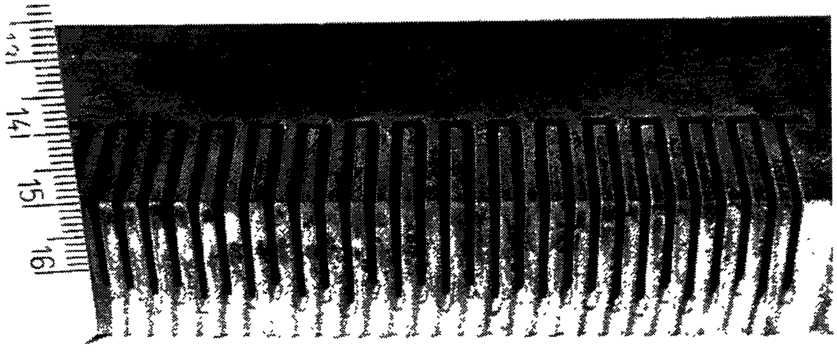

Figure 45 Cross-section of a kerfed test plate (kerfing of copper - 20 mm thickness)

B.4.3. Methods to lower the spreading out of the emissions

The expense of handling the secondary waste is mostly influenced by the spreading out of the abrasives after machining. A reduction of the spreading out causes a decrease of mass of material which has to be treated to separate all the waste from the environment.
In order to find a way to lower the spreading out the two methods of abrasive machining - cutting through and kerfing - have to be investigated separately.

Cutting through

In case of cutting through the abrasive water jet is passing the workpiece producing the cut. A reduction of the spreading out of the used particles can be realised by using a catcher system on the opposite side of the workpiece. The passing jet enters this catcher system and the remaining kinetic energy of the jet is changed into heat by friction of the catcher material. The abrasive can be sucked out of the catcher and has to be treated for disposal in case of cutting radioactive components.

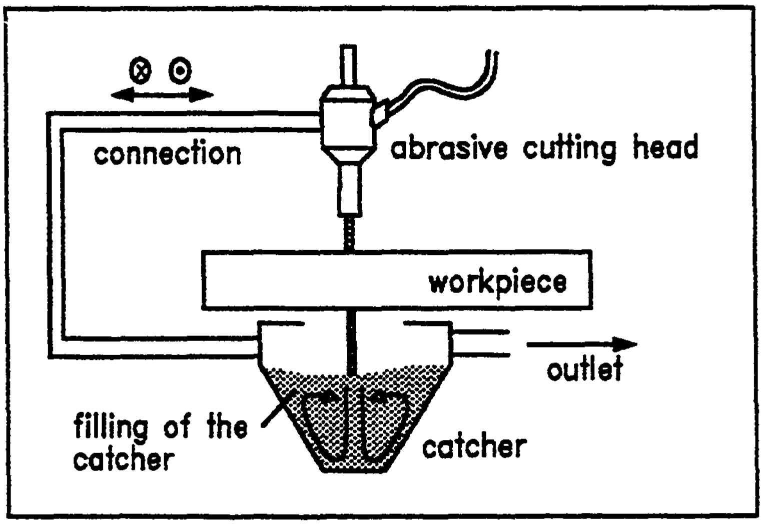

Figure 46 Catcher system for cutting through

Such systems are working in manufacturing industry sufficiently because of the small size of the workpieces. During cutting operation the catcher system has to be moved in the same manner as the abrasive cutting head. Therefore either a connection of the cutting head and the catcher is necessary (see fig. 46) or a second handling system has to be installed to move the catcher. The use of such systems for cutting large structures is nearly impossible because of the size of the workpieces. A connection of cutting head and catcher can't be realised; a second handling system needs a sophisticated controlling unit to follow the jet on the rear side of the workpiece. In many cases the rear side is not accessible (tubes, housing of machines and pumps).

So for decommissioning purposes a general solution of the problem in case of cutting through is not possible. For most applications the only way seems to be to filter the water of the basin in which the cutting takes place. To reduce the amount of water which has to be filtered the size of such a basin has to be as small as possible.

To separate the particles from the water different techniques can be used. With regard to the reduction of "tertiary" waste such as filters the use of a hydrocyclone for separation seems to be a sufficient solution. The working principle of a hydrocyclone is given in figure 47.

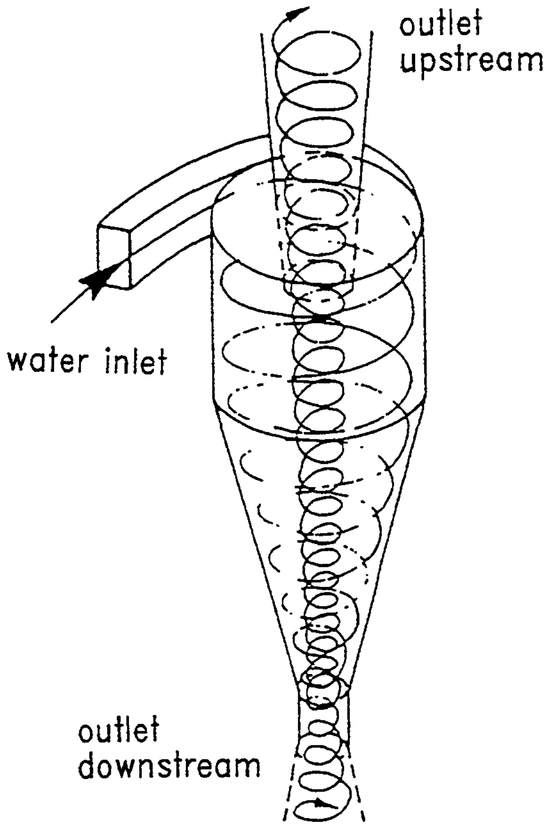

Figure 47 Working principle of a hydrocyclone

The tangential inlet of the suspension flow causes a vortex inside the cylindrical part of the cyclone. The flow runs downwards according to the effect of gravity. When reaching the conical part a second vortex is being created. Because of the decreasing diameter of the cyclone the whole suspension flow is not able to pass the conical part, so the inner vortex runs upwards. Using the effect of inertia the solid particles remain in the downward flow while the water flow leaves the cyclone through the upper outlet. The solid particles are gathered in a hopper at the bottom. The geometry of the conical part and the size of the cyclone effects the cut-off-diameter. Because of the disintegration of the abrasive particles during the cutting process the size of some particles to be separated is very small. Hydrocyclones in general are able to separate particles starting at a size of a few μm. In addition the use of a filter seems to be useful to gather the smallest-sized particles, too.

A hydrocyclone which is designed for cleaning applications in nuclear power plants was tested during the reported research work. The results of the tests are given in B.4.4.

The system has been lend to the project by the company GRADEL. The technical details are given in annex 4.

Another possibility to lower the spreading out in case of cutting through is the method of multiple-pass cutting. During a first pass the workpiece is kerfed as deep as possible. The remaining thickness is only a few mm. A second pass is used for cutting through the workpiece.

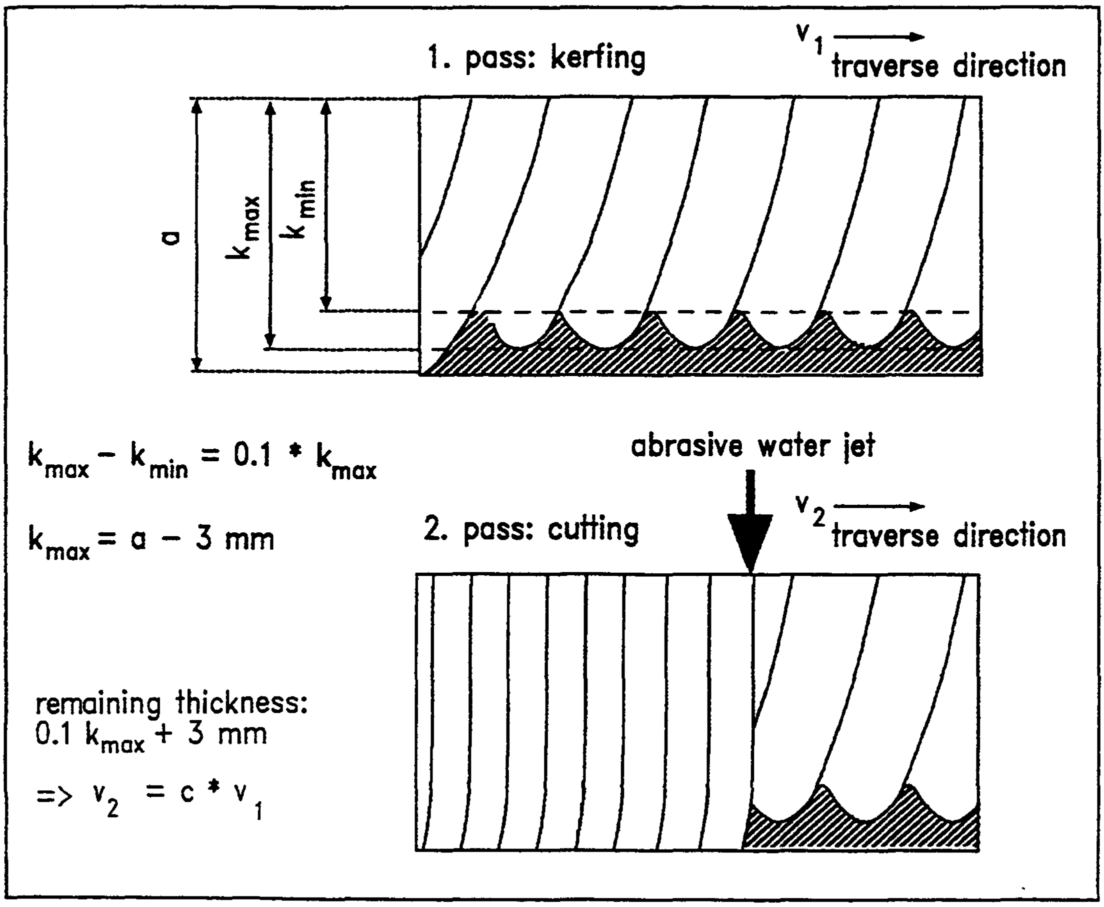
1. pass: kerfing
v_1 traverse direction
a
k_{max}
k_{min}
$k_{max} - k_{min} = 0.1 * k_{max}$
$k_{max} = a - 3$ mm
abrasive water jet
2. pass: cutting
v_2 traverse direction
remaining thickness:
$0.1\ k_{max} + 3$ mm
$=> v_2 = c * v_1$

Figure 48 Multiple-pass cutting

Because of the small remaining thickness the traverse rate can be very high. A calculation is given in figure 48. The waviness of the ground of the kerf is about 10 % of the maximum kerfing depth. Additionally there has to be a remaining thickness of the workpiece of about 3 mm to be sure to kerf only. Both together - remaining thickness and waviness of the ground of the kerf - effect the traverse speed of the second pass for cutting through. The speed can be calculated according to the figures of B.1. (fig. 5 and 6). For material thicker than 20 mm the traverse speed of the second pass can be more than 5 times higher than the first pass. This fact causes a reduction of spread out abrasives by the factor of 5, too, in case the reflected particles during kerfing are caught in total by a hood.

During kerfing the particles are reflected by the ground of the kerf and can be sucked away by a hood which is adapted at the cutting head. In this case there are no problems regarding the connection and movement of the hood; access to the rear side of the workpiece is not necessary. The application of such a hood is tested during the contract. The results are reported in the following.

Kerfing

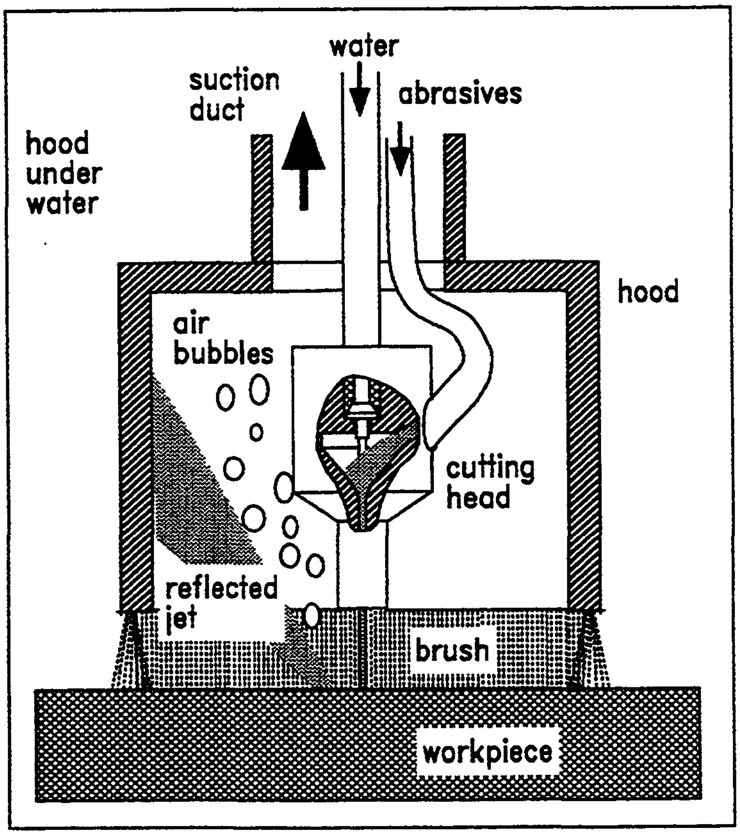

Figure 49 Suction hood

According to the principle given in figure 31 the reflected particles can be caught by a hood during kerfing. The hood has to be fixed as close as possible to the cutting head and the workpiece to catch as much reflected abrasives as possible. The volume of the hood can be sucked away continuously and has to be treated for final storage or recycling. The water inlet into the hood is realised by the gap between workpiece and hood. The flow through this gap makes sure that the particles are not spread out.

The first type of such a hood is shown in figure 49.

The hood is fixed at the cutting head and covers it symmetrically. The high pressure water feed and the abrasive transport hose are integrated in the suction duct. To obtain a small gap and therefore a high water flow velocity into the hood the gap is closed partly by brushes.

The hood was tested by a kerfing test (test nr. 12 in the following chapter).

The main problem to use such a hood is caused by the air entrainment of the abrasive water jet. The abrasive transport is realised by an air flow. This air flow causes air bubbles during kerfing operation, which are gathered inside the hood. When using the mentioned hydrocyclone and the adapted water pump to aspirate the flow from the hood the system breaks down because the equipment is not able to handle the air. The water flow through the hood amounts according to the performance of the pump to about 350 l/min, the air flow into the cutting head and so the hood was less than 30 l/min. The hydrocyclone wasn't able to aspirate and separate the resulting flow with an air content of less than 10 vol.-%.

For that reason the hood was modified as given in figure 50.

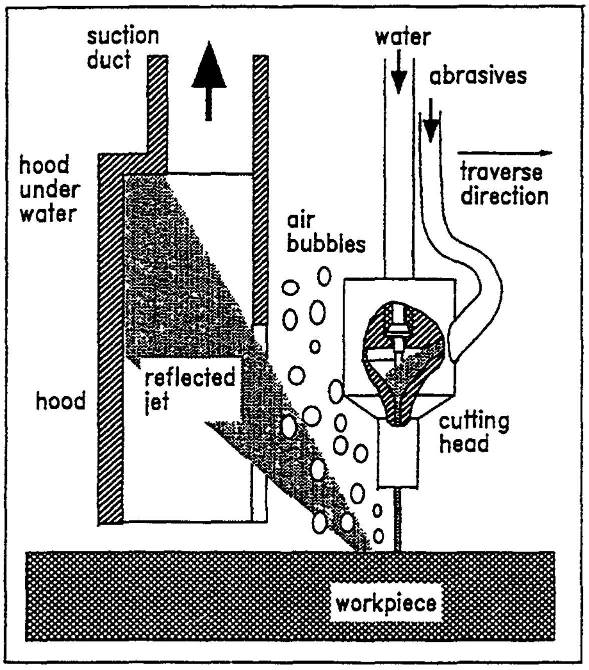

Figure 50 Modified hood

The hood was adapted in the zone of jet reflection but not covering the cutting head. This geometry allows most of the air bubbles to rise in the water according to the effect of buoyancy. Because of the low density they are rising very fast and close to the cutting head while the reflected particles are reflected in a certain angle. By this effect the bubbles and the reflected particles can be separated by finding an adequate position for the hood as shown in figure 50. The flow which can be sucked away from the hood includes only a small amount of air which can be handled by the hydrocyclone. A view of the hood is given in figure 51. The total setup including the vacuum cleaner (hydrocyclone) and the cartridge filter system is shown in figure 52.

Figure 51 Suction hood

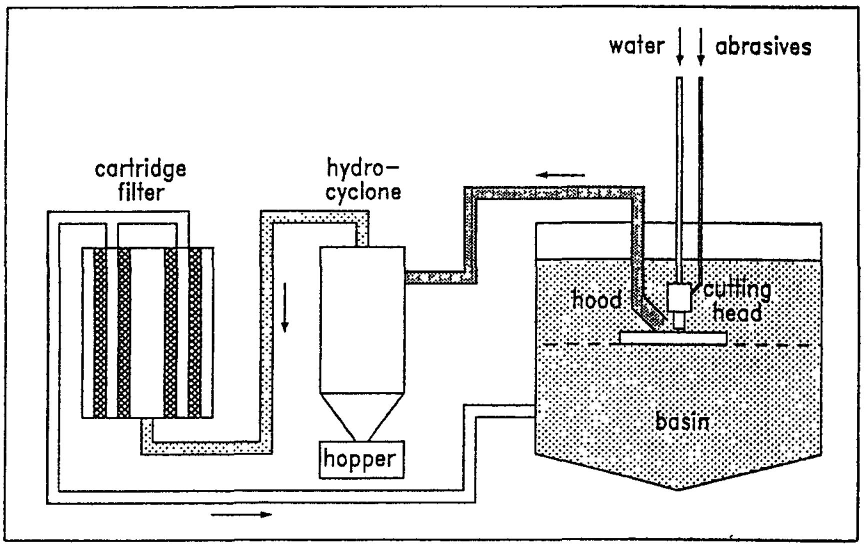

Figure 52 Setup of basin, cyclone and cardridge filter

The detailed worksheets are given in annex 1.

To compare the results from both series of tests a comparison test was carried out (nr. 11). The results of this test has to be compared with nr. 6/7 in B.4.2 (table XII).

	Cut length mm	Workpiece mass loss $g.m^{-1}$	Used abrasive $g.m^{-1}$	Sedimented dross		Suspended particles		Aerosols		Used water $g.m^{-1}$	Water in exhaust duct		Aerosols $g.m^{-2}$ of cut edge
				$g.m^{-1}$	% TC	$g.m^{-1}$	% TC	$g.m^{-1}$	% TC		$g.m^{-1}$	% of used water	
Exp 6/7 Phase 1	6 533	152.9	2 532	2 324	98.7	31.5	1.3	7.10^{-4}	3.10^{-5}	11 679	5.5	0.05	$4.2.10^{-2}$
Exp 11 Phase 2	21 252	144.2	2 612	2 644	99.3	17.7	0.7	1.10^{-4}	4.10^{-6}	11 669	8.1	0.07	6.10^{-3}

Table XII Comparison of 1. and 2. test series

The results obtained in the two experiments are in the same order of magnitude. The quantity of aerosols is divided by 7 in the second experimental phase but the aerosol collected mass is very small because operation takes place under water; so the uncertainty is important.

Experiment 12 was carried out with the vacuum cleaner (B.4.3.) and the directly working hood (fig. 49).

In this configuration, the vacuum cleaner was not operating correctly because the system was sucking air coming from the cutting hood. In fact, the abrasive transport is realised by an air flow. This air causes bubbles inside the hood during kerfing. The bubbles were sucked into the cyclone, the pump cannot work with air. The air flow rate into the cutting head was less than 30 l/min and the water flow was about 350 l/min but the system was not able to handle this proportion of air.

Furthermore the abrasive focusing nozzle was disconnected after 18 min of kerfing and the test was stopped after another 15 min.

Experiment 13 was carried out with the vacuum cleaner associated with the cartridge filter. The suction point was positioned at the side of the basin. A hood closed by a rubber membrane was placed directly at the cutting head. The membrane was inflating during the kerfing due to the bubbles of air coming from the cutting head. Compared to test 11 the quantity of aerosols is divided by almost 5, probably due to the trapping effect of the hood.

Test 14 concerned the kerfing of a bigger plate (thickness: 100 mm, depth of kerf: 70 mm).

Following the poor collection of the waste when filtering the whole basin (test 13) by cyclone and cartridge filter and the impossibility of using the direct hood (test 12) experiments 15 and 16 were carried out with an indirect hood (see fig. 50) and without cartridge filters because of their high pressure drop. With this hood arrangement the bubbles are not caught by the hood contrarily to the solid waste which is reflected during kerfing.

The data for the sedimentation process in the basin after finishing kerfing are given in figure 53. Also the result for the experiment nr. 1 is shown there.

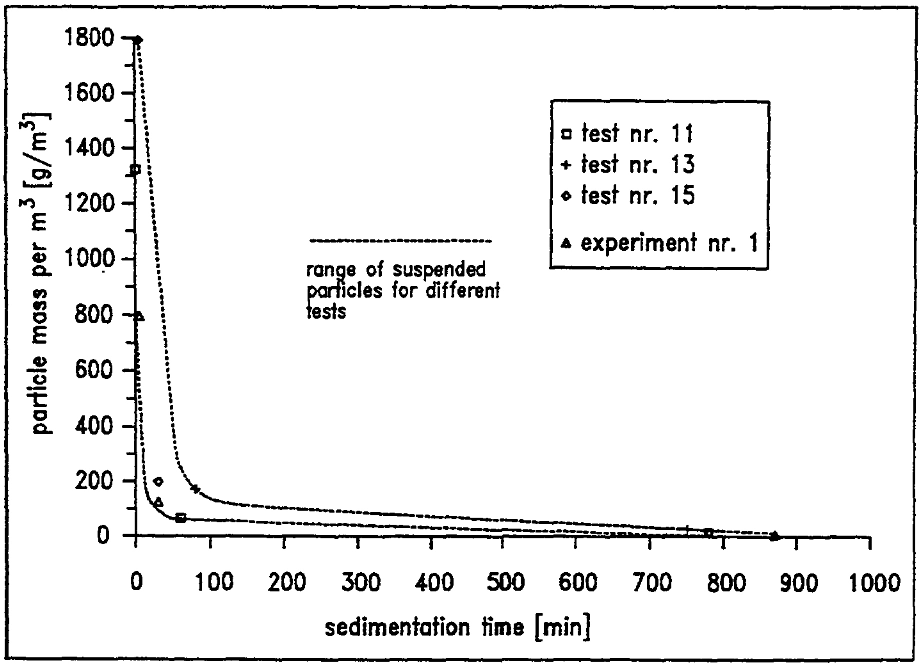

Figure 53 Sedimentation process

The quantity of suspended particles is extremely dependent upon the sedimentation time. A difference of a few minutes just after kerfing can induce a decrease factor of 2.

A) Balance of secondary emissions

Solid emissions

- 6.10^{-6} % to 2.10^{-3} % of the total solid mass is drawn into the exhaust duct (M4).
- 0.5 to 2.8 % of the total solid mass is composed by suspended particles (M3).

By chemical analyses of the water (annex 3) it can be noted:

- the proportion of copper and abrasives in solution in the sampling bottles three months after the experiments is in the range 1 to 3 % for copper, inferior to 0.1 % for particles of abrasives,
- the ratio of

$$\frac{\text{mass of particles of copper}}{\text{mass of particles of abrasives + mass of particles of copper}}$$

in the suspended particles five minutes after the cut is comprised between 5 and 12 %. These values are in agreement with the first test series.

- The remainder of the solid emissions is composed by dross sedimented in the tank (M1).
As sedimented dross represents almost all the solid secondary emissions especially when the operation takes place under water, the ratio

$$\frac{\text{used abrasives}}{\text{used abrasives + workpiece mass loss}}$$

can be considered coarsely as a representative of the proportion of abrasives in the sedimented dross.

Exp. No.	Material thickness mm	Operation place	Cut length mm	Workpiece mass loss $g.m^{-1}$	Used abrasive $g.m^{-1}$	Sedimented dross $g.m^{-1}$	Sedimented dross % TC	Suspended particles	Suspended particles %	Aerosols $g.m^{-1}$	Aerosols % TC	Used water $g.m^{-1}$	Water in exhaust duct $g.m^{-1}$	Water in exhaust duct % of used water	Aerosols $g.m^{-2}$ of cut edge
11	20	Underwater	21 252	144.2	2 612	2 644	99.3	17.7	0.7	1.10^{-4}	4.10^{-6}	11 669	8.1	0.07	6.10^{-3}
12	20	Underwater	2 500	15.6	4 200	NM		NM		$1.8.10^{-4}$		21 600	NS		6.10^{-2}
13	20	Underwater	21 252	152.8	2 922	3 051	97.2	88.2	2.8	$2.2.10^{-5}$	7.10^{-7}	11 669	11.7	0.10	$1.3.10^{-3}$
14	100	Underwater	3 036	729.2	19 779	19 679	99.5	105.2	0.5	$4.2.10^{-4}$	2.10^{-6}	81 686	81.9	0.10	6.10^{-3}
15	20	Underwater	21 252	126.4	2 580	2 312	99.4	13.8	0.6	8.10^{-6}	3.10^{-7}	11 905	15.1	0.13	$4.7.10^{-4}$
16	20	Underwater	21 252	117.7	1 704	1 700	99.3	12.5	0.7	1.10^{-6}	6.10^{-8}	22 586	73.6	0.33	$5.6.10^{-5}$

TC = Total solid mass collected
NM = not measured
NS = not significative

Table XIII Recapitulative secondary emissions results

No. of experiment	Depth of kerf (mm)	Abrasive flow rate (g/s)	% of abrasives in the sedimented dross
11	17	6.1	94.8
13	17	6.8	95.0
14	70	6.6	96.4
15	17	6.2	95.3
16	17	2.05	93.5

Table XIV Proportion of abrasives in the sedimented dross

The proportion of abrasives in the sedimented dross is in agreement with previous experiments. It increases with the kerfing depth (test 14) and with the abrasive flow rate (compared to test 16).

Liquid emissions (vapours)

Between 0.07 to 0.4 % of the used mass of water is drawn into the exhaust duct (M2).

B) Size distribution of abrasives and sedimented dross

Regarding the handling and the recycling capacity of the secondary waste it is useful to get knowledge about the proportion of eroded material in the sedimented dross depending on the size. Therefore for the tests 1 and 2 of the first series chemical analysis were carried out to determine the proportion of copper in the waste.

Dimensions of the particles in micrometers	Proportion of copper in % on each sieve	
	Experiment 1	Experiment 2
< 37	11.0	12.2
37-63	9.8	6.7
63-125	5.2	2
125-250	0.17	0.09
250-500	0.02	0.02
> 500	N.D.	N.D.

N.D. = not detectable

Table XV Proportion of copper in the sedimented dross according to the size distribution

The particles of copper are more concentrated in the finest particles. The quantity of copper is more important in particles which dimensions are inferior to 125 µm for experiment 1 (mean proportion of copper: 3 %) and to 63 µm for experiment 2 (mean proportion: 3.6 %).

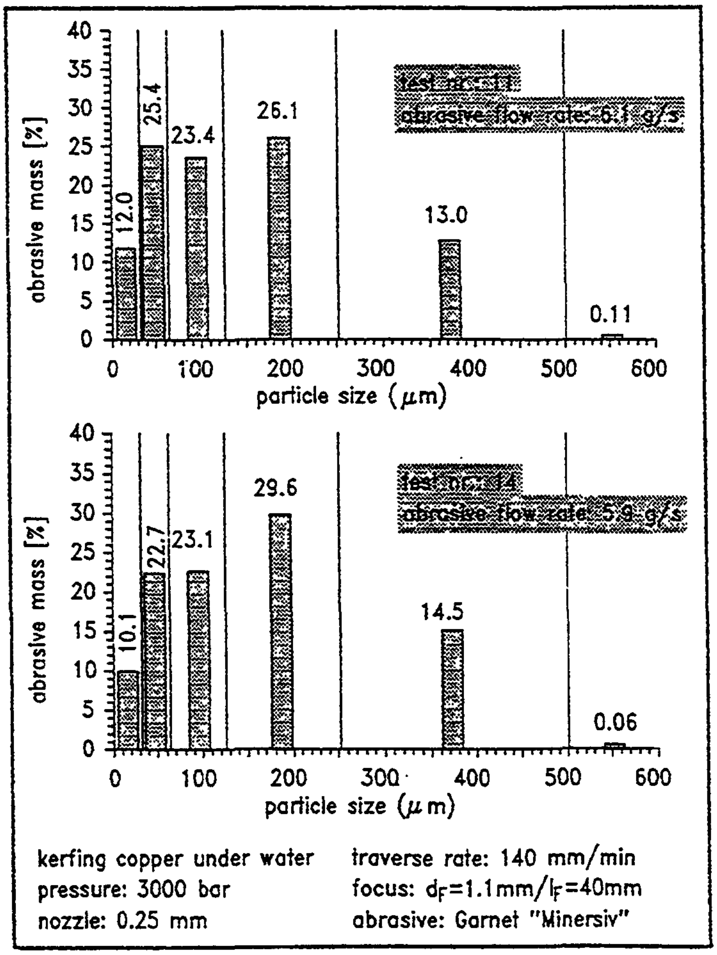

kerfing copper under water
pressure: 3000 bar
nozzle: 0.25 mm
traverse rate: 140 mm/min
focus: d_F=1.1mm/l_F=40mm
abrasive: Garnet "Minersiv"

Figure 54 Size distribution of used abrasives

Figure 54 gives the result for the tests nr. 11 and 14.
The percentage of the abrasive that is retained on each sieve is plotted versus the corresponding particle range. The bars represent the percentage of abrasive that is retained in each particle range. All percentage values are related to the mean (arithmetic) particle size of each range. The result of test nr. 11 can be compared with test nr. 6/7 of B.4.2. because of the use of the same machining conditions. The particle disintegration of test nr. 11 is not as high as the one of test nr. 6/7. Especially the amount of abrasives of the smallest sieve range (0-32 µm) is much smaller. A comparison of all tests which are comparable is given in table XVI.

Particle size [µm]	Percentage of mass in experiment No.					
	6/7	11	13	14	15	16
0-32	19.8	12.0	9.3	10.1	6.8	5.2
32-63	19.4	25.4	21.5	22.7	25.2	28.9
63-125	24.2	23.4	23.1	23.0	27.5	29.4
125-250	28.3	26.1	30.7	29.6	29.3	28.1
250-500	8.4	13.0	15.4	14.5	11.0	10.4
> 500	-	0.1	0.1	0.1	0.3	-
Σ	100.1	100.0	100.1	100.0	100.1	100.0

Table XVI Size distribution of sedimented dross

For all tests carried out in the second series of experiments the size distribution is the same in the range of scattering.
When separation methods were used the mass mean diameter is calculated for the whole waste.

No. of experiment	Abrasive flow rate [g/s]	Mass median diameter [µm]
6/7	5.9	120
11	6.1	134
13	6.8	149
14	6.6	144
15	6.2	136
16	2.05	134

Table XVII Mass mean diameter of used abrasives

Obviously the medium particle size of the second series is in general a little bit bigger than for test nr. 6/7. The experiments of the second series are more reliable because of the long machining time compared to nr. 6/7.

Comparing the results of test nr. 11 and 14 there seems to be no influence of the kerfing depth on the particle disintegration. The size distribution (fig. 54) as well as the median diameter (table XVII) are nearly not affected.

The kerf of test nr. 14 was produced by using only 20 % of the traverse speed of the other test. As the result the kerfing depth was increased by the factor of 4, but not by a factor of 5 as expected. So for deep kerfing the efficiency of the abrasive water jet decreases according to the increased friction of the jet with the shoulder of the deep kerf.

As mentioned before test nr. 12 wasn't successful. Using the direct hood the aspirated air causes problems with the suction pump and the hydrocyclone for separation.

Additionally the use of the cartridge filters (Type U2-20Z, 2 μm) lead to problems regarding the circulated water flow rate. Although 10 filters were used parallel the pressure drop after few minutes of filtering was very high. The total capacity of each cartridge filter is between 200 and 2000 g (according to the manufacturer) depending on the conditions and especially on the formation of the cake but the suction system was not able to overcome the pressure drop of the wet and dirty filters.

This effect was verified in test nr. 13. To simulate an operation without any hood (simulation of kerfing as well as cutting through) it has been tried to filter the basin in total. For this test the hydrocyclone as well as the cartridge filters were used. Starting with a water flow rate of 350 l/min through the filtration system the pressure drop increased very fast. After a few minutes the flow was decreased to 90 l/min water. One used cartridge filter is shown in figure 55. The filtering paper is clogged by particles from the cutting process. According to this effect the pressure drop has been increased.

Figure 55 Used cartridge filter (filter length 250 mm)

mean diameter of 152 µm.

Tests nr. 15 and 16 point out the effect of the abrasive flow rate on the cutting efficiency (see experiments 2,9 and 10 of first series). According to table XVII the mass mean diameter is not affected by the abrasive flow rate. The cutting efficiency related to the abrasive flow is increased by using smaller abrasive flow rates. This is in accordance with the results presented in B.1.

The size distributions of the used particles for tests nr. 15 and 16 are given in figure 57 and 58. Both tests were carried out with the indirect hood (see B.4.3.), the hydrocyclone for separation but without the cartridge filter system.

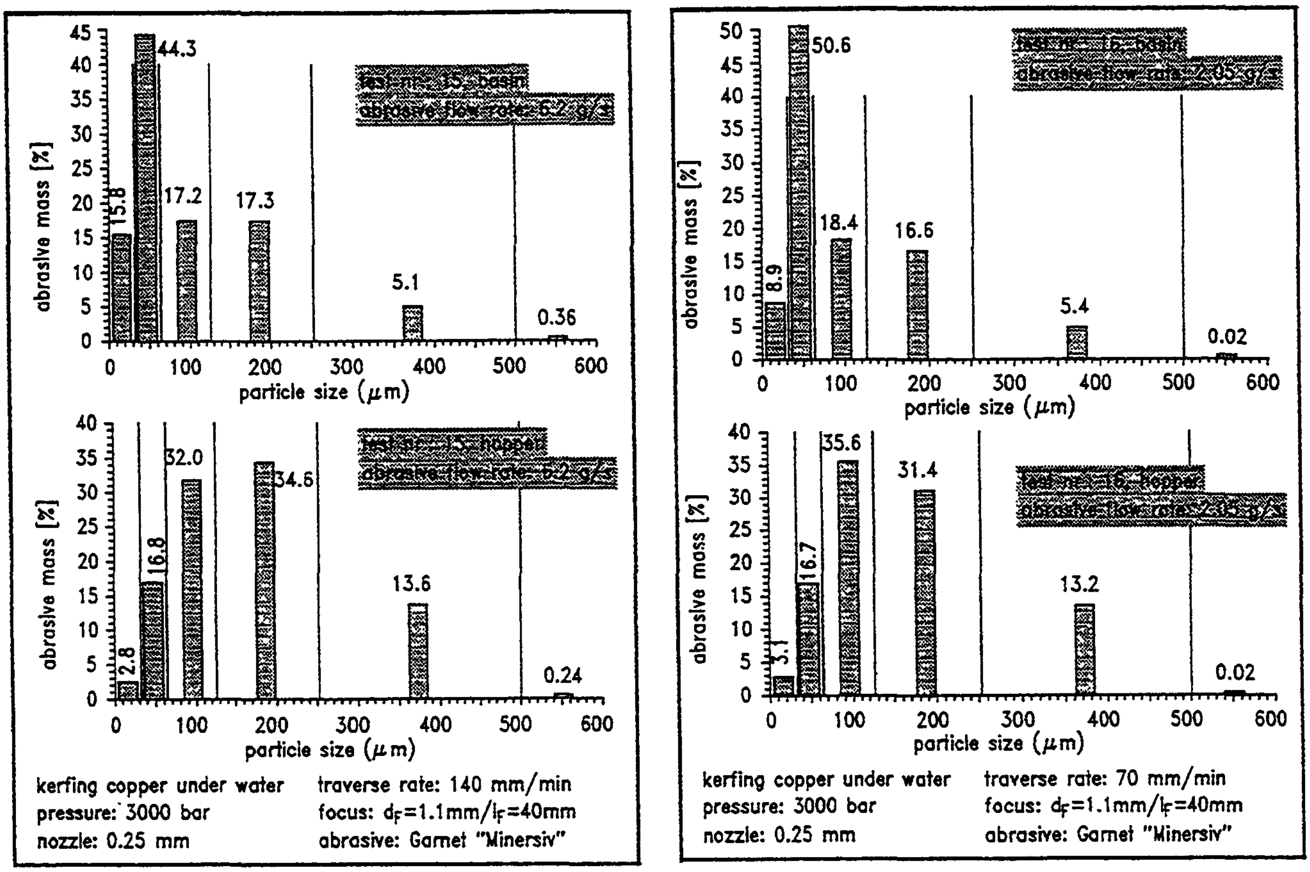

Figure 57, 58 Size distribution of used abrasives

The mean diameter of the particles which are remaining in the basin is of smaller size than the particles gathered by the cyclone. The mass-% of the abrasives is related to the total amount of abrasives remaining in the basin (upper part of fig. 57, 58) resp. the hopper (lower part), but not related to the total mass of waste.
This is given in figure 59.

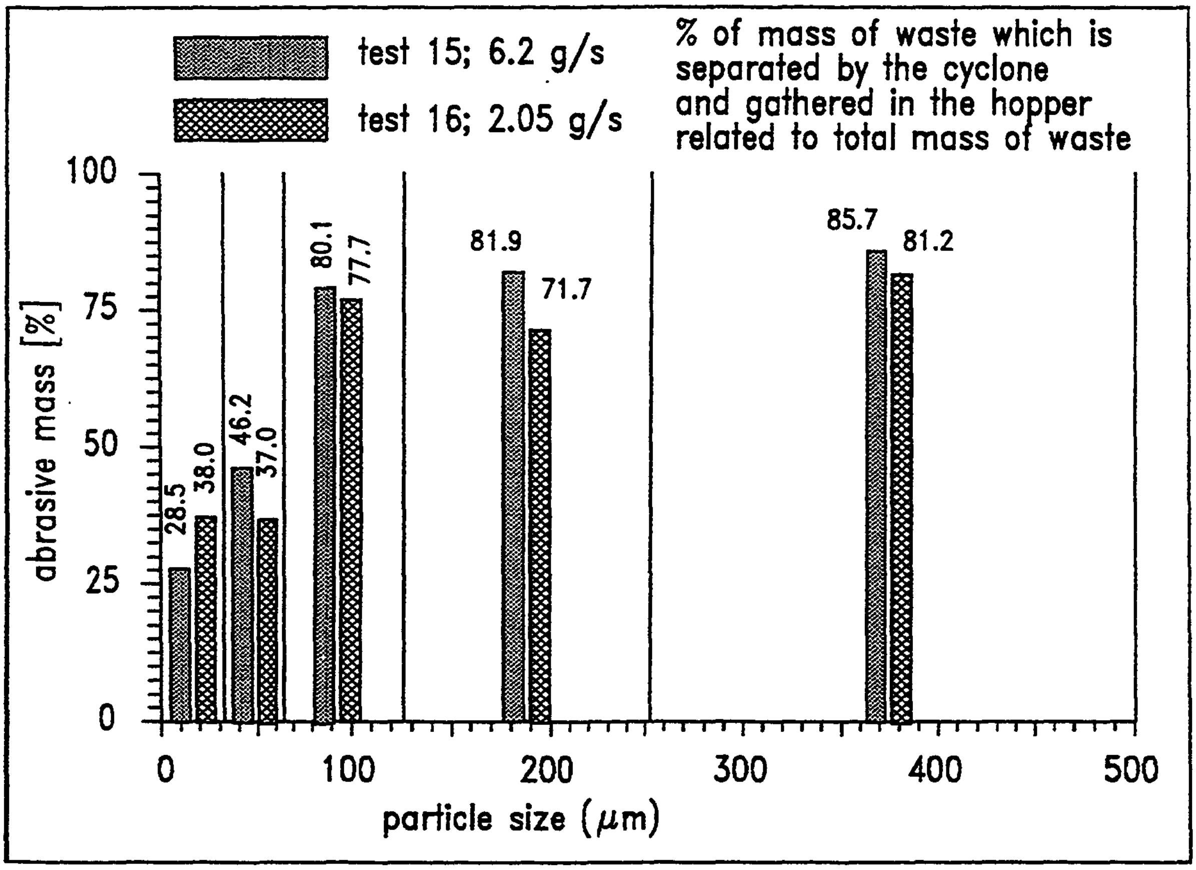

Figure 59 Size distribution of used abrasives
- gathered by the hydrocyclone
- related to the total mass of waste

For both tests the mass-% of the particles gathered in the hopper of the hydrocyclone are given related to the total mass of solid waste. For bigger particles the efficiency of the cyclone is quite good. For particles bigger than about 100 μm for both tests more than 80% of the mass was filtered by the cyclone. For smaller particles the efficiency decreases. According to figure 54 (result test nr. 11) 30 - 40 % of the total mass of solid waste consists out of particles smaller than 100 μm when kerfing copper under water (assumption: same size distribution of solid waste of test 11 and 15 / 16). With respect to this fact it is necessary to increase the efficiency of the hydrocyclone regarding parti-

cles smaller than 100 μm to gather more mass in the filtration system.
Nevertheless, the use of a hydrocyclone seems to be a useful technique to separate solid and liquid waste produced during abrasive water jet cutting. For the tests nr. 15 and 16 an indirect hood without optimisation has been used. 64.1 resp. 69.4 mass-% of the solid waste were separated by the cyclone (table XVIII).

Experiment No.	Mass of waste [g] % of total mass [-]		
	Basin	Hopper of cyclone	Cartridge filters
13	59 235 91.4	756 1.2	4 844 7.4
15	15 022 30.6	34 106 69.4	-
16	12 972 35.9	23 146 64.1	-

Table XVIII Separation efficiency of hydrocyclone and filter

The use of cartridge filters is no sufficient way because of the high amount of smallest particles which clog the filters very fast. Only when using a hydrocyclone which is able to separate a much higher percentage of particle mass even for particles smaller than 100 μm the additional use of a cartridge filter can be a good method to separate the remaining small amount of particles from the water.

C) Characterisation of the aerosols in the exhaust duct

The concentration of aerosols in the exhaust duct in all experiments of the second series is inferior to 0.05 mg/m^3. this concentration is low and the masses collected in the filters are small, so the figures obtained have to be considered as an order of magnitude.
As in previous experiments, taking into consideration the very small masses collected on each stage of the Andersen impactor during kerfing under water,, the size distribution cannot be determined in mass. On the stages of the impactor cellulose filters were used instead of fibre glass because they have a lower background for the researched elements (factor of 30 for Fe and Mg). Therefore, it was necessary to use a fibre glass filter as final filter because the cellulose filter has a poorer collection efficiency.
By the chemical analysis (annex 2) it can be deduced the size distribution of the particles of Cu, Fe and Mg. For each experiment, the size distribution is bimodal (and sometimes trimodal) with one mode below 0.3 μm and another mode mainly between 1 and 4

μm (annex 3).

For the experiments where the size distribution is almost unimodal, the mass mean aerodynamic diameter (MMAD; see B.4.2) is indicated (table XIX).

Compared to the previous results (B.4.2.), the particles collected in the exhaust duct for underwater operations are smaller than for operations in air.

Exp n°	Abrasive flow rate g/s	Reference	Mass mean aerodynamic diameter 10^{-6} m	Geometric standard deviation
11	6.1	Cu Fe Mg	NA NA NA	
13	6.8	Cu Fe	NA NA	
14	6.6	Cu Fe	NA NA	
15	6.2	Cu Fe	2.06 NA	3.07
16	2.05	Cu Fe	1.72 1.61	2.86 3.01

NA: not applicable (the size distributions are multimodal)

Table XIX Aerosol size (MMAD)

Conclusions and Outlook

In the reported project different aspects have been investigated regarding the application of abrasive water jets in nuclear decommissioning. Especially the minimisation of secondary waste, the handling of aerosols and the control of the tool during operation are of interest.

It was shown that abrasive water jets are able to cut steel up to more than 100 mm thickness. To do so the consumption of abrasives can be reduced by special measures. In detail the use of medium sized nozzles (0.25 mm) and the reduction of the abrasive flow rate as well as the increase of the pressure as high as possible are methods to reduce the abrasive consumption related to the produced area of cut. This fact can reduce the amount of secondary waste, too. In addition to these methods for reducing the consumption of water and abrasives it seems to be necessary to find ways to recycle the used abrasives.

The cutting has to be operated remote controlled. Therefore methods to control the tool as well as the cutting result are necessary to ensure the reliability.

Various techniques are applicable:

- Measuring the pressure loss of the sucked-in air in the transport hose is a method to calculate the diameter of the focusing nozzle during operation.
- Sound analysis are not reliable to detect the result of machining.
- The application of an accelerometer to detect the state of kerfing seems to be useful.

Regarding the wear of the focusing nozzle the standing time was increased by the factor of 10 - 50 by the use of composite carbide nozzles. Therefore no special methods to replace worn parts are necessary because the operation time of one nozzle reaches about 100 h.

In the reported project the secondary waste was quantified and analysed. This was done for kerfing and cutting through for application in air as well as under water. Only a very small amount of the waste is spread into the air as aerosols, most of the waste are sedimented particles. Analysing these particles it can be said that the particles are destroyed during the cutting process. To reduce the waste which has to be conditioned for final storage recycling seems to be a possible route. Although the particles disintegrate during cutting recycling can be realised /11/: Even particles, which have been broken during previous cutting processes, are able to remove material. Particles with a diameter of about 50 μm are able to reach the same efficiency as the same particle mass consisting out of particles with 500 μm diameter.

This fact indicates that it can be possible to reuse most of the abrasives. But it was shown that there is an enrichment of cut material in smaller particle sizes so that special treatment is necessary to separate these material from the abrasives. Further investigations have to be carried out to develop an efficient method of recycling.

Regarding the aerosols working under water reduces the amount by the factor of 200 compared to application in air. In addition the use of a suction hood near the cutting head lowers the spreading of the particles. A cyclone seems to be useful to separate the particles from the water.

Summing up the abrasive water jet technique is able to work reliable in the field of nuclear decommissioning. To find real applications methods of recycling the abrasive particles have to be investigated to reduce the amount of secondary waste. First tests have pointed out that it could be possible to reuse about 80 - 90 % of the abrasives.

References

/1/ Abudaka, M. and P.S.J. Crofton
"Abrasive water jets for controlled demolition and dismantling"
In: Proc. of the 1. Intern. Conf. on Offshore, Onshore and Nuclear Works (Manchester, England, 1988), UMIST, Manchester, England, 1988

/2/ Bach, F.-W.; Steiner, H.; Pilot, G. and E. Skupinski
"Analysis of results obtained with different cutting techniques and associated filtration systems"
Decommissioning of Nuclear Installations
Ed.: Pflugrad, Bisci, Huber, Skupinski
Elsevier Science Publishers Ltd.; Essex, England, 1990

/3/ Haferkamp, H.; Louis, H. and G. Meier
"Submerged cutting of steel by abrasive water jets"
Decommissioning of Nuclear Installations
Ed.: Pflugrad, Bisci, Huber, Skupinski
Elsevier Science Publishers Ltd.; Essex, England, 1990

/4/ Haferkamp, H.; Louis, H. and G. Meier
"Submerged cutting of contaminated material by abrasive water jets under the protection of water shield".
In: Proc. of the 9th International Symposium on Jet Cutting Technology (Sendai, Japan, Oct. 1988) BHRA, The Fluid Engineering Centre, Cranfield, U.K., 1988

/5/ Haferkamp, H.; Louis, H. and G. Meier
"Weiterentwicklung des Abrasivstrahl-Schneidverfahrens zum Trennen ferritischer und austenitischer Stähle unter Wasser"
Final Report Contract FI1D-0069, EUR 12684 DE
Commission of the European Communities, Luxembourg, 1990

/6/ Meier, G.:
"Unterwassereinsatz von Wasserabrasivstrahlen"
VDI-Fortschrittbericht, Reihe 2 (Fertigungstechnik)
VDI-Verlag, Düsseldorf, 1993

/7/ Louis, H. and G. Meier
"Process Control for Submerged Cutting by Abrasive water Jets"
In: Proceeding of the 3. Intern. Symposium on Underwater Technology, GKSS Forschungszentrum, Geesthacht, Germany, 1991

/8/ Louis, H. and G. Meier
"Methods of Process Control for of Abrasive Water Jets"
In: Proc. of the 6th American Water Jet Technology Conference (Houston, USA, Aug. 1991) Water Jet Technology Association, St. Louis, USA, 1991

/9/ G.A. Mort
"Long Life Abrasive Water Jet Nozzles and Their Effect on AWJ Cutting"
In: Proc. of the 6th American Water Jet Technology Conference (Houston, USA, Aug. 1991) Water Jet Technology Association, St. Louis, USA, 1991

/10/ Rouviere, R.; Pinault, M.; Gasc, B.; Guiadeur, R. and G. Pilot
"Adaptation des jets d'eau haute pression avec abrasif au demantèlement des installations nucléaires"
Final Report Contract FI1D-0067, EUR 12490 FR
Commission of the European Communities, Luxembourg, 1989

/11/ Guo, N.S.; Louis, H.; Meier, G. and J. Ohlsen
"Recycling Capacity of Abrasives in Abrasive Water Jet Cutting"
Jet Cutting Technology
Ed.: A. Lichtarowicz
Kluwer Academic Press; Dordrecht, Netherlands, 1992

ANNEX 1

Sheets of results

EXPERIMENT No. 1 (CUTTING)		**Date: 26/11/91**	
PLACE: UNDERWATER		**TOOL: WATER JET**	
MATERIAL NATURE:	**COPPER**	**WATER DEPTH:** **AIR VOLUME OF BASIN:** **WATER VOLUME OF BASIN:** **VENTILATION FLOW RATE:**	**100 mm** **0.360 m³** **0.780 m³** **24 m³.h⁻¹**
THICKNESS: **CUT LENGTH:**	**10 mm** **6528 mm**		
WATER PRESSURE: **WATER FLOW RATE:**	**3000 bar** **1.63 ℓ/min**	**ABRASIVE NATURE:** **ABRASIVE FLOW RATE:**	**GARNET** **7.2 g/s**

TOOL								
OPERATION	ABRASIVE		WATER		FOCUSING NOZZLE		OPERATION	
MODE AND POSITION	M6 mass used (g)	M'6 (g/m)	M7 mass used (g)	M'7 (g/m)	M5 mass loss (g)	M'5 (g/m)	CUTTING SPEED (mm/min)	TIME (min)
AUTOMATIC GRAVITY	20 070	3 074.4	76 300	11 688	0.0112	0.0017	140	46 9

SECONDARY EMISSIONS											
MATERIAL WEIGHT (g)			SEDIMENTED DROSS			EXHAUST WATER			SUSPENDED PARTICLES		
Before after	M0 Removed (g)	M'0 (g/m)	M1 (g)	M'1 (g/m)	M1/TC (%)	M2 (g)	M'2 (g/m)	M2/M7 (%)	M3 (g)	M'3 (g/m)	M3/TC (%)
4 083 3 433	650	99.6	19 607	3 003.5	97.5	30.8	4.7	0.04	504**	77	2.4**

** 5 min after cutting

AEROSOLS								
FILTER Ø mm	SAMPLED MASS (mg)	SAMPLED VOLUME (m³)	C1 gross (mg/m³)	C0 background (mg/m³)	C1 net (mg/m³)	M4 (g) aerosol mass	M4 (g/m)	M4/TC (%)
Ø 47 Ø 130	0.06 0.20	0.4452 1.033	0.13 0.19	0.06 0.08	0.07 0.11			
Integral Ø 160	1.53	16.1	0.095	0.055	0.04	0.00075	0.00012	3 6.10⁻⁶

TC = TOTAL SOLID MASS COLLECTED = M1 + M3 + M4 = 20 111 g

T1C1 = TOTAL SOLID MASS REMOVED = M0 + M6 = 20 720 g

$\frac{TC}{T1C1}$ = 97.0 %

NOTES:

KERF WIDTH	TOP: 1.2 mm	BOTTOM: 0.9 mm

EXPERIMENT No. 2 (CUTTING)		**Date: 27/11/91**	
PLACE: IN AIR		**TOOL: WATER JET**	
MATERIAL NATURE:	**COPPER**	**WATER DEPTH:** **AIR VOLUME OF BASIN:** **WATER VOLUME OF BASIN:** **VENTILATION FLOW RATE:**	**-** **0.650 m³** **0.490 m³** **24 m³.h⁻¹**
THICKNESS: **CUT LENGTH:**	**10 mm** **6528 mm**		
WATER PRESSURE: **WATER FLOW RATE:**	**3000 bar** **1.63 ℓ/min**	**ABRASIVE NATURE:** **ABRASIVE FLOW RATE:**	**GARNET** **6.8 g/s**

TOOL								
OPERATION	ABRASIVE		WATER		FOCUSING NOZZLE		OPERATION	
MODE AND POSITION	M6 mass used (g)	M'6 (g/m)	M7 mass used (g)	M'7 (g/m)	M5 mass loss (g)	M'5 (g/m)	CUTTING SPEED (mm/min)	TIME (min)
AUTOMATIC GRAVITY	19 020	2 914	76 300	11 688	0.0112	0.0017	140	46.9

SECONDARY EMISSIONS											
MATERIAL WEIGHT (g)			SEDIMENTED DROSS			EXHAUST WATER			SUSPENDED PARTICLES		
Before after	M0 Removed (g)	M'0 (g/m)	M1 (g)	M'1 (g/m)	M1/TC (%)	M2 (g)	M'2 (g/m)	M2/M7 (%)	M3 (g)	M'3 (g/m)	M3/TC (%)
4 086 3 367	719	110.1	18 404	2 819.2	99 3	127.2	19.5	0.17	128.1*	19.6*	0.7*

* water under material

AEROSOLS								
FILTER Ø mm	SAMPLED MASS (mg)	SAMPLED VOLUME (m³)	C1 gross (mg/m³)	C0 background (mg/m³)	C1 net (mg/m³)	M4 (g) aerosol mass	M4 (g/m)	M4/TC (%)
Ø 47 Ø 130	3.69 8.72	0.4680 0.8610	7.88 10.13	0.05 0.08	7.83 10.05			
Integral Ø 160	156.37	16.31	9 59	0.055	9.54	0.179	0.027	9.7.10⁻⁴

TC = TOTAL SOLID MASS COLLECTED = M1 + M3 + M4 = 18 532 g

T1C1 = TOTAL SOLID MASS REMOVED = M0 + M6 = 19 739 g

$\frac{TC}{T1C1}$ = 93.9 %

NOTES:

KERF WIDTH	TOP. 1.3 mm	BOTTOM: 1 mm

EXPERIMENT No. 3 (CUTTING)	Date: 28/11/91
PLACE: IN AIR	TOOL: WATER JET
MATERIAL NATURE· STEEL	WATER DEPTH: - AIR VOLUME OF BASIN: 0 650 m^3 WATER VOLUME OF BASIN: 0.490 m^3 VENTILATION FLOW RATE: 24 $m^3.h^{-1}$
THICKNESS: 10 mm CUT LENGTH: 3 672 mm	
WATER PRESSURE: 3 000 bar WATER FLOW RATE: 1.63 ℓ/min	ABRASIVE NATURE: GARNET ABRASIVE FLOW RATE: 6.8 g/s

TOOL								
OPERATION	ABRASIVE		WATER		FOCUSING NOZZLE		OPERATION	
MODE AND POSITION	M6 mass used (g)	M'6 (g/m)	M7 mass used (g)	M'7 (g/m)	M5 mass loss (g)	M'5 (g/m)	CUTTING SPEED (mm/min)	TIME (min)
AUTOMATIC GRAVITY	13 602	3 704	54 300	14 788	0 0093	0.0025	110	33.3

SECONDARY EMISSIONS											
MATERIAL WEIGHT (g)			SEDIMENTED DROSS			EXHAUST WATER			SUSPENDED PARTICLES		
Before after	M0 Removed (g)	M'0 (g/m)	M1 (g)	M'1 (g/m)	M1/TC (%)	M2 (g)	M'2 (g/m)	M2/M7 (%)	M3 (g)	M'3 (g/m)	M3/TC (%)
3 552 3 057	295	80.3	12 723	3 464.9	98 6	86.6	23.6	0.16	181.9*	49.6*	1.4

* water under material

AEROSOLS								
FILTER Ø mm	SAMPLED MASS (mg)	SAMPLED VOLUME (m^3)	C1 gross (mg/m^3)	C0 background (mg/m^3)	C1 net (mg/m^3)	M4 (g) aerosol mass	M4 (g/m)	M4/TC (%)
Ø 47 Ø 130	2.41 10.79	0.3019 0.7842	7.98 13.76	0.06 0.08	7.92 13.68			
Integral Ø 160	111.81	11.67	9.58	0.055	9.53	0.127	0.035	$9.8.10^{-4}$

TC = TOTAL SOLID MASS COLLECTED = M1 + M3 + M4 = 12 905 g
T1C1 = TOTAL SOLID MASS REMOVED = M0 + M6 = 13 897 g

$$\frac{TC}{T1C1} = 92.9\ \%$$

NOTES:

KERF WIDTH	TOP: 1.3 mm	BOTTOM: 1 mm

EXPERIMENT No. 5 (KERFING)	Date: 27/11/91
PLACE: IN AIR	TOOL: WATER JET
MATERIAL NATURE· COPPER	WATER DEPTH: - AIR VOLUME OF BASIN· 0.600 m^3 WATER VOLUME OF BASIN: 0.540 m^3 VENTILATION FLOW RATE: 24 $m^3.h^{-1}$
THICKNESS: 20 mm CUT LENGTH: 3 672 mm	
WATER PRESSURE: 3 000 bar WATER FLOW RATE: 1.63 ℓ/min	ABRASIVE NATURE: GARNET ABRASIVE FLOW RATE: 6.3 g/s

TOOL								
OPERATION	ABRASIVE		WATER		FOCUSING NOZZLE		OPERATION	
MODE AND POSITION	M6 mass used (g)	M'6 (g/m)	M7 mass used (g)	M'7 (g/m)	M5 mass loss (g)	M'5 (g/m)	CUTTING SPEED (mm/min)	TIME (min)
AUTOMATIC GRAVITY	9 980	2 693	42 900	11 683	0.0063	0.0017	140	26 3

SECONDARY EMISSIONS											
MATERIAL WEIGHT (g)			SEDIMENTED DROSS			EXHAUST WATER			SUSPENDED PARTICLES		
Before after	M0 Removed (g)	M'0 (g/m)	M1 (g)	M'1 (g/m)	M1/TC (%)	M2 (g)	M'2 (g/m)	M2/M7 (%)	M3 (g)	M'3 (g/m)	M3/TC (%)
4 736 4 154	582	158.5	982.1	2 674.6	99.1	715.6	194.9	1.7	92.3*	25.1*	0.9

* water under material

AEROSOLS								
FILTER Ø mm	SAMPLED MASS (mg)	SAMPLED VOLUME (m^3)	C1 gross (mg/m^3)	C0 background (mg/m^3)	C1 net (mg/m^3)	M4 (g) aerosol mass	M4 (g/m)	M4/TC (%)
Ø 47 Ø 130	12.33 34.5	0.2418 0.5637	51.0 61.2	0.06 0.08	50.9 61.1			
Integral Ø 160	428.8	9.03	47.49	0.055	47.4	0.499	0.136	5.10^{3}

TC = TOTAL SOLID MASS COLLECTED = M1 + M3 + M4 = 9 913.8 g
T1C1 = TOTAL SOLID MASS REMOVED = M0 + M6 = 10 472 g

$$\frac{TC}{T1C1} = 94.7\ \%$$

NOTES: KERFING DEPTH: 15-18 mm

KERF WIDTH	TOP· 1.2mm	BOTTOM: 0.9 mm

EXPERIMENT N° 11 (KERFING)	DATE: 02/06/1992
PLACE: UNDERWATER	TOOL: WATER JET
MATERIAL NATURE: COPPER	WATER DEPTH: 180 mm AIR VOLUME OF BASIN: 0.27 m³ WATER VOLUME OF BASIN: 0.85 m³ + 0.25 m³ VENTILATION FLOW RATE: 24 m³/h
THICKNESS: 20 mm CUT LENGTH: 21 252 mm	
WATER PRESSURE: 3000 bar WATER FLOW RATE: 1.63 ℓ/min	ABRASIVE NATURE: GARNET ABRASIVE FLOW RATE: 6.1 g/s

TOOL								
OPERATION MODE AND POSITION	ABRASIVE		WATER		FOCUSING NOZZLE		OPERATION	
	M6 mass used (g)	M'6 (g/m)	M7 mass used (g)	M'7 (g/m)	M5 mass loss (g)	M'5 (g/m)	CUTTING SPEED (mm/min)	TIME (min)
AUTOMATIC GRAVITY	55 510	2 612	248 000	11 669	0.035	0.0016	140	152

SECONDARY EMISSIONS											
MATERIAL WEIGHT (G)			SEDIMENTED DROSS			EXHAUST WATER			SUSPENDED PARTICLES		
Before after	M0 Removed (g)	M'0 (g/m)	M1 (g)	M'1 (g/m)	M1/TC (%)	M2 (g)	M'2 (g/m)	M2/M7 (%)	M3 (g)	M'3 (g/m)	M3/TC (%)
16 619 13 554	3 065	144.2	56 184	2 644	99.3	172.7	8.1	0.07	377.2	17.7	0.7

AEROSOLS								
FILTER mm	SAMPLED MASS (mg)	SAMPLED VOLUME (m³)	C1 gross (mg/m³)	C0 background (mg/m³)	C1 NET (mg/m³)	M4 (g) aerosol mass	M4 (g/m)	M4/TC (%)
Ø 47 Ø 130	NS NS							
Integral Ø 160	2.8	51.5	0.054	0.010	0.044	$2.3\ 10^{3}$	1.10^{-4}	4.10^{-4}

TC = TOTAL SOLID MASS COLLECTED = M1 + M3 + M4 = 56 561.2
T1C1 = TOTAL SOLID MASS REMOVED = M0 + M6 = 58 575

$\frac{TC}{T1C1} = 96.6\ \%$

NOTES: KERF DEPTH: 17 mm

KERF WIDTH	TOP:	BOTTOM:

NS = NOT SIGNIFICATIVE

EXPERIMENT N° 12 (KERFING)	DATE: 03/06/1992
PLACE: UNDERWATER	TOOL: WATER JET
MATERIAL NATURE: COPPER	WATER DEPTH: 180 mm AIR VOLUME OF BASIN: 0.27 m³ WATER VOLUME OF BASIN: 0.85 m³ VENTILATION FLOW RATE: 24 m³/h
THICKNESS: 20 mm CUT LENGTH: 2 500 mm	
WATER PRESSURE: 3000 bar WATER FLOW RATE: 1.63 ℓ/min	ABRASIVE NATURE: GARNET ABRASIVE FLOW RATE: 9.7 g/s

TOOL								
OPERATION MODE AND POSITION	ABRASIVE		WATER		FOCUSING NOZZLE		OPERATION	
	M6 mass used (g)	M'6 (g/m)	M7 mass used (g)	M'7 (g/m)	M5 mass loss (g)	M'5 (g/m)	CUTTING SPEED (mm/min)	TIME (min)
AUTOMATIC GRAVITY	10 500	4 200	54 000	21 600	0.004	0.0016	140	18*

* + 15 min without abrasives

SECONDARY EMISSIONS											
MATERIAL WEIGHT (G)			SEDIMENTED DROSS			EXHAUST WATER			SUSPENDED PARTICLES		
Before after	M0 Removed (g)	M'0 (g/m)	M1 (g)	M'1 (g/m)	M1/TC (%)	M2 (g)	M'2 (g/m)	M2/M7 (%)	M3 (g)	M'3 (g/m)	M3/TC (%)
16 633 16 594	39	15.6				NS					

AEROSOLS								
FILTER mm	SAMPLED MASS (mg)	SAMPLED VOLUME (m³)	C1 gross (mg/m³)	C0 background (mg/m³)	C1 NET (mg/m³)	M4 (g) aerosol mass	M4 (g/m)	M4/TC (%)
Ø 47 Ø 130	NS NS							
Integral Ø 160	0.6	13.97	0.043	0.010	0.033	$4.6\ 10^{-4}$	$1.8\ 10^{-4}$	

TC = TOTAL SOLID MASS COLLECTED = M1 + M3 + M4 =
T1C1 = TOTAL SOLID MASS REMOVED = M0 + M6 =

$\frac{TC}{T1C1} =$

NOTES: 1) Vacuum cleaner + cartridges + direct hood with suction
2) The vacuum cleaner was not operating correctly because the pump was sucking air coming from the cutting head
3) The abrasive tube was disconnected after 18 minutes

KERF WIDTH	TOP:	BOTTOM:

NS = NOT SIGNIFICATIVE

EXPERIMENT N° 13 (KERFING)	DATE: 03/06/1992
PLACE: UNDERWATER	TOOL: WATER JET
MATERIAL NATURE: COPPER	WATER DEPTH: 180 mm AIR VOLUME OF BASIN: 0.27 m³ WATER VOLUME OF BASIN: 0.85 m³ + 0.25 m³ VENTILATION FLOW RATE: 24 m³/h
THICKNESS: 20 mm CUT LENGTH: 21 252 mm	
WATER PRESSURE: 3000 bar WATER FLOW RATE: 1.63 ℓ/min	ABRASIVE NATURE: GARNET ABRASIVE FLOW RATE: 6.8 g/s

TOOL								
OPERATION MODE AND POSITION	ABRASIVE		WATER		FOCUSING NOZZLE		OPERATION	
	M6 mass used (g)	M'6 (g/m)	M7 mass used (g)	M'7 (g/m)	M5 mass loss (g)	M'5 (g/m)	CUTTING SPEED (mm/min)	TIME (min)
AUTOMATIC GRAVITY	62 090	2 922	248 000	11 669	0.035	0.0016	140	152

SECONDARY EMISSIONS											
MATERIAL WEIGHT (G)			SEDIMENTED DROSS			EXHAUST WATER			SUSPENDED PARTICLES		
Before after	M0 Removed (g)	M'0 (g/m)	M1 (g)	M'1 (g/m)	M1/TC (%)	M2 (g)	M'2 (g/m)	M2/M7 (%)	M3 (g)	M'3 (g/m)	M3/TC (%)
16 611 13 364	3 247	152.8	64 835	3 051	97.2	249.3	11.7	0.1	1 874.4	88.2	2.8

AEROSOLS								
FILTER mm	SAMPLED MASS (mg)	SAMPLED VOLUME (m³)	C1 gross (mg/m³)	C0 background (mg/m³)	C1 NET (mg/m³)	M4 (g) aerosol mass	M4 (g/m)	M4/TC (%)
Ø 47 Ø 130	NS NS							
Integral Ø 160	1.0	53.75	0.019	0.010	0.009	4.7 10^{-4}	2.2 10^{5}	7.10^{7}

TC = TOTAL SOLID MASS COLLECTED = M1 + M3 + M4 = 66 709.4
T1C1 = TOTAL SOLID MASS REMOVED = M0 + M6 = 65 337

$$\frac{TC}{T1C1} = 102\ \%$$

NOTES: 1) Vacuum cleaner + cartridges + suction at basin side
2) Hood at the cutting head
3) M1: 4 844 g in cartridge / 756 g in hopper / 59 235 g in basin
4) Vacuum cleaner flow rate: Start: 450 ℓ/min, End: 90 ℓ/min
5) Kerf depth : 17 mm

KERF WIDTH	TOP:	BOTTOM:

NS = NOT SIGNIFICATIVE

EXPERIMENT N° 14 (KERFING)	DATE: 04/06/1992
PLACE: UNDERWATER	TOOL: WATER JET
MATERIAL NATURE: COPPER	WATER DEPTH: 180 mm AIR VOLUME OF BASIN: 0.27 m³ WATER VOLUME OF BASIN: 0.85 m³ + 0.25 m³ VENTILATION FLOW RATE: 24 m³/h
THICKNESS: 100 mm CUT LENGTH: 3 036 mm	
WATER PRESSURE: 3000 bar WATER FLOW RATE: 1.63 ℓ/min	ABRASIVE NATURE: GARNET ABRASIVE FLOW RATE: 6.6 g/s

TOOL								
OPERATION MODE AND POSITION	ABRASIVE		WATER		FOCUSING NOZZLE		OPERATION	
	M6 mass used (g)	M'6 (g/m)	M7 mass used (g)	M'7 (g/m)	M5 mass loss (g)	M'5 (g/m)	CUTTING SPEED (mm/min)	TIME (min)
AUTOMATIC GRAVITY	60 050	19 779	248 000	81 686	0.028	0.0092	20	152

SECONDARY EMISSIONS											
MATERIAL WEIGHT (G)			SEDIMENTED DROSS			EXHAUST WATER			SUSPENDED PARTICLES		
Before after	M0 Removed (g)	M'0 (g/m)	M1 (g)	M'1 (g/m)	M1/TC (%)	M2 (g)	M'2 (g/m)	M2/M7 (%)	M3 (g)	M'3 (g/m)	M3/TC (%)
29 171 26 957	2 214	729.2	59 746	19 679	99.5	248.7	81.9	0.1	319.5	105.2	0.5

AEROSOLS								
FILTER mm	SAMPLED MASS (mg)	SAMPLED VOLUME (m³)	C1 gross (mg/m³)	C0 background (mg/m³)	C1 NET (mg/m³)	M4 (g) aerosol mass	M4 (g/m)	M4/TC (%)
Ø 47 Ø 130	NS NS							
Integral Ø 160	1.8	53.75	0.033	0.010	0.023	1.3 10^{-3}	4.2 10^{4}	2.10^{-4}

TC = TOTAL SOLID MASS COLLECTED = M1 + M3 + M4 = 60 065.5
T1C1 = TOTAL SOLID MASS REMOVED = M0 + M6 = 62 264.0

$$\frac{TC}{T1C1} = 96.5\%$$

NOTES: KERF DEPTH: 70 mm

KERF WIDTH	TOP:	BOTTOM:

NS = NOT SIGNIFICATIVE

EXPERIMENT N° 15 (KERFING)	DATE: 04/06/1992
PLACE: UNDERWATER	TOOL: WATER JET
MATERIAL NATURE: COPPER	WATER DEPTH: 180 mm AIR VOLUME OF BASIN: 0.27 m³ WATER VOLUME OF BASIN: 0.85 m³ + 0.25 m³ VENTILATION FLOW RATE: 24 m³/h
THICKNESS: 20 mm CUT LENGTH: 21 252 mm	
WATER PRESSURE: 3000 bar WATER FLOW RATE: 1.63 ℓ/min	ABRASIVE NATURE: GARNET ABRASIVE FLOW RATE: 6.2 g/s

TOOL								
OPERATION MODE AND POSITION	ABRASIVE		WATER		FOCUSING NOZZLE		OPERATION	
	M6 mass used (g)	M'6 (g/m)	M7 mass used (g)	M'7 (g/m)	M5 mass loss (g)	M'5 (g/m)	CUTTING SPEED (mm/min)	TIME (min)
AUTOMATIC GRAVITY	54 840	2 580	253 000	11 905	0.028	0.0013	140	155

SECONDARY EMISSIONS											
MATERIAL WEIGHT (G)			SEDIMENTED DROSS			EXHAUST WATER			SUSPENDED PARTICLES		
Before after	M0 Removed (g)	M'0 (g/m)	M1 (g)	M'1 (g/in)	M1/TC (%)	M2 (g)	M'2 (g/m)	M2/M7 (%)	M3 (g)	M'3 (g/m)	M3/TC (%)
16 615 13 929	2 686	126.4	49 128	2 312	99.4	321.2	15.1	0.13	293.9	13.8	0.6

AEROSOLS								
FILTER mm	SAMPLED MASS (mg)	SAMPLED VOLUME (m³)	C1 gross (mg/m³)	C0 background (mg/m³)	C1 NET (mg/m³)	M4 (g) aerosol mass	M4 (g/m)	M4/TC (%)
Ø 47 Ø 130	NS NS							
Integral Ø 160	0.7	53.75	0.013	0.010	0.003	$1.7\ 10^{-4}$	$9.\ 10^{-6}$	3.10^{-7}

TC = TOTAL SOLID MASS COLLECTED = M1 + M3 + M4 = 49 421.9
T1C1 = TOTAL SOLID MASS REMOVED = M0 + M6 = 57 526.0

$$\frac{TC}{T1C1} = 85.9\%$$

NOTES: 1) Vacuum cleaner without cartridge, Flow rate: 350 ℓ/min
2) M1: 34 106 g in hopper, 15 022 g in basin
3) Suction by hood running behind cutting head
4) Kerf depth: 17 mm

KERF WIDTH	TOP:	BOTTOM:

NS = NOT SIGNIFICATIVE

EXPERIMENT N° 16 (KERFING)	DATE: 05/06/1992
PLACE: UNDERWATER	TOOL: WATER JET
MATERIAL NATURE: COPPER	WATER DEPTH: 180 mm AIR VOLUME OF BASIN: 0.27 m³ WATER VOLUME OF BASIN: 0.85 m³ + 0.5 m³ VENTILATION FLOW RATE: 24 m³/h
THICKNESS: 20 mm CUT LENGTH: 21 252 mm	
WATER PRESSURE: 3000 bar WATER FLOW RATE: 1.63 ℓ/min	ABRASIVE NATURE: GARNET ABRASIVE FLOW RATE: 2.05 g/s

TOOL								
OPERATION MODE AND POSITION	ABRASIVE		WATER		FOCUSING NOZZLE		OPERATION	
	M6 mass used (g)	M'6 (g/m)	M7 mass used (g)	M'7 (g/m)	M5 mass loss (g)	M'5 (g/m)	CUTTING SPEED (mm/min)	TIME (min)
AUTOMATIC GRAVITY	36 210	1 704	480 000	22 586	0.022	0.0010	70	301

SECONDARY EMISSIONS											
MATERIAL WEIGHT (G)			SEDIMENTED DROSS			EXHAUST WATER			SUSPENDED PARTICLES		
Before after	M0 Removed (g)	M'0 (g/m)	M1 (g)	M'1 (g/m)	M1/TC (%)	M2 (g)	M'2 (g/m)	M2/M7 (%)	M3 (g)	M'3 (g/m)	M3/TC (%)
16 594 14 093	2 501	117.7	36 118	1 700	99.3	1 565.2	73.6	0.33	266.3	12.5	0.7

AEROSOLS								
FILTER mm	SAMPLED MASS (mg)	SAMPLED VOLUME (m³)	C1 gross (mg/m³)	C0 background (mg/m³)	C1 NET (mg/m³)	M4 (g) aerosol mass	M4 (g/m)	M4/TC (%)
Ø 47 Ø 130	NS NS							
Integral Ø 160	1.1	107.8	0.010	0.010	2.10^{-4}	$2.2\ 10^{-5}$	1.10^{-6}	6.10^{-8}

TC = TOTAL SOLID MASS COLLECTED = M1 + M3 + M4 = 36 384.3
T1C1 = TOTAL SOLID MASS REMOVED = M0 + M6 = 38 711

$$\frac{TC}{T1C1} = 94\%$$

NOTES: 1) Vacuum cleaner without cartridge, Flow rate: 350 ℓ/min
2) M1: 23 146 g in hopper, 12 972 g in basin
3) Suction by hood running behind cutting head
4) Kerf depth: 17 mm

KERF WIDTH	TOP:	BOTTOM:

NS = NOT SIGNIFICATIVE

ANNEX 2

Chemical analysis of the waste

Réf.	Exp. n° 1 Microgrammes totaux			Exp. n° 6/7 Microgrammes totaux			Exp. n° 2 Microgrammes totaux			Exp. n° 10 Microgrammes totaux		
N°	Cu	Fe	Mg	Cu	Fe	Mg	Cu	Fe	Mg	Cu	Fe	Mg
0	< 1	65	80	7	700	930	110	980	870	73	800	800
1	< 1	65	80	7	820	770	60	865	910	38	700	700
2	< 1	60	80	6	590	820	43	900	1020	25	900	1200
3	< 1	60	80	7	625	900	41	860	960	15	900	900
4	< 1	65	80	7	700	950	35	980	860	34	800	1100
5	< 1	75	100	7	740	880	24	750	960	23	800	1000
6	< 1	65	80	6	610	875	20	680	930	11	900	1200
7	< 1	60	75	7	660	880	15	720	1070	11	800	1100
Fin	< 1	70	80	7	660	900	14	670	930	3	800	1100
Blanc	< 1	10	10	6	650	850	6	650	850	6	650	850

Réf.	Exp. n° 8 Microgrammes totaux				Exp. n° 3 Microgrammes totaux				Exp.	Filtres diamètre 160 mm milligrammes totaux				
N°	Cr	Fe	Mg	Ni	Cr	Fe	Mg	Ni	N°	Cr	Cu	Fe	Mg	Ni
0	450	5800	1500	230	< 10	100	70	< 10						
1	240	3400	1250	110	< 10	95	60	< 10	1		0.01	0.17	6.0	
2	170	2600	1100	70	< 10	87	70	< 10	5		44.3	73.3	20.2	
3	160	2200	700	33	< 10	84	60	< 10	6/7		0.21	0.98	9.4	
4	90	1700	1050	40	< 10	96	70	< 10	2		6.2	28.5	11.1	
5	45	1100	970	45	< 10	90	80	< 10	8	6.50	0.001	164	17.1	3.6
6	20	730	920	25	< 10	60	80	< 10	3	0.37	0.11	19.7	10.3	0.3
7	18	660	880	26	< 10	50	80	< 10	9		3.05	14.3	9.2	
Fin	17	710	540	50	< 10	50	80	< 10	10		2.4	10.1	11.0	
Blanc	17	540	730	16	< 10	8	6	< 10	Blanc	0.015	<0.001	0.15	6.1	< 0.01

Référence	Cu	Fe	Mg	Unité
Eau propre	26	< 5	4.4	Microgrammes/litres
Exp. n° 1 (520 ml)				
Surnageant	480	< 5	5.8	Microgrammes/litres
Dépôt	25	77	10	Milligrammes
Exp. n° 6/7 (520 ml)				
Surnageant	500	< 5	4.8	Microgrammes/litres
Dépôt	8.2	21	3.1	Milligrammes

CENTRE D'ETUDES DE SACLAY

D.C.C. / D.P.E.
S.P.E.A / S.A.I.S
Laboratoire d'Analyses Physico-Chimiques

Saclay, le 3 novembre 1992

R.A. 92-142

Analyse de filtres diamètre 80 mm

Série 11	Cu	Fe	Mg
filtre 0	1,06	0,60	1,25
filtre 1	1,32	0,60	1,22
filtre 2	1,52	0,77	1,37
filtre 3	2,06	0,80	1,63
filtre 4	2,49	1,30	1,50
filtre 5	2,22	1,12	1,45
filtre 6	2,05	1,62	1,49
filtre 7	1,80	1,12	1,27
11 F millipore	1,85	1,77	1,97
11 F pall	5,35	8,37	16,8

Série 13	Cu	Fe	Mg
Filtre 0	1,12	0,60	1,12
filtre 1	1,30	0,60	1,47
filtre 2	1,32	1,02	1,60
filtre 3	1,55	1,07	1,62
filtre 4	1,47	1,55	1,70
filtre 5	1,32	1,22	1,87
filtre 6	1,40	1,72	1,87
filtre 7	1,12	2,17	1,77
F millipore	2,05	3,00	3,30
F pall	0,82	12,5	31,3

Série 14	Cu	Fe	Mg
filtre 0	0,65	1,45	0,95
filtre 1	0,55	0,75	0,75
filtre 2	0,60	0,87	1,22
filtre 3	0,70	1,10	1,42
filtre 4	1,00	2,02	2,90
filtre 5	0,92	1,60	1,90
filtre 6	0,75	1,62	2,02
filtre 7	0,80	1,52	2,05
F millipore	1,00	3,00	4,25
F pall	1,22	10,9	27,3

D.C.C. / D.P.E.
S.P.E.A / S.A.I.S
Laboratoire d'Analyses Physico-Chimiques

R.A. 92-142

Analyse de filtres diamètre 80 mm

Série 15	Cu	Fe	Mg
filtre 0	1,15	1,12	1,55
filtre 1	1,37	1,92	1,62
filtre 2	1,87	2,05	2,00
filtre 3	2,80	2,42	2,55
filtre 4	3,15	2,67	3,05
filtre 5	1,70	1,42	2,02
filtre 6	1,00	1,47	1,50
filtre 7	0,70	0,62	1,30
F millipore	1,62	2,42	2,50
F pall	0,92	11,4	23,3

Série 16	Cu	Fe	Mg
filtre 0	1,40	0,98	1,20
filtre 1	1,50	0,92	1,30
filtre 2	2,40	1,50	1,52
filtre 3	4,00	1,87	1,92
filtre 4	5,70	2,45	2,57
filtre 5	3,87	1,90	1,97
filtre 6	2,40	1,40	1,70
filtre 7	1,45	0,95	1,37
F millipore	2,70	1,87	3,25
F pall	0,85	9,38	25,3

Analyse de filtres diamètre 160 mm

Référence	Cu	Fe	Mg
BDF pall	4,45	10,2	23,9
BDF millipore	3,90	12,4	9,50
BDF nuit pall	14,9	47,9	32,4
BDF nuit millipore	5,00	10,5	7,20
11 pall	4,80	10,2	32,9
11 millipore	36,4	20,3	17,9
12 pall	5,40	18,5	35,3
12 millipore	7,95	10,9	12,4
13 pall	4,45	9,90	27,5
13 millipore	15,9	15,6	17,0
14 pall	3,40	10,5	25,8
14 millipore	9,40	20,7	25,1
15 pall	4,50	9,0	26,6
15 millipore	20,9	19,9	19,0
16 pall	7,50	11,8	34,2
16 millipore	41,6	31,3	23,7
filtre blanc pall	1,80	11,4	40,0
filtre blanc millipore	1,90	2,70	2,60

D.C.C. / D.P.E.
S.P.E.A / S.A.I.S
Laboratoire d'Analyses Physico-Chimiques

R.A. 92-142

Analyse de filtres diamètre 47 mm

Référence	Cuivre	Fer
mouvement propre	1,10	24,2
bruit de fond nuit	11,0	66,0
filtre 11	4,22	24,2
filtre 12	2,25	25,0
filtre 13	3,50	24,6
filtre 14	2,12	27,2
filtre 15	5,25	23,9
filtre 16	10,5	40,0
(Pour mémoire:)		
blanc filtre	0,92	21,6

Analyse de filtres diamètre 130 mm

Référence	Cuivre	Fer
mouvement propre	1,37	5,62
bruit de fond nuit	35,4	85,2
filtre 11	16,0	9,65
filtre 12	2,40	6,12
filtre 13	3,18	5,07
filtre 14	1,95	5,37
filtre 15	3,33	5,87
filtre 16	6,21	8,07

Les résultats sont exprimés en microgrammes recueillis sur le filtre.

Limites de confiance (p=0,95): 0,3 microgramme.

D.C.C. / D.P.E.
S.P.E.A / S.A.I.S
Laboratoire d'Analyses Physico-Chimiques

C.R. N° 92-142

Analyse de solutions de découpe et de dépôts.

Référence	Cu	Fe	Mg
Solution	µg/l	µg/l	µg/l
11 (475 ml)	605	<20	6620
13 (50 ml)	430	135	6880
14 (475 ml)	835	<20	6720
15 (475 ml)	600	<20	6480
16 (525 ml)	815	<20	6560
Dépôt	mg	mg	mg
11	20,3	44,9	7,60
13	32,0	130	20,2
14	16,9	41,4	6,80
15	25,4	55,1	9,00
16	17,8	25,6	4,10

Ecart-type relatif sur les mesures: 2 %

C. BLAIN
Responsable du laboratoire

D.C.C. / D.P.E.
S.P.E.A / S.A.I.S
Laboratoire d'Analyses Physico-Chimiques

F.A.R, le 18 décembre 1992

R.A. N° 92-010

Analyse de poudres tamisées

Référence	Cu %
1 A	12,2
1 W	11,0
2 A	6,7
2 W	9,8
3 A	2,0
3 W	5,2
4 A	0,09
4 W	0,17
5 A	0,02
5 W	0,02

Cuivre non dosable dans les échantillons 6 et 7. Présence d'un résidu insoluble (proportion >30 %) dans les échantillons 4 W, 5, 6 et 7.

C. BLAIN
Responsable du Laboratoire

ANNEX 3

Aerosol size distribution

Figure 10 - Aerosol size distribution based on chemical analysis for Fe
Experiment n° 16 (copper underwater kerfing, e = 20 mm, hood running after cutting head, abrasive flow rate = 2.05 g/s)

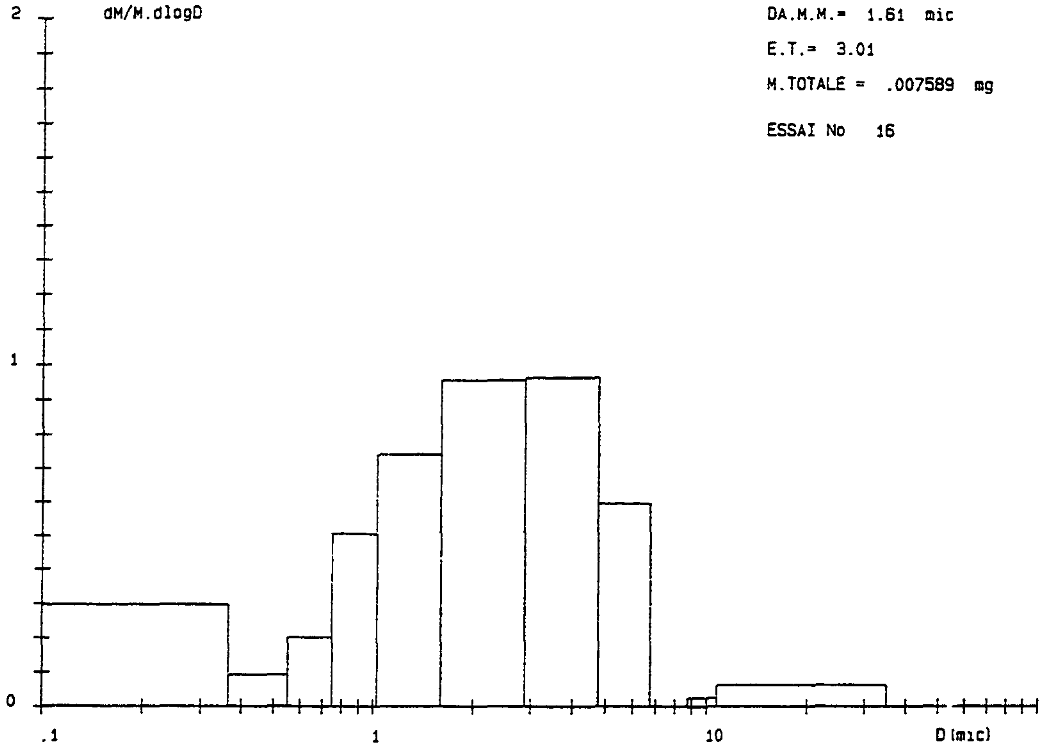

Figure 11 - Aerosol size distribution based on chemical analysis for Mg
Experiment n° 11 (copper underwater kerfing, e = 20 mm)

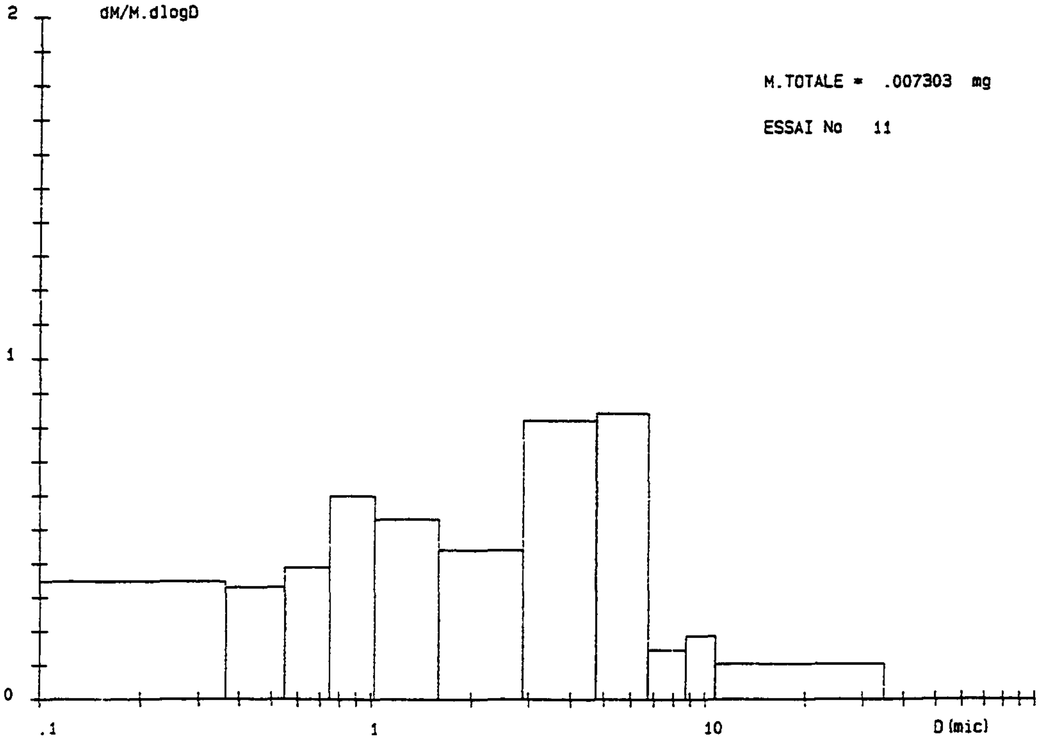

Figure 8 - Aerosol size distribution based on chemical analysis for Fe
Experiment n° 14 (copper underwater kerfing, e = 100 mm)

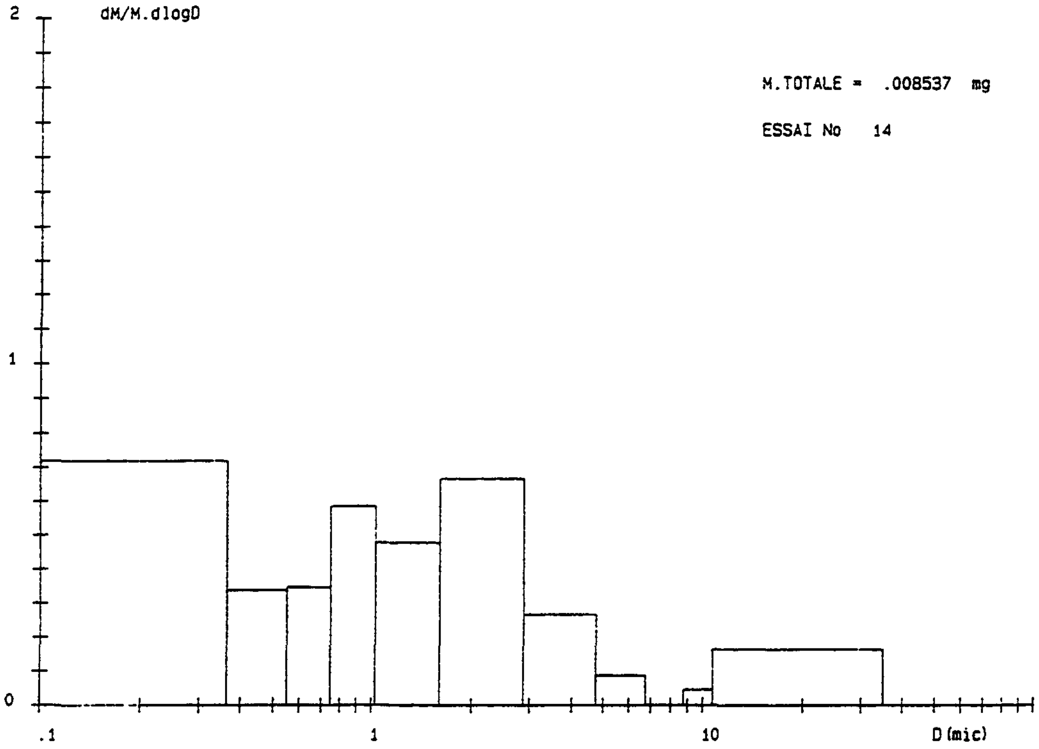

Figure 9 - Aerosol size distribution based on chemical analysis for Fe
Experiment n° 15 (copper underwater kerfing, e = 20 mm, hood running after cutting head)

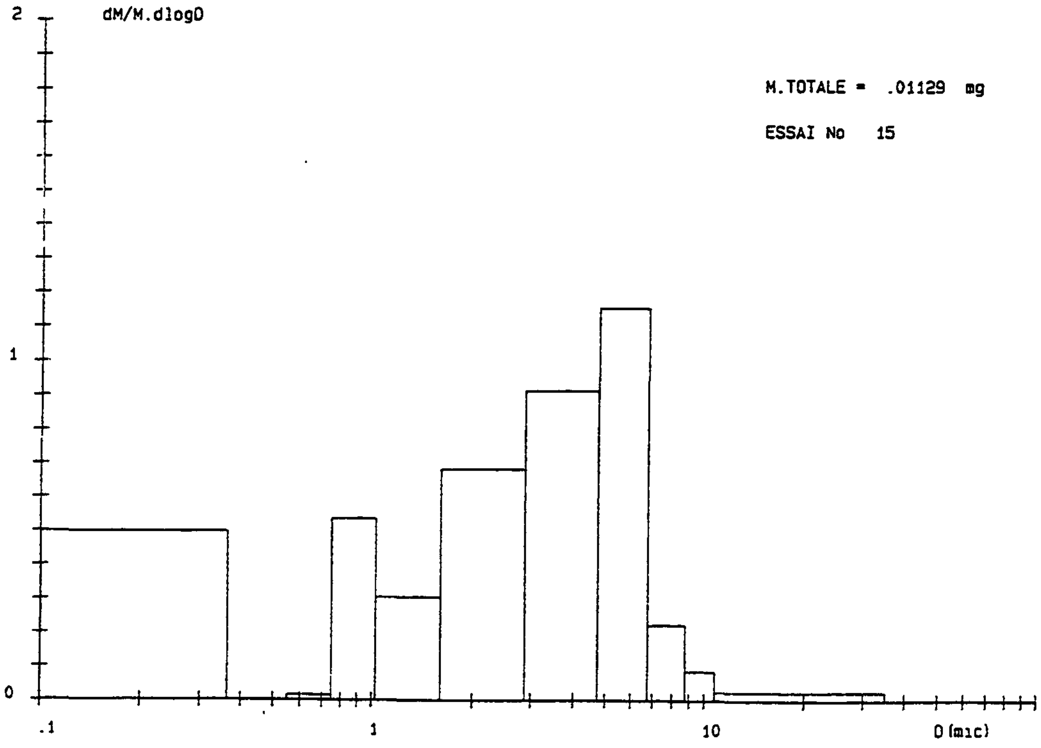

Figure 6 - Aerosol size distribution based on chemical analysis for Fe
Experiment n° 11 (copper underwater kerfing, e = 20 mm)

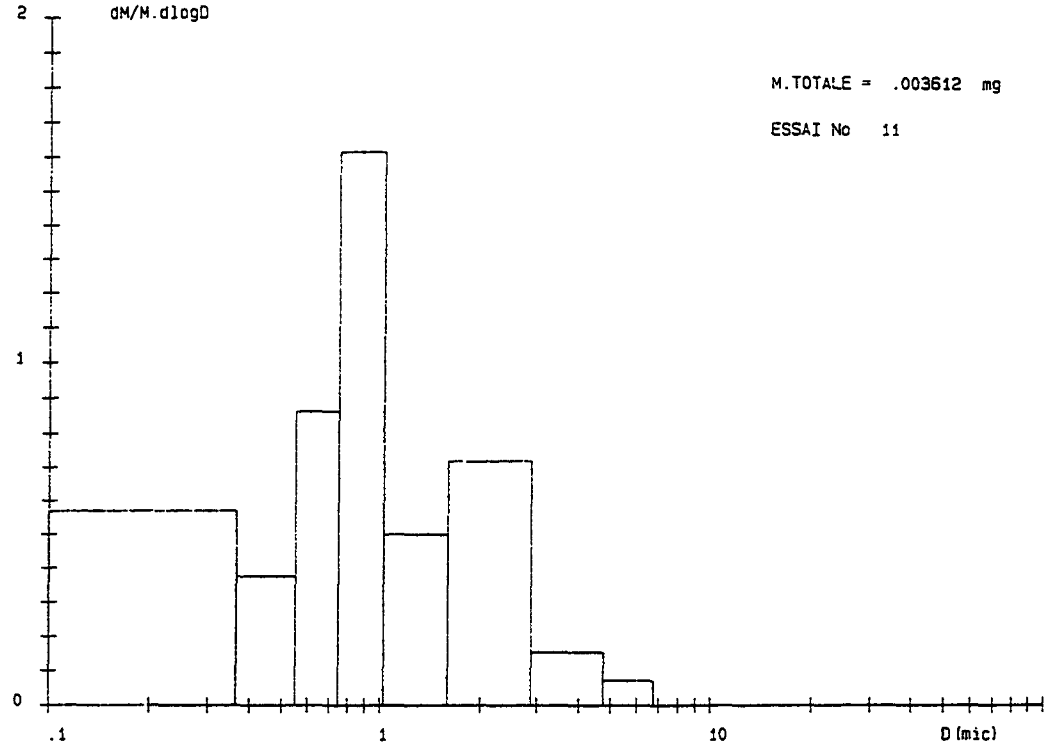

Figure 7 - Aerosol size distribution based on chemical analysis for Fe
Experiment n° 13 (copper underwater kerfing, e = 20 mm, independent hood at cutting head)

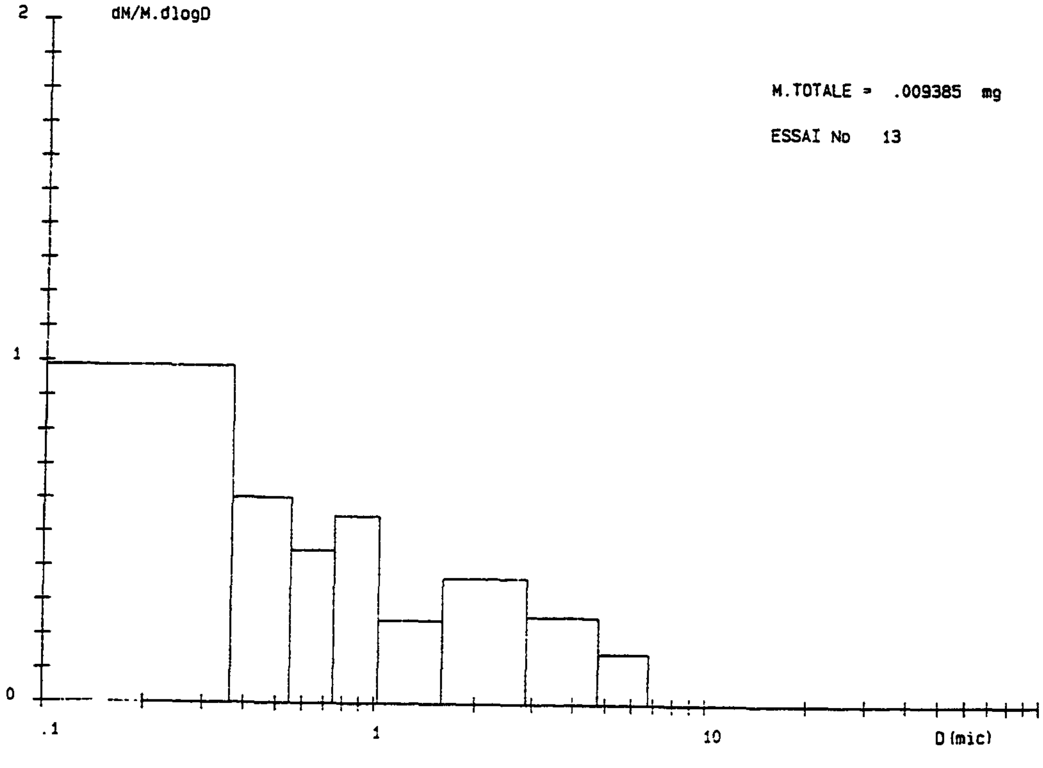

Figure 4 - Aerosol size distribution based on chemical analysis for Cu
Experiment n° 15 (copper underwater kerfing, e = 20 mm, hood running after cutting head)

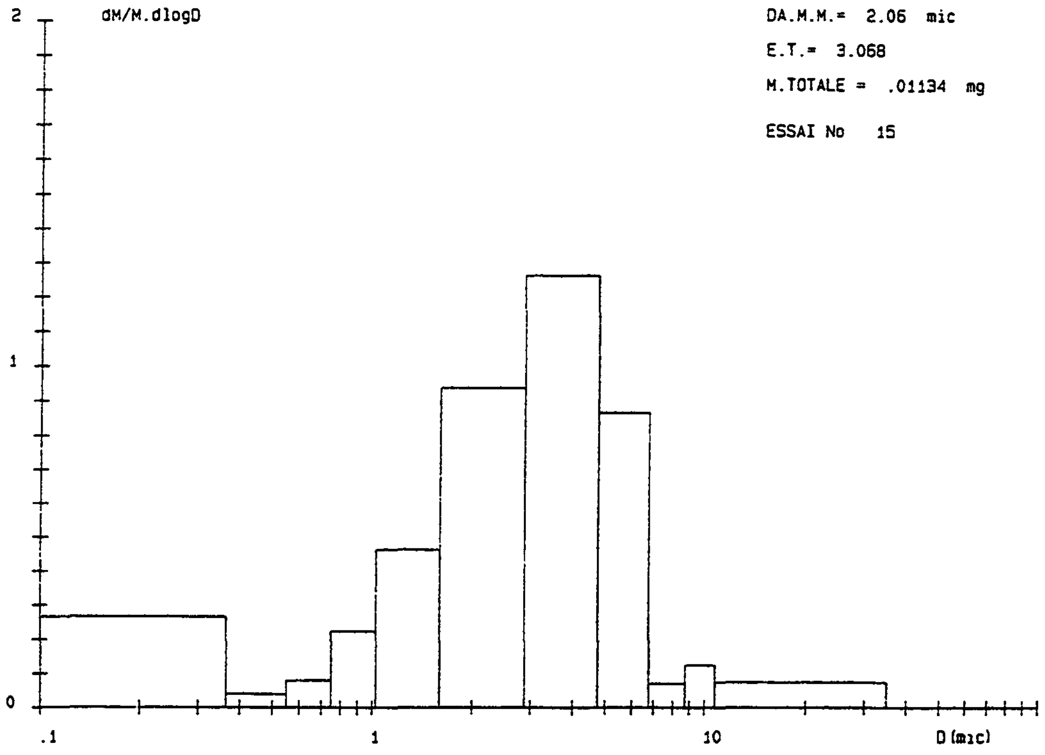

Figure 5 - Aerosol size distribution based on chemical analysis for Cu
Experiment n° 16 (copper underwater kerfing, e = 20 mm, hood running after cutting head, abrasive flow rate = 2.05 g/s)

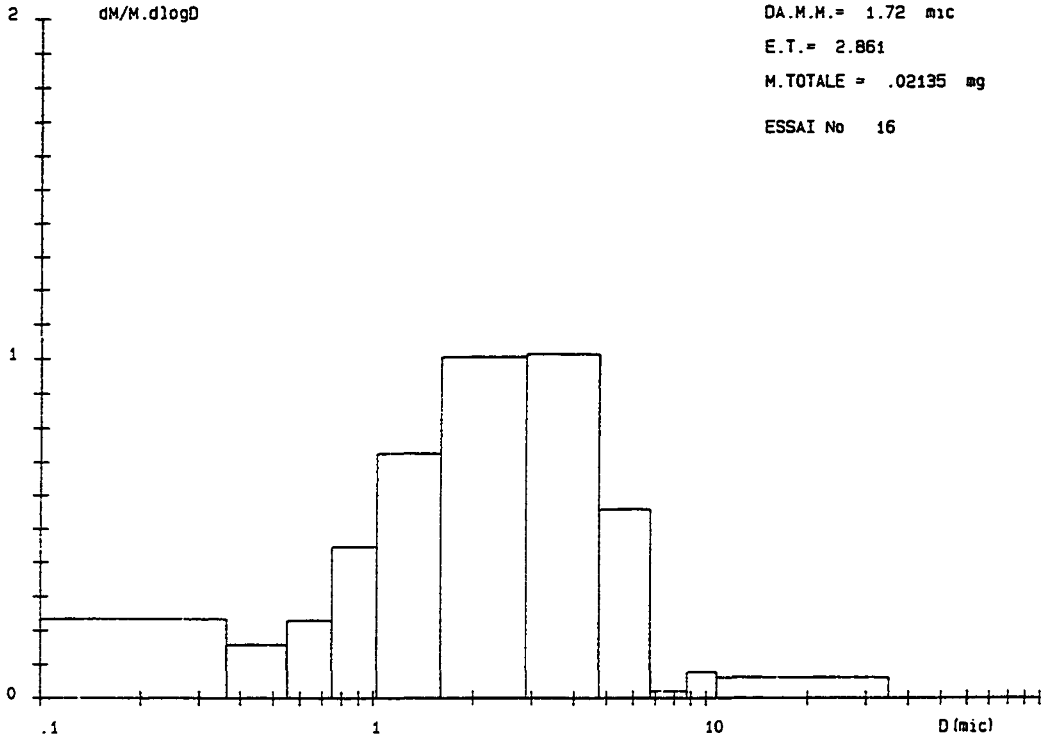

Figure 2 - Aerosol size distribution based on chemical analysis for Cu
Experiment n° 13 (copper underwater kerfing, e = 20 mm, independent hood at cutting head)

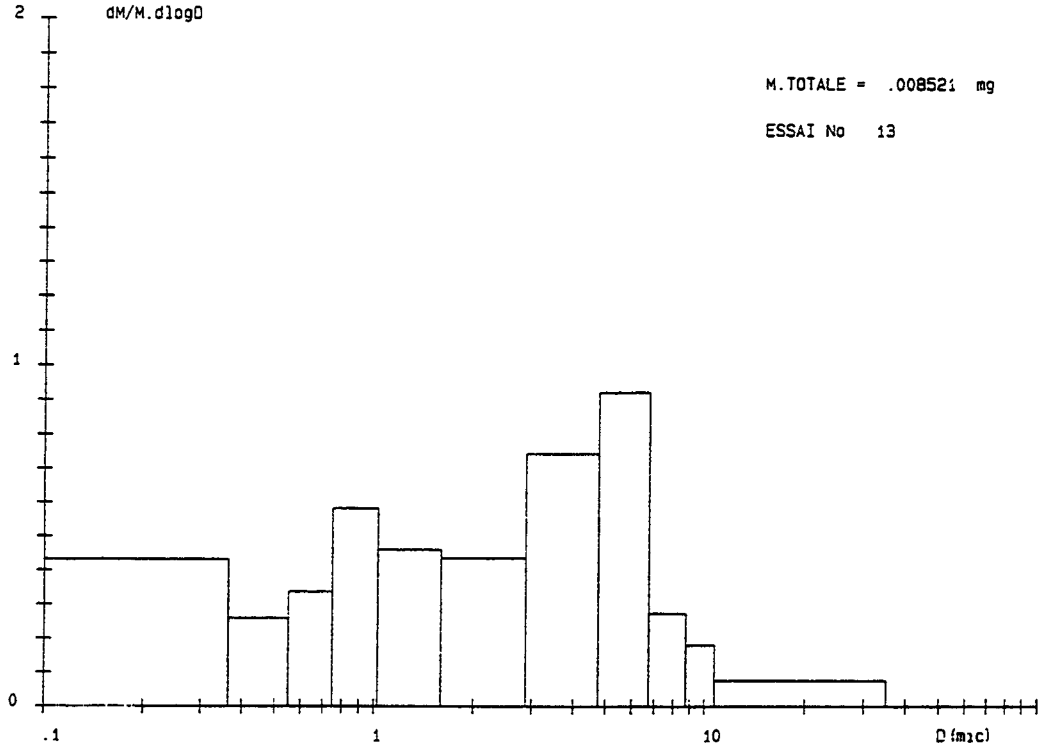

Figure 3 - Aerosol size distribution based on chemical analysis for Cu
Experiment n° 14 (copper underwater kerfing, e = 100 mm)

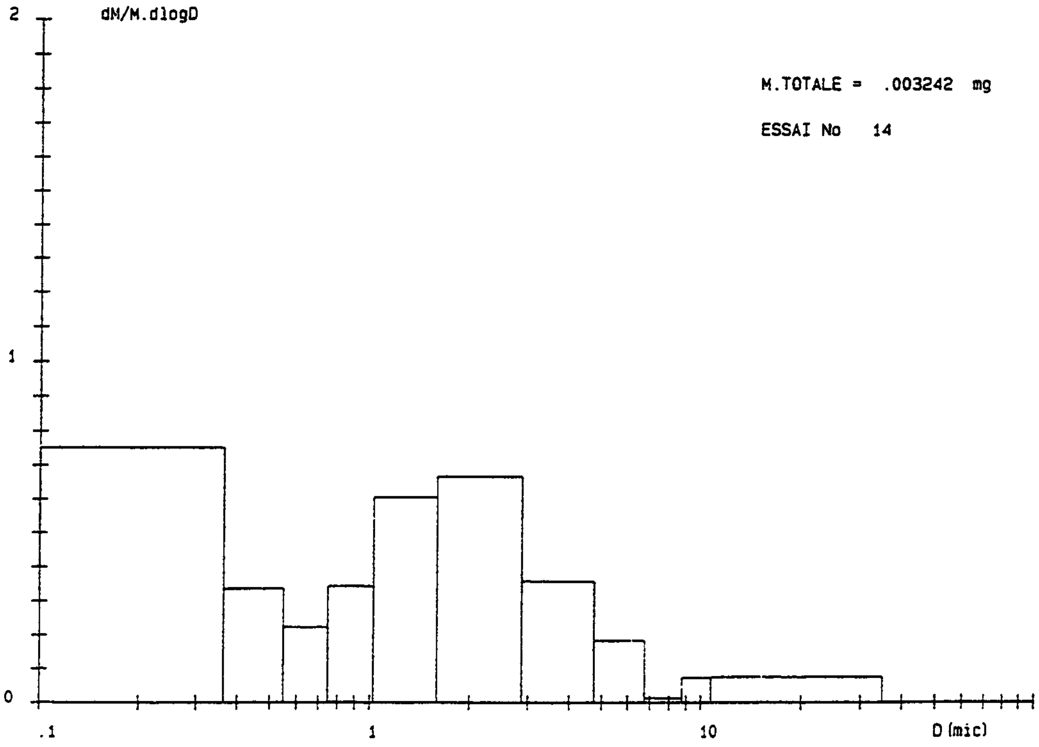

Figure 11 - Aerosol size distribution based on chemical analysis for Ni. Experiment n° 8 (steel kerfing in air, e = 20 mm)

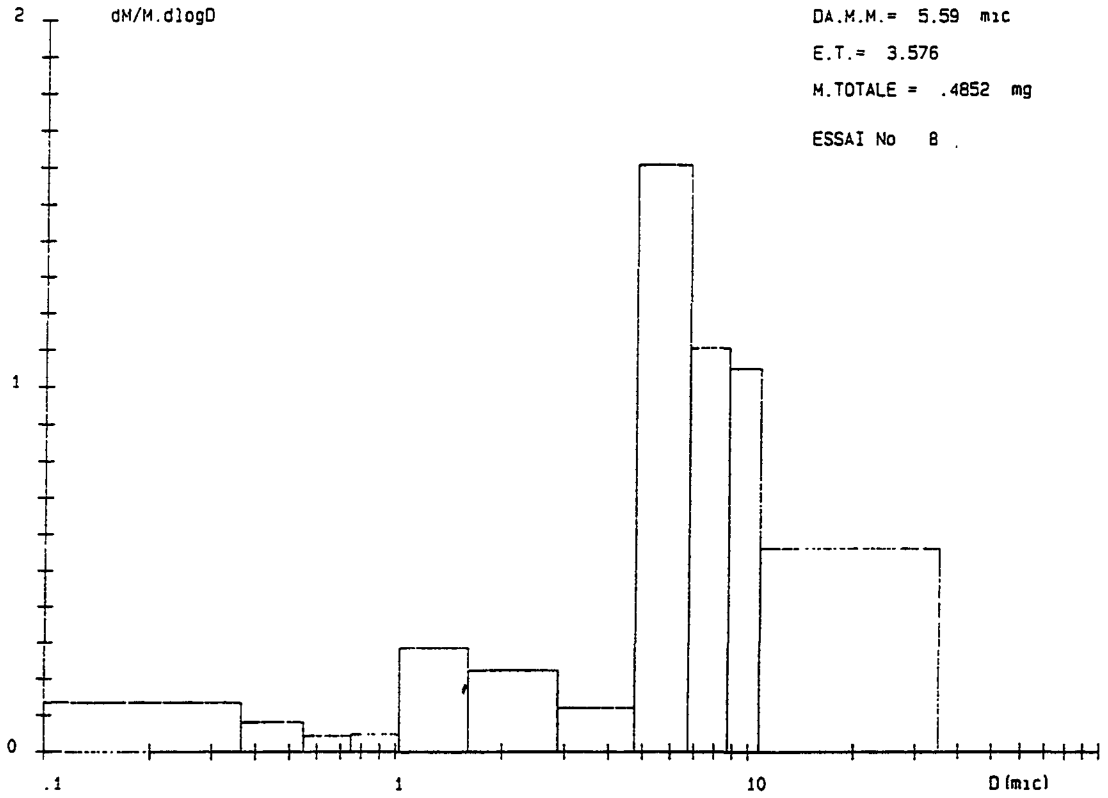

Figure 1 - Aerosol size distribution based on chemical analysis for Cu
Experiment n° 11 (copper underwater kerfing, e = 20 mm)

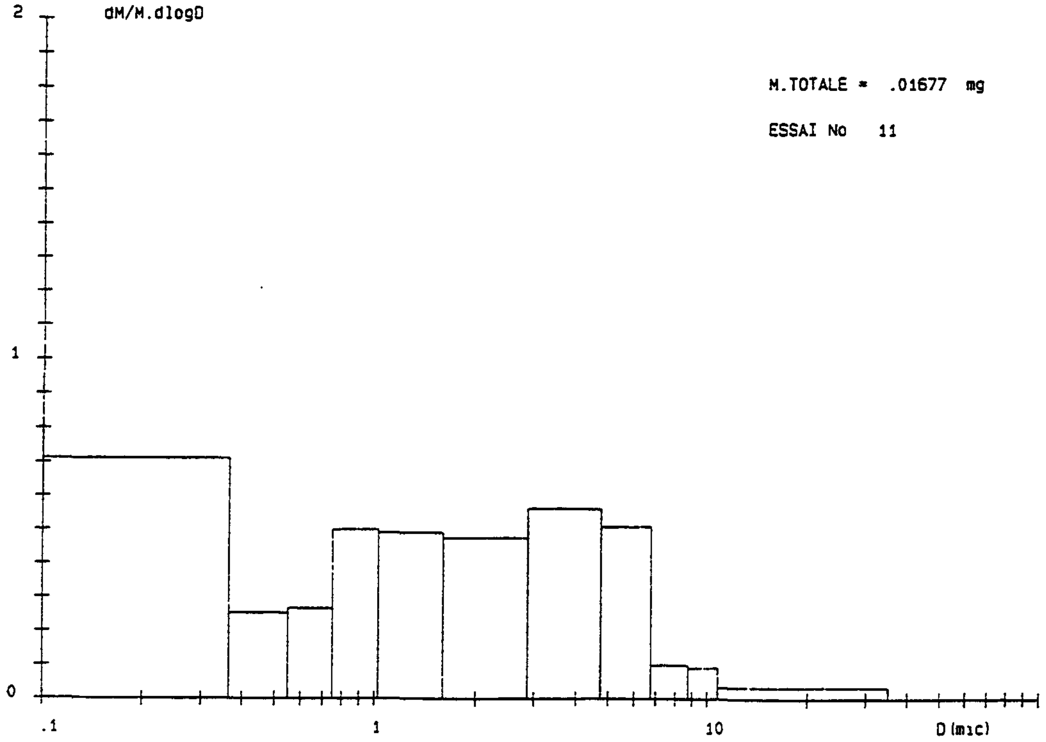

Figure 9 - Aerosol size distribution based on chemical analysis for Fe. Experiment n° 8 (steel kerfing in air, e = 20 mm)

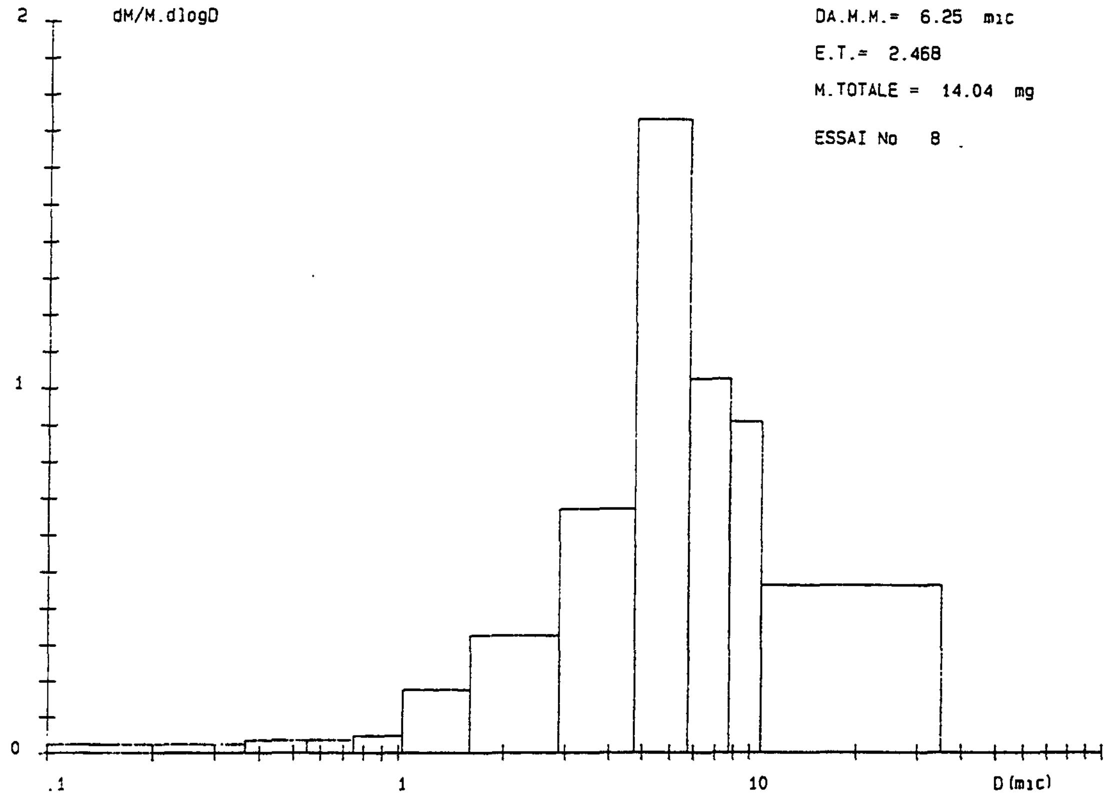

Figure 10 - Aerosol size distribution based on chemical analysis for Cr. Experiment n° 8 (steel kerfing in air, e = 20 mm)

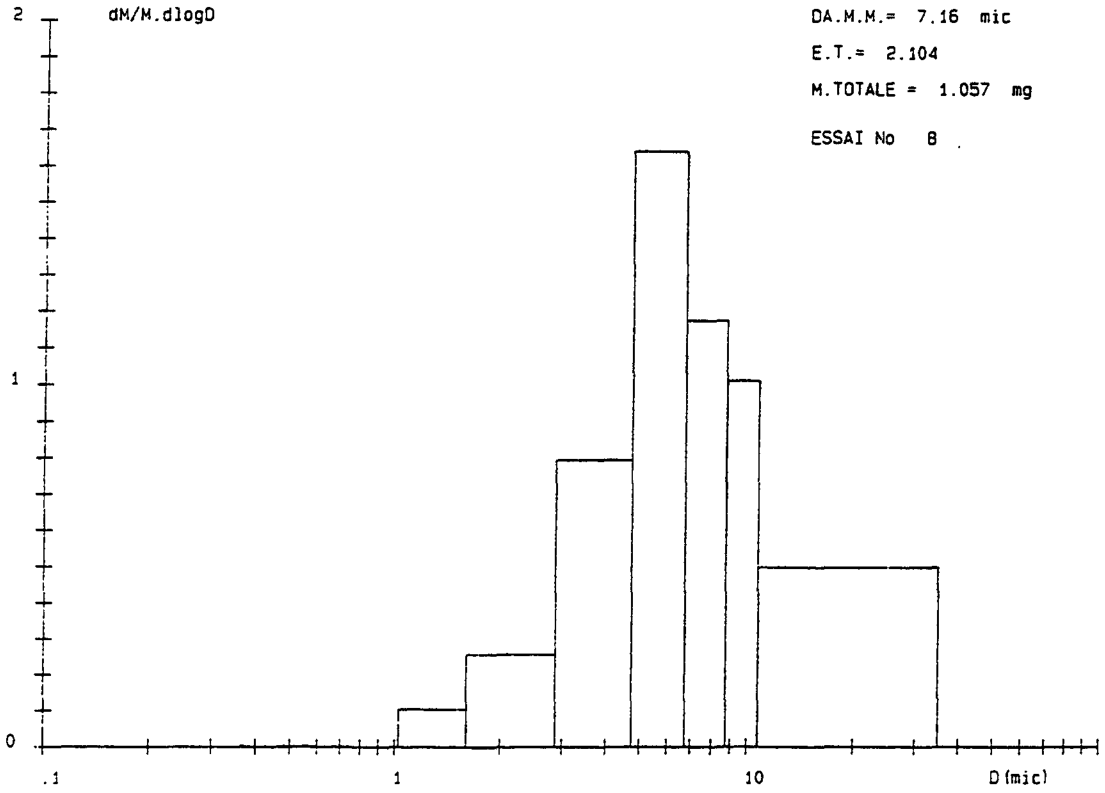

Figure 7 - Aerosol size distribution based on chemical analysis for Cu. Experiment n° 2 (conper cutting in air, e = 10 mm)

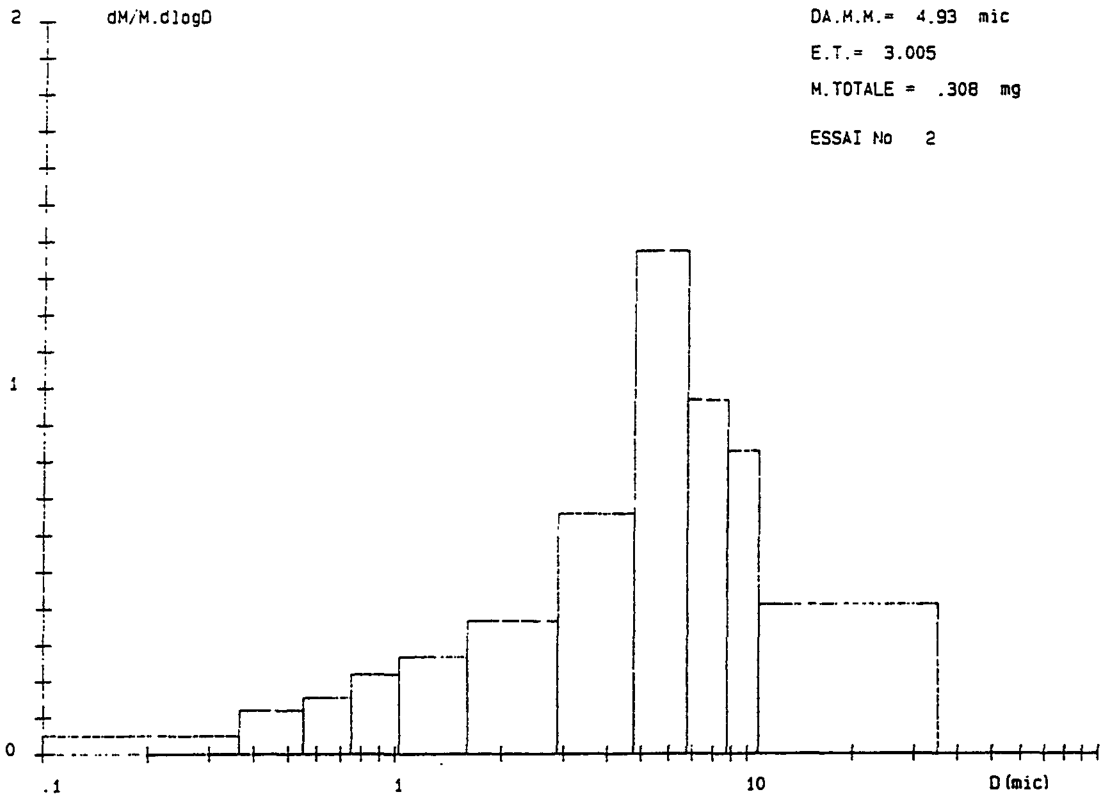

Figure 8 - Aerosol size distribution based on chemical analysis for Fe. Experiment n° 3 (steel cutting in air, e = 10 mm)

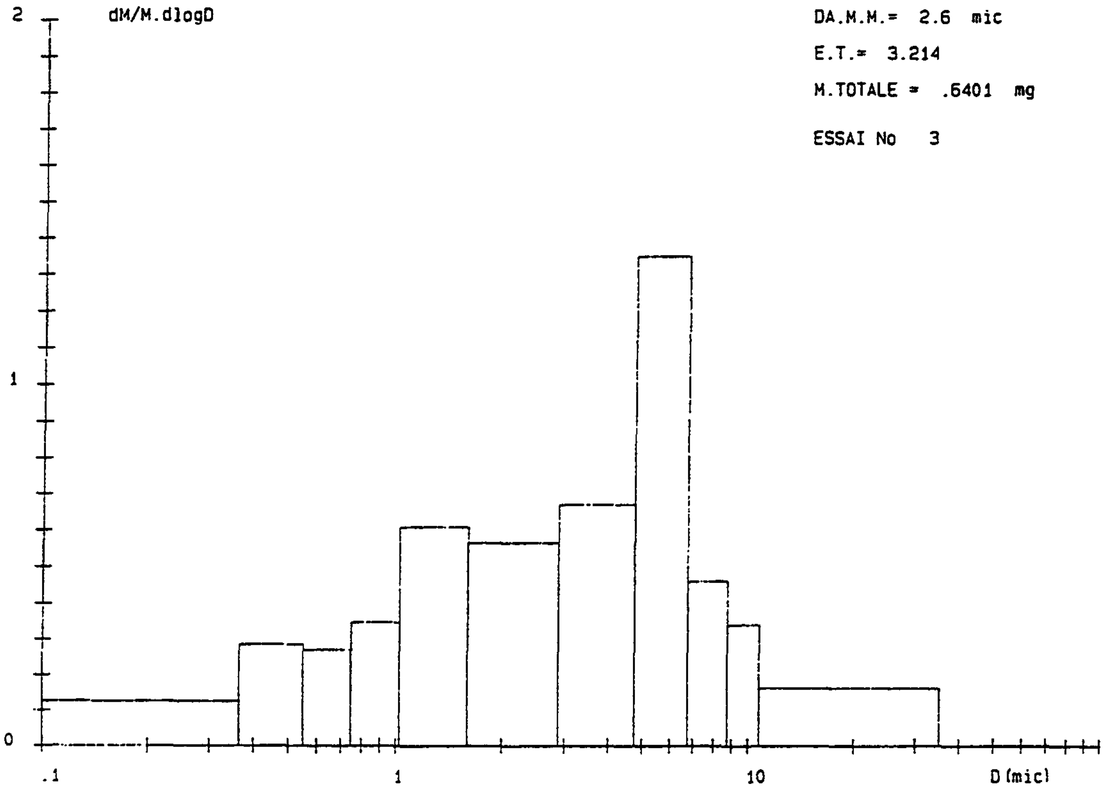

Figure 5 - Aerosol size distribution in mass for experiment n° 9 (copper cutting in air, e = 10 mm, abrasive flow rate = 3.4 g/s)

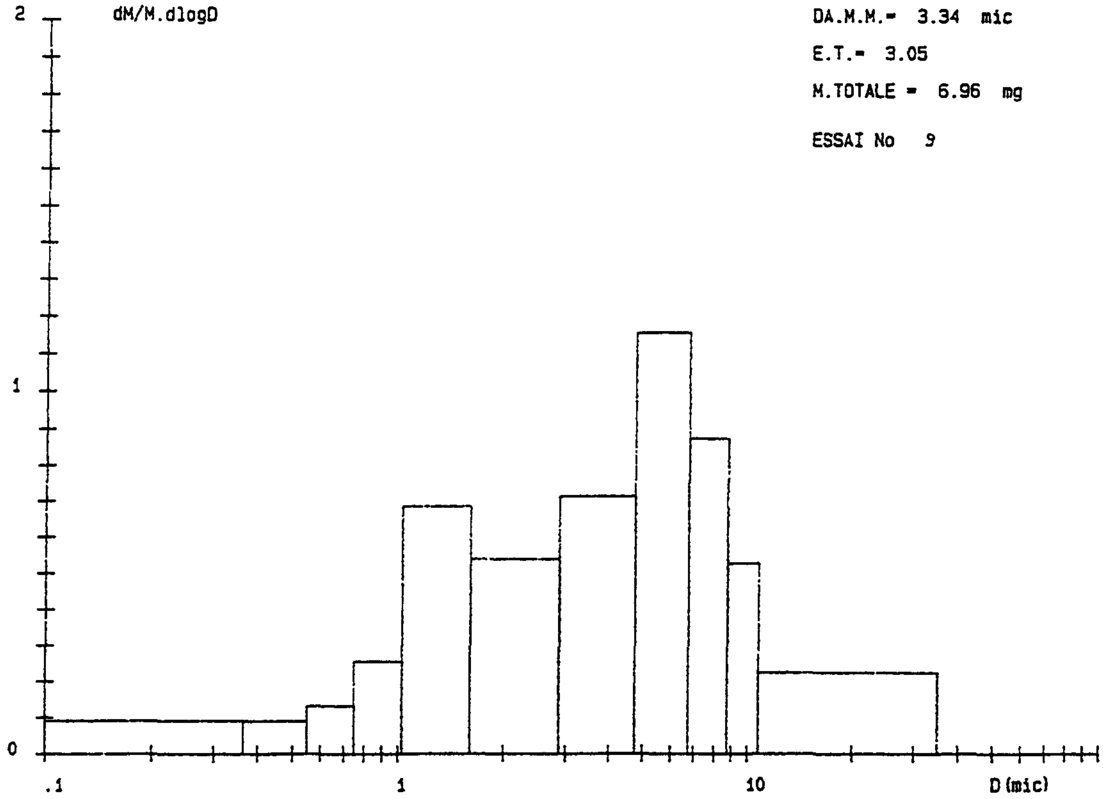

Figure 6 - Aerosol size distribution in mass for experiment n° 10 (copper cutting in air, e = 10 mm, abrasive flow rate = 1.8 g/s)

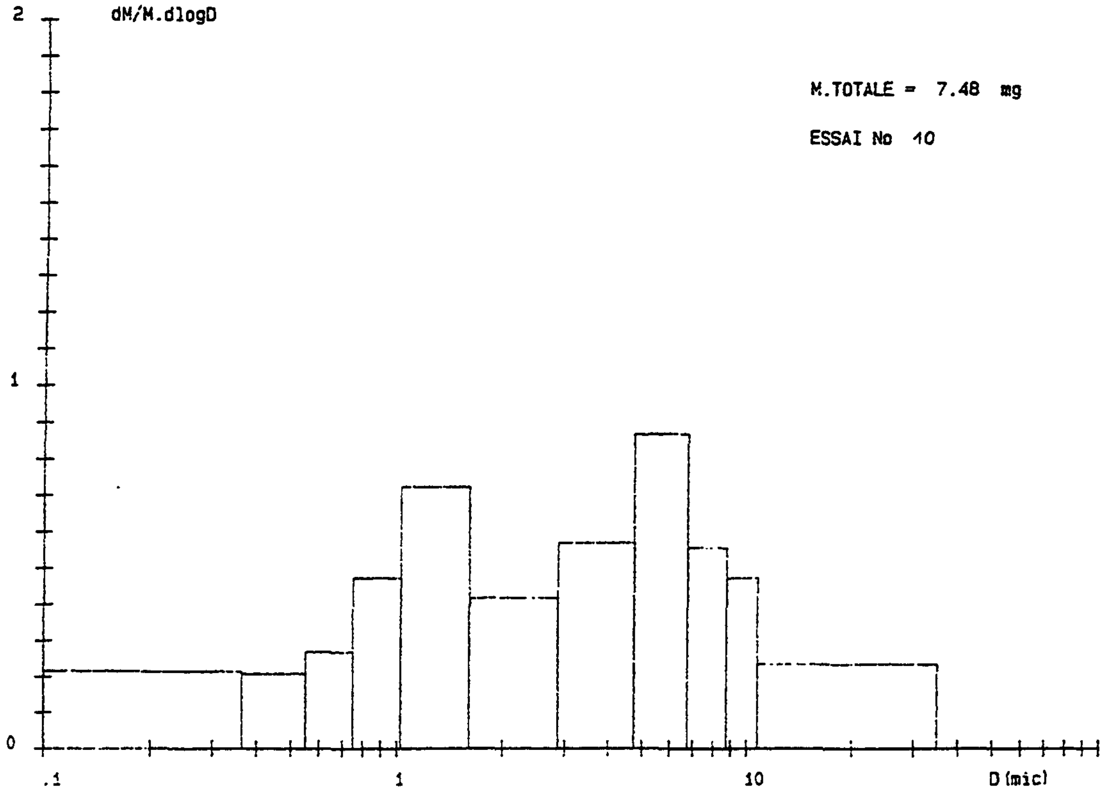

Figure 3 - Aerosol size distribution in mass for experiment n° 5 (copper kerfing in air, e = 20 mm)

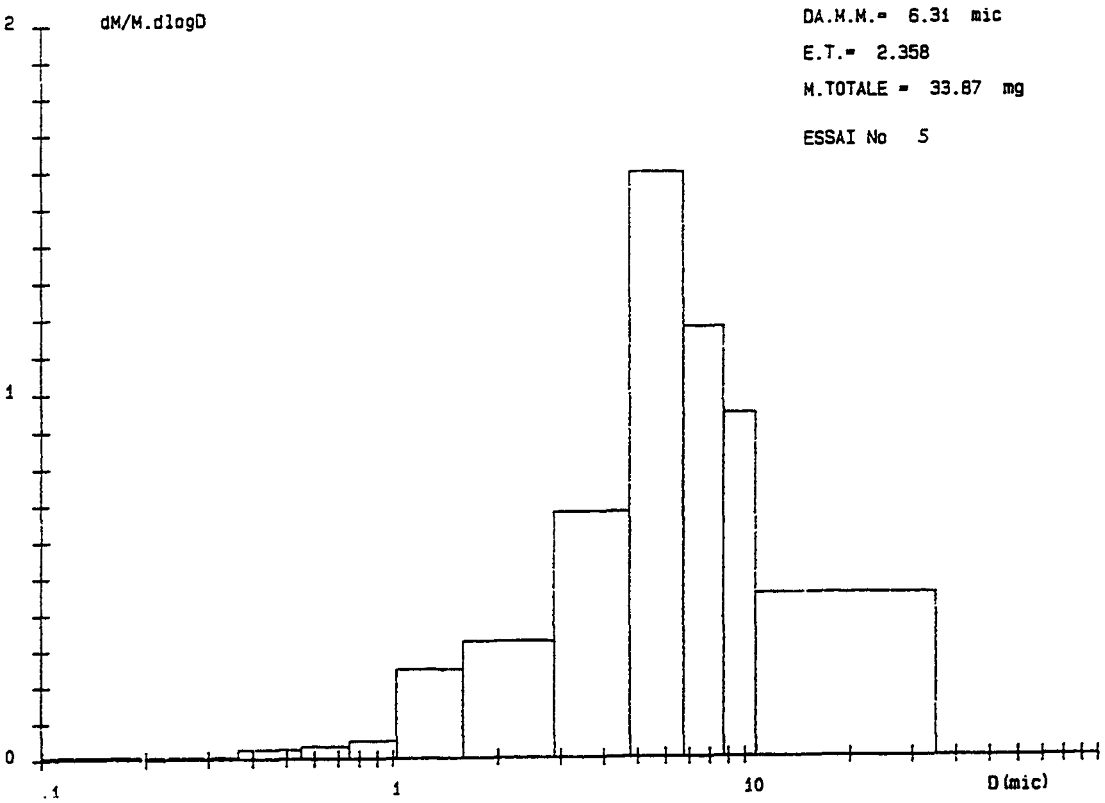

Figure 4 - Aerosol size distribution in mas for experiment n° 8 (steel kerfing in air, e = 20 mm)

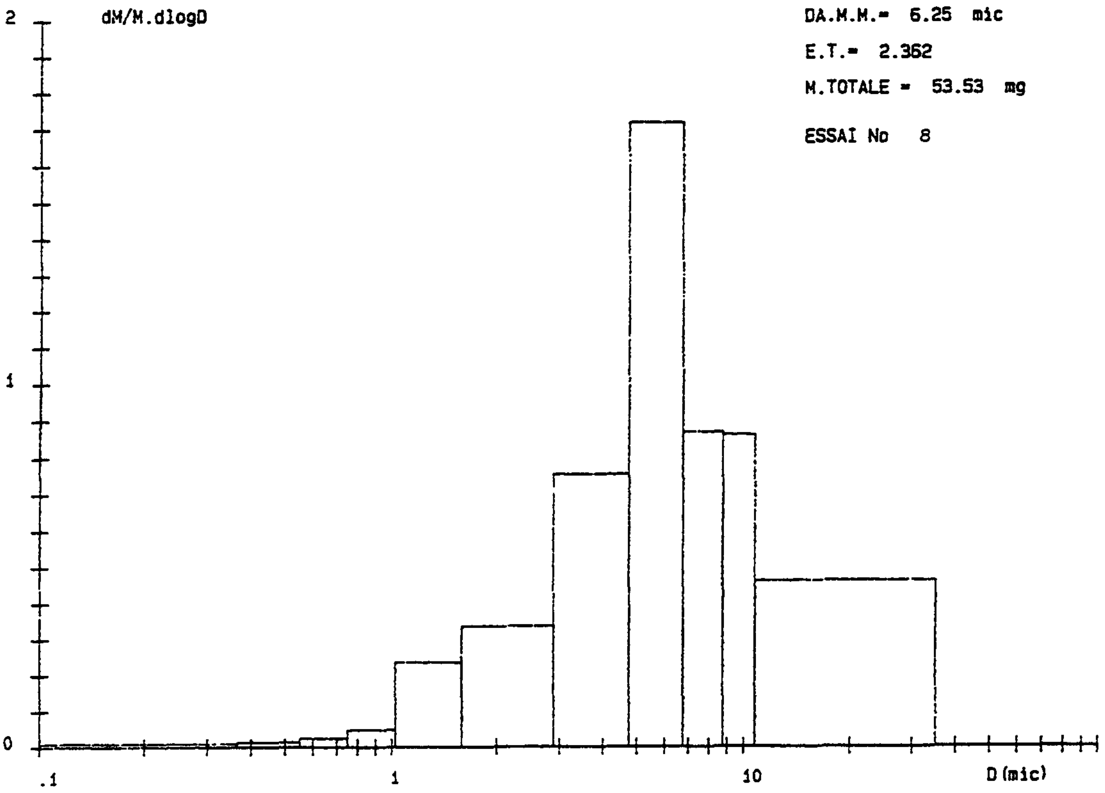

Figure 1 - Aerosol size distribution in mass for experiment n° 2 (copper cutting in air, e = 10 mm)

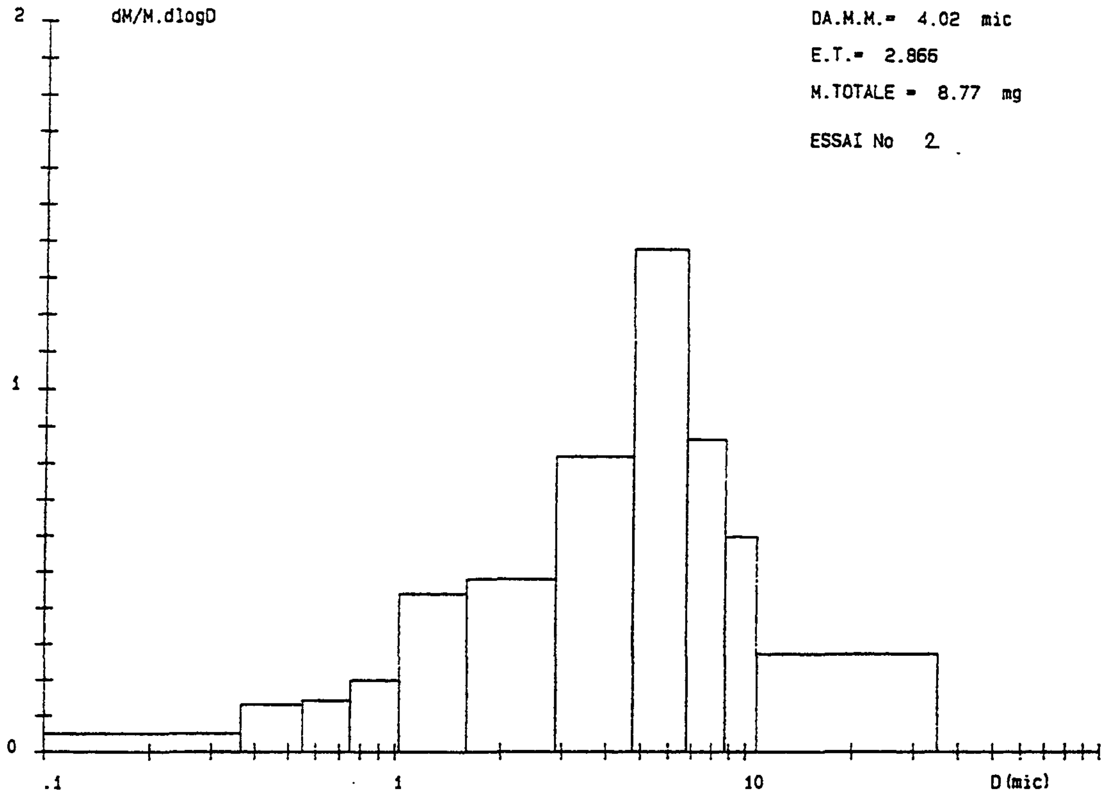

Aerosol size distribution

Figure 2 - Aerosol size distribution in mass for experiment n° 3 (steel cutting in air, e = 10 mm)

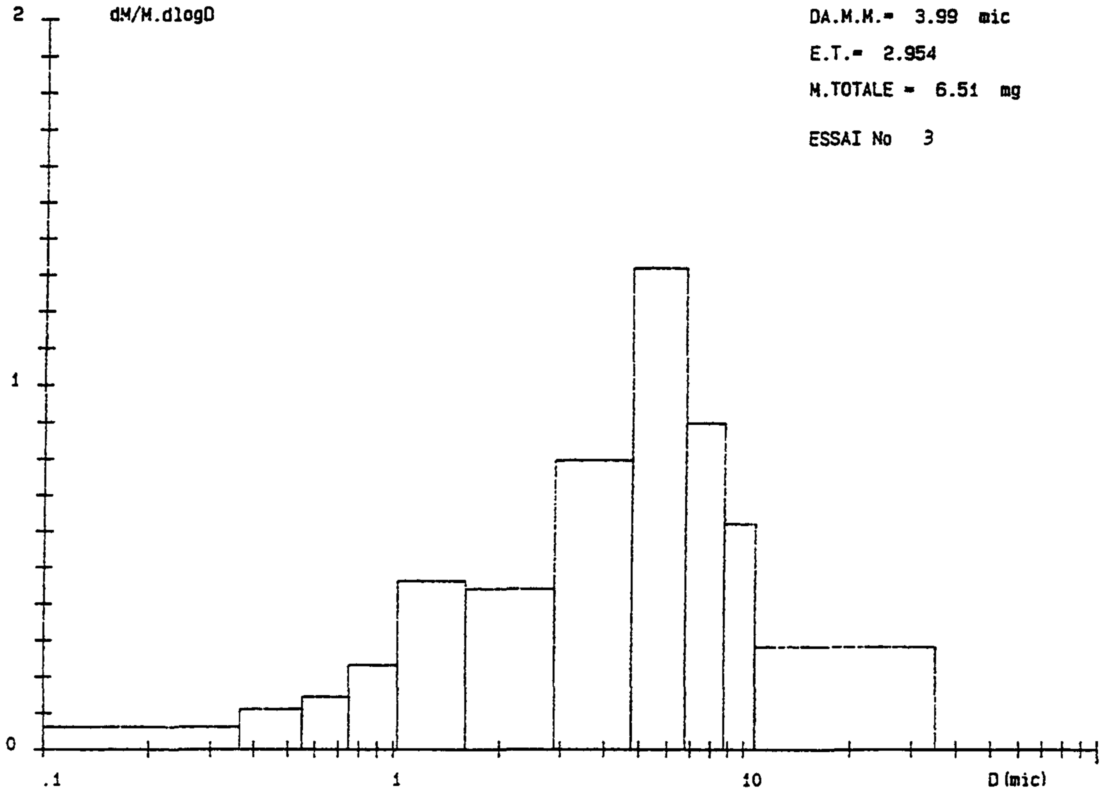

Figure 12 - Aerosol size distribution based on chemical analysis for Cu. Experiment n° 10 (copper cutting in air, e = 10 mm, abrasive flow rate = 1.8 g/s)

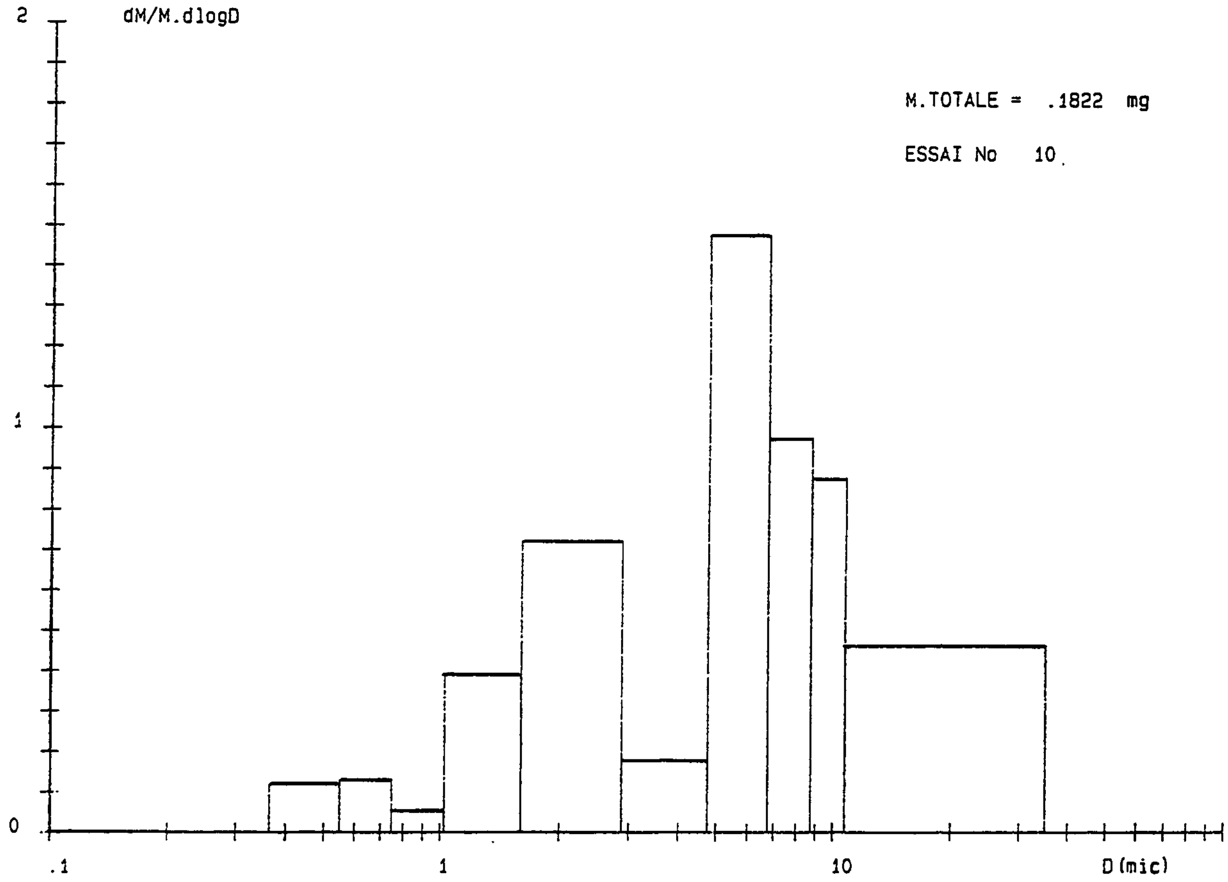

ANNEX 4

Data of cyclone

ASPIRATEUR SOUS EAU
UNDERWATER-VACUUMCLEANER
UNTERWASSER-ABSAUGGERÄT

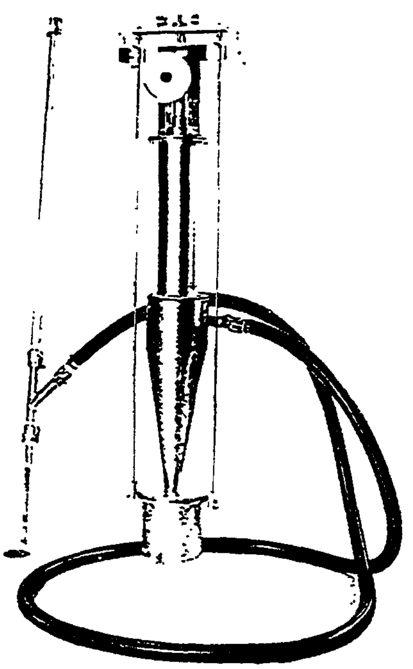

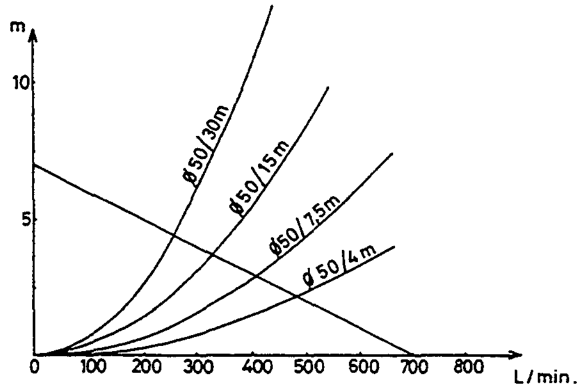

Caractéristiques techniques
Technical characteristics
Technische Daten

Puissance	: 2 CV
Courant	: 220 V ou 380 V alternatif - 50 périodes
Débit	: 400 l/min (7 m tuyau d'aspiration)
Dépression	: 0,5 kg/cm^2
Dimensions de particules	: 40 à 5000 µ m
Densité de particules	: 1,5 à 20 kp/cm^3
Efficacité du cyclône	: 95 - 98%
Poids total	: 100 kg.

Power	: 2 H. P.
Current	: 220 V or 380 V, 50 ph.
Flow	: 400 l/min (7 m suction hose)
Under pressure	: 0,5 Kg/cm^2
Particle sizes	: 40 - 5000 µ m
Density of particles	: 1,5 - 20 gm/cm^3
Efficiency of cyclone	: 95 - 98%
Total weight	: approx. 100 kg.

Leistung	: 2 PS
Anschluß	: 220 V oder 380 V, 50 Hz
Fördermenge	: 400 l/min (7 m Ansaugleitung)
Saugdruck	: 0,5 kp/cm^2
Partikel: Größe	: 40 : 5000 µ m
Dichte	: 1,5 : 20 kg/dm^3
Abscheidungswirkungsgrad	: 95 - 98%
Gesamtgewicht	: za. 100 kp

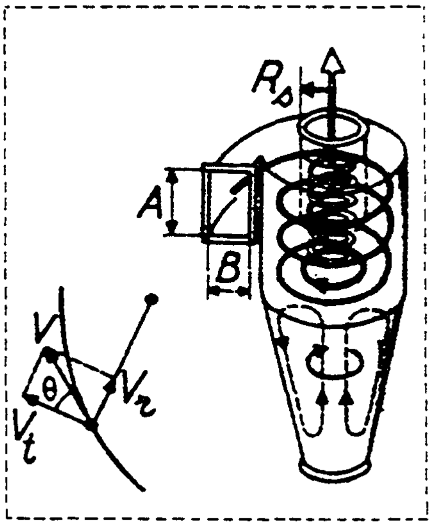

Construction entièrement en acier inoxydable
All stainless steel structure
Säurebeständige Stahlkonstruktion

C O R D I S

The Communities research and development information service

CORDIS

A vital part of your programme's dissemination strategy

CORDIS is the information service set up under the VALUE programme to give quick and easy access to information on European Community research programmes. It is available free-of-charge online via the European Commission host organization (ECHO), and now also on a newly released CD-ROM.

CORDIS offers the European R&D community:

— a comprehensive up-to-date view of EC R&TD activities, through a set of databases and related services,

— quick and easy access to information on EC research programmes and results,

— a continuously evolving Commission service tailored to the needs of the research community and industry,

— full user support, including documentation, training and the CORDIS help desk.

The CORDIS Databases are:

R&TD-programmes – R&TD-projects – R&TD-partners – R&TD-results
R&TD-publications – R&TD-comdocuments – R&TD-acronyms – R&TD-news

Make sure your programme gains the maximum benefit from CORDIS

— Inform the CORDIS unit of your programme initiatives,

— contribute information regularly to CORDIS databases such as R&TD-news, R&TD-publications and R&TD-programmes,

— use CORDIS databases, such as R&TD-partners, in the implementation of your programme,

— consult CORDIS for up-to-date information on other programmes relevant to your activities,

— inform your programme participants about CORDIS and the importance of their contribution to the service as well as the benefits which they will derive from it,

— contribute to the evolution of CORDIS by sending your comments on the service to the CORDIS Unit.

For more information about contributing to CORDIS,
contact the DG XIII CORDIS Unit

Brussels
Ms I. Vounakis
Tel. +(32) 2 299 0464
Fax +(32) 2 299 0467

Luxembourg
M. B. Niessen
Tel. +(352) 4301 33638
Fax +(352) 4301 34989

To register for online access to CORDIS, contact:

ECHO Customer Service
BP 2373
L-1023 Luxembourg
Tel. +(352) 3498 1240
Fax +(352) 3498 1248

If you are already an ECHO user, please mention your customer number.

European Commission

EUR 15241 — Abrasive water-jet cutting technique from the laboratory stage into real application

G. Meier, H. Louis, G. Pilot

Luxembourg: Office for Official Publications of the European Communities

1995 — IV, 101 pp., num. tab., fig. — 21.0 x 29.7 cm

Nuclear science and technology series

ISBN 92-827-0222-7

Price (excluding VAT) in Luxembourg: ECU 11.50

The objective of the project was to adapt and qualify the commercial abrasive water-jet cutting technique for application in nuclear decommissioning.

The cutting has to be remote controlled. Therefore, methods are required to control the state of the wear of the cutting tool as well as the cutting result.

Experiments have shown that sound analysis is not a sufficient method to check the cutting result (cutting through or kerfing only). But in the case of kerfing the reflected jet can be detected by a deflector plate and an adapted accelerometer. Abrasive water-jet cutting produces a small amount of aerosols, especially when cutting under water.

It was shown that using optimized cutting parameters to minimize the consumption of water and abrasives and separating the waste from the water by using a cyclone can considerably reduce the secondary waste generation. More investigation should be done to recycle the separated abrasives. First tests indicate that a recycling of 80 to 90% of the abrasives may be attainable.

Venta • Salg • Verkauf • Πωλήσεις • Sales • Vente • Vendita • Verkoop • Venda • Myynti • Försäljning

BELGIQUE / BELGIË

Moniteur belge/
Belgisch Staatsblad

Rue de Louvain 42/Leuvenseweg 42
B-1000 Bruxelles/B-1000 Brussel
Tél. (02) 512 00 26
Fax (02) 511 01 84

Jean De Lannoy

Avenue du Roi 202/Koningslaan 202
B-1060 Bruxelles/B-1060 Brussel
Tél. (02) 538 51 69
Fax (02) 538 08 41

Autres distributeurs/
Overige verkooppunten:

Librairie européenne/
Europese boekhandel

Rue de la Loi 244/Wetstraat 244
B-1040 Bruxelles/B-1040 Brussel
Tél. (02) 231 04 35
Fax (02) 735 08 60

Document delivery:

Credoc

Rue de la Montagne 34/Bergstraat 34
Boîte 11/Bus 11
B-1000 Bruxelles/B-1000 Brussel
Tél. (02) 511 69 41
Fax (02) 513 31 95

DANMARK

J. H. Schultz Information A/S

Herstedvang 10-12
DK-2620 Albertslund
Tlf. 43 63 23 00
Fax (Sales) 43 63 19 69
Fax (Management) 43 63 19 49

DEUTSCHLAND

Bundesanzeiger Verlag

Breite Straße 78-80
Postfach 10 05 34
D-50445 Köln
Tel. (02 21) 20 29-0
Fax (02 21) 2 02 92 78

GREECE/ΕΛΛΑΔΑ

G.C. Eleftheroudakis SA

International Bookstore
Nikis Street 4
GR-10563 Athens
Tel. (01) 322 63 23
Telex 219410 ELEF
Fax 323 98 21

ESPAÑA

Boletín Oficial del Estado

Trafalgar, 27-29
E-28071 Madrid
Tel. (91) 538 22 95
Fax (91) 538 23 49

Mundi-Prensa Libros, SA

Castelló, 37
E-28001 Madrid
Tel. (91) 431 33 99 (Libros)
431 32 22 (Suscripciones)
435 36 37 (Dirección)
Télex 49370-MPLI-E
Fax (91) 575 39 98

Sucursal:

Librería Internacional AEDOS

Consejo de Ciento, 391
E-08009 Barcelona
Tel. (93) 488 34 92
Fax (93) 487 76 59

Llibreria de la Generalitat
de Catalunya

Rambla dels Estudis, 118 (Palau Moja)
E-08002 Barcelona
Tel. (93) 302 68 35
Tel. (93) 302 64 62
Fax (93) 302 12 99

FRANCE

Journal officiel
Service des publications
des Communautés européennes

26, rue Desaix
F-75727 Paris Cedex 15
Tél. (1) 40 58 77 01/31
Fax (1) 40 58 77 00

IRELAND

Government Supplies Agency

4-5 Harcourt Road
Dublin 2
Tel. (1) 66 13 111
Fax (1) 47 80 645

ITALIA

Licosa SpA

Via Duca di Calabria 1/1
Casella postale 552
I-50125 Firenze
Tel. (055) 64 54 15
Fax 64 12 57
Telex 570466 LICOSA I

GRAND-DUCHÉ DE LUXEMBOURG

Messageries du livre

5, rue Raiffeisen
L-2411 Luxembourg
Tél. 40 10 20
Fax 49 06 61

NEDERLAND

SDU Servicecentrum Uitgeverijen

Postbus 20014
2500 EA 's-Gravenhage
Tel. (070) 37 89 880
Fax (070) 37 89 783

ÖSTERREICH

Manz'sche Verlags-
und Universitätsbuchhandlung

Kohlmarkt 16
A-1014 Wien
Tel. (1) 531 610
Telex 112 500 BOX A
Fax (1) 531 61-181

Document delivery:

Wirtschaftskammer

Wiedner Hauptstraße
A-1045 Wien
Tel. (0222) 50105-4356
Fax (0222) 50206-297

PORTUGAL

Imprensa Nacional

Casa da Moeda, EP
Rua D. Francisco Manuel de Melo, 5
P-1092 Lisboa Codex
Tel. (01) 387 30 02/385 83 25
Fax (01) 384 01 32

Distribuidora de Livros
Bertrand, Ld.ª

Grupo Bertrand, SA

Rua das Terras dos Vales, 4-A
Apartado 37
P-2700 Amadora Codex
Tel. (01) 49 59 050
Telex 15798 BERDIS
Fax 49 60 255

SUOMI/FINLAND

Akateeminen Kirjakauppa

Keskuskatu 1
PO Box 218
FIN-00381 Helsinki
Tel. (0) 121 41
Fax (0) 121 44 41

SVERIGE

BTJ AB

Traktorvägen 13
S-22100 Lund
Tel. (046) 18 00 00
Fax (046) 18 01 25
30 79 47

UNITED KINGDOM

HMSO Books (Agency section)

HMSO Publications Centre
51 Nine Elms Lane
London SW8 5DR
Tel. (0171) 873 9090
Fax (0171) 873 8463
Telex 29 71 138

ICELAND

BOKABUD
LARUSAR BLÖNDAL

Skólavördustíg, 2
IS-101 Reykjavik
Tel. 11 56 50
Fax 12 55 60

NORGE

Narvesen Info Center

Bertrand Narvesens vei 2
Postboks 6125 Etterstad
N-0602 Oslo 6
Tel. (22) 57 33 00
Fax (22) 68 19 01

SCHWEIZ/SUISSE/SVIZZERA

OSEC

Stampfenbachstraße 85
CH-8035 Zürich
Tel. (01) 365 54 49
Fax (01) 365 54 11

BĂLGARIJA

Europress Klassica BK Ltd

66, bd Vitosha
1463 Sofia
Tel./Fax (2) 52 74 75

ČESKÁ REPUBLIKA

NIS ČR

Havelkova 22
130 00 Praha 3
Tel./Fax (2) 24 22 94 33

HRVATSKA (CROATIE)

Mediatrade

P. Hatza 1
4100 Zagreb
Tel. (041) 43 03 92
Fax (041) 45 45 22

MAGYARORSZÁG

Euro-Info-Service

Honvéd Europá Ház
Margitsziget
H-1138 Budapest
Tel./Fax (1) 111 60 61, (1) 111 62 16

POLSKA

Business Foundation

ul. Krucza 38/42
00-512 Warszawa
Tel. (2) 621 99 93, 628 28 82
International Fax&Phone (0-39) 12 00 77

ROMÂNIA

Euromedia

65, Strada Dionisie Lupu
RO-70184 Bucuresti
Tel./Fax 1-31 29 646

RUSSIA

CCEC

9,60-letiya Oktyabrya Avenue
117312 Moscow
Tel./Fax (095) 135 52 27

SLOVAKIA

Slovak Technical
Library

Nàm. slobody 19
812 23 Bratislava 1
Tel. (7) 52 204 52
Fax : (7) 52 957 85

CYPRUS

Cyprus Chamber of Commerce
and Industry

Chamber Building
38 Grivas Dhigenis Ave
3 Deligiorgis Street
PO Box 1455
Nicosia
Tel. (2) 44 95 00, 46 23 12
Fax (2) 45 86 30

MALTA

Miller Distributors Ltd

PO Box 25
Malta International Airport LQA 05 Malta
Tel. 66 44 88
Fax 67 67 99

TÜRKIYE

Pres AS

Istiklal Caddesi 469
80050 Tünel-Istanbul
Tel. (1) 520 92 96, 528 55 66
Fax (1) 520 64 57

ISRAEL

ROY International

31, Habarzel Street
69710 Tel Aviv
Tel. (3) 49 78 02
Fax (3) 49 78 12

EGYPT/
MIDDLE EAST

Middle East Observer

41 Sherif St.
Cairo
Tel/Fax (2) 393 97 32

UNITED STATES OF AMERICA/
CANADA

UNIPUB

4611-F Assembly Drive
Lanham, MD 20706-4391
Tel. Toll Free (800) 274 48 88
Fax (301) 459 00 56

CANADA

Subscriptions only
Uniquement abonnements

Renouf Publishing Co. Ltd

1294 Algoma Road
Ottawa, Ontario K1B 3W8
Tel. (613) 741 43 33
Fax (613) 741 54 39

AUSTRALIA

Hunter Publications

58A Gipps Street
Collingwood
Victoria 3066
Tel. (3) 417 53 61
Fax (3) 419 71 54

JAPAN

Procurement Services Int. (PSI-Japan)

Koru Dome Postal Code 102
Tokyo Kojimachi Post Office
Tel. (03) 32 34 69 21
Fax (03) 32 34 69 15

Sub-agent

Kinokuniya Company Ltd
Journal Department

PO Box 55 Chitose
Tokyo 156
Tel. (03) 34 39-0124

SOUTH-EAST ASIA

Legal Library Services Ltd

Orchard
PO Box 0523
Singapore 9123
Tel. 243 24 98
Fax 243 24 79

SOUTH AFRICA

Safto

5th Floor, Export House
Cnr Maude & West Streets
Sandton 2146
Tel. (011) 883-3737
Fax (011) 883-6569

ANDERE LÄNDER
OTHER COUNTRIES
AUTRES PAYS

Office des publications officielles
des Communautés européennes

2, rue Mercier
L-2985 Luxembourg
Tél. 29 29-1
Télex PUBOF LU 1324 b
Fax 48 85 73, 48 68 17

4/9

NOTICE TO THE READER

All scientific and technical reports published by the European Commission are announced in the monthly periodical '**euro abstracts**'. For subscription (1 year: ECU 63) please write to the address below.

Price (excluding VAT) in Luxembourg: ECU 11.50

OFFICE FOR OFFICIAL PUBLICATIONS
OF THE EUROPEAN COMMUNITIES

L-2985 Luxembourg

ISBN 92-827-0222-7

9 789282 702222